

Io's Volcanic Activity from Time Domain Adaptive Optics Observations: 2013-2018

KATHERINE DE KLEER,¹ IMKE DE PATER,² EDWARD M. MOLTER,² ELIZABETH BANKS,³ ASHLEY GERARD DAVIES,⁴
CARLOS ALVAREZ,⁵ RANDY CAMPBELL,⁵ JOEL AYCOCK,⁵ JOHN PELLETIER,⁵ TERRY STICKEL,⁵ GLENN G. KACPRZAK,⁶
NIKOLE M. NIELSEN,⁶ DANIEL STERN,⁴ AND JOSHUA TOLLEFSON²

¹*California Institute of Technology
1200 E California Blvd M/C 150-21
Pasadena, CA 91125, USA*

²*University of California, Berkeley, Berkeley CA*

³*The Pembroke Hill High School, Kansas City MO*

⁴*Jet Propulsion Laboratory, California Institute of Technology, Pasadena CA*

⁵*W. M. Keck Observatory, Waimea HI*

⁶*Swinburne University of Technology, Hawthorn, Victoria, Australia*

(Accepted May 14, 2019)

Submitted to AJ

ABSTRACT

We present measurements of the near-infrared brightness of Io's hot spots derived from 2-5 μm imaging with adaptive optics on the Keck and Gemini N telescopes. The data were obtained on 271 nights between August 2013 and the end of 2018, and include nearly 1000 detections of over 75 unique hot spots. The 100 observations obtained between 2013 and 2015 have been previously published in de Kleer and de Pater (2016a); the observations since the start of 2016 are presented here for the first time, and the analysis is updated to include the full five-year dataset. These data provide insight into the global properties of Io's volcanism. Several new hot spots and bright eruptions have been detected, and the preference for bright eruptions to occur on Io's trailing hemisphere noted in the 2013-2015 data (de Kleer and de Pater 2016a) is strengthened by the larger dataset and remains unexplained. The program overlapped in time with *Sprint-A/EXCEED* and *Juno* observations of the jovian system, and correlations with transient phenomena seen in other components of the system have the potential to inform our understanding of the impact of Io's volcanism on Jupiter and its neutral/plasma environment.

1. INTRODUCTION

Io's dramatic volcanic activity exhibits a high degree of spatial and temporal variability. The distribution of volcanic thermal emission in space and time contains information on the underlying volcanic advection processes, providing a window into the nature of Io's geological processes as well as into how tidal heating impacts the characteristics of the volcanism it powers.

While some of Io's volcanoes have remained persistently active since the *Voyager* fly-bys in 1979, numerous transient eruptions appear and subside in a matter of days, hours, or even minutes (e.g. Johnson et al. 1988; Veeder et al. 1994; de Pater et al. 2014; de Kleer et al. 2014; Tsang et al. 2014; Davies et al. 2018). The timeline of thermal activity for a given volcano is indicative of the style of volcanism and hence geological processes active at that site (Davies et al. 2010). The time intervals between eruptions at a given site can provide information on characteristic resupply timescales, while a comparison of eruption timing between sites has the potential to illuminate eruption clustering if present. Finally, the periodic forcing of Io may translate into specific temporal signatures that may be apparent in thermal timelines.

Volcanoes are also distributed non-randomly across Io’s surface, showing in particular a dearth of activity at the sub- and anti-jovian longitudes, as well as in polar regions (Hamilton et al. 2013; Veeder et al. 2015; de Kleer and de Pater 2016b), although no dataset published to date has had good coverage of the high latitudes. The spatial distribution of Io’s surface heat flow may place constraints on models for tidal heat dissipation in Io’s interior, or may indicate the degree of fluid flow in Io’s mantle through the amount of smoothing in the observed spatial trends relative to the expected patterns. Without allowing for lateral movement of melt, the end-member case of heat deposition in a shallow aesthenosphere predicts higher heat flow at lower latitudes with the greatest heat flow centered at the sub-jovian and anti-jovian regions. In contrast, the end-member case of deep mantle heating results in enhanced heat flow at the poles (Gaskell et al., 1988; Segatz et al., 1988).

Determining the temporal and spatial distribution of Io’s volcanism requires a large sample size of hot spot detections over a range of timescales. We have been building up a database of thermal emission from individual volcanoes on Io’s surface since 2013, when we initiated a time domain campaign of adaptive optics imaging of Io’s volcanoes at the Keck and Gemini N telescopes. Io has been observed using adaptive optics on Keck since 2001 (Marchis et al. 2002), but only since 2013 has there been a dedicated Io observing program at such high cadence. These observations spatially resolve Io, permitting the identification of individual active volcanoes, and are often made at multiple wavelengths in the 2-5 μm range in order to constrain temperature and total power output. The observations have a typical spatial resolution of $\sim 100\text{-}500$ km depending on telescope, wavelength, and sky conditions. The collective dataset is well suited to an investigation into the volcanic eruption processes at individual hot spots, which requires data capturing the time evolution of the eruptions, and to identification of spatial and temporal patterns in the distribution of activity.

The prior Io dataset that is most comparable in cadence, wavelength, and spatial resolution is from the *Galileo* Near-Infrared Mapping Spectrometer (NIMS; Carlson et al. 1992), which observed Io on 25 distinct passes with a typical spatial resolution of 100-400 km on Io’s surface, including some images with resolutions as coarse as 725 km and as fine as 100 meters (see Table 3.2 in Davies 2007). NIMS detected thermal emission from 115 unique hot spots (Davies et al. 2012; Veeder et al. 2012; 2015), each detected between one and 50+ times over the course of the mission. Long-term programs observing Io’s thermal emission from the NASA InfraRed Telescope Facility have also been very successful (Spencer et al. 1990; Veeder et al. 1994; Rathbun and Spencer 2010). While such data do not spatially resolve Io, techniques such as lucky imaging and observing Io as the satellite enters or emerges from occultation behind Jupiter have permitted brightness measurements of individual volcanoes. Though sensitive only to the brightest events and only to the Jupiter-facing hemisphere, occultation observations have by far the longest time baseline, having been made on more than 100 occasions over the past >2 decades (Rathbun et al. 2018), albeit at only one wavelength (3.5 or 3.8 μm).

Our spatial resolution and sensitivity to faint hot spots is intermediate between NIMS data and occultation observations, and is comparable to a typical NIMS observation. Our cadence and total number of observations are higher than all prior datasets, although the time baseline of our high cadence campaign is much shorter than the decadal timescales covered by the occultation datasets.

Our campaign is introduced in de Kleer et al. (2014), and the analysis methods and results from the first 2.5 years of the program (100 nights of observation) are given in de Kleer and de Pater (2016a). Here we present results from the 2016-2018 observations, and a joint analysis of all data to date, 2013-2018. The flexible scheduling capabilities at Gemini N, and our Twilight Zone observing program at Keck¹, have been instrumental in achieving the high cadence and quantity of observations. The observations and data analysis methods are reviewed in Section 2, the results are presented and discussed in Section 3, and the conclusions are summarized in Section 4.

2. OBSERVATIONS AND DATA ANALYSIS

We observed Io in the near-infrared with adaptive optics on 271 nights between August 2013 and July 2018; the observing dates and details are given in Table A.1. Observations were made with the NIRI imager on Gemini N (Hodapp et al. 2003) combined with the ALTAIR adaptive optics system in Natural Guide Star (NGS) mode, and with the NIRC2 imager on Keck II also using NGS adaptive optics (Wizinowich et al. 2000). The Gemini N data constitute 80% of the total visits, and include images in the L’ (3.78 μm) and K-cont (2.27 μm) filters. The Keck images were taken in a variety of filters from H-cont (1.58 μm) to Ms (4.67 μm), shown in Figure 1.

¹ <https://www2.keck.hawaii.edu/inst/tda/TwilightZone.html>

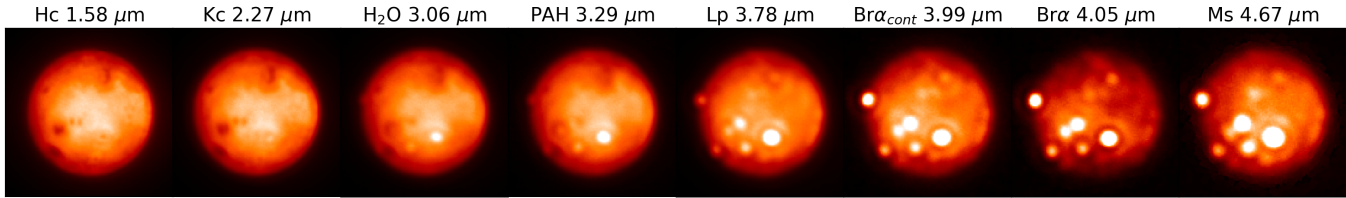


Figure 1. Images from Keck on 2017 May 28 demonstrating the range of filters used in the observations. All images were taken within a 30-minute window, and each is labeled with the filter name and central wavelength.

Images are flux calibrated to a standard star if a star was observed and the night was photometric; otherwise the images are calibrated to volcano-free regions of Io's disk, which do not change measurably with time. Within each image, all hot spots are identified; their pixel locations are translated to latitude and longitude coordinates on Io's disk based on Io's ephemeris; and their intensity is measured based on an aperture photometry approach adapted to point sources on a bright background (de Pater et al. 2014). All observing, data reduction, and analysis procedures are described in detail in de Kleer and de Pater (2016a), and an identical approach is used here. Of the full dataset, the 100 observations from 2013 through the end of 2015 were published in de Kleer and de Pater (2016a), while the 171 observations from 2016-2018 are presented here for the first time.

The detection limits for hot spots in the Keck and Gemini N images are given as a function of emission angle in Appendix A of de Kleer and de Pater (2016a). We use these limits to define the sensitivity of the dataset as a whole to hot spots at different longitudes. This sensitivity varies by up to 20% across Io's surface, and is used to correct the longitudinal hot spot distribution described in Section 3.4.

3. RESULTS & DISCUSSION

The coordinates, number of detections, and average brightness of each of the 75 hot spots detected and tracked by our program are listed in Table 1. The full set of near-infrared brightnesses in all filters for all 980 hot spot detections are tabulated in Table A.2. In some cases, the location of a hot spot appears to shift over time or transition from one active site to another nearby; in cases where it is not clear from the data whether the emission over time is produced by a single site or multiple nearby sites, we tabulate all detections under a single site name. The timeline of L'-band (3.78 μm) brightness of all volcanoes is shown in Figure 2, which gives a sense for the global variability of Io's volcanism over this period.

3.1. Energetic eruptions

Since 2013 we have detected bright eruptions at eighteen sites, where we define "bright" as a maximum L'-band brightness greater than 20 $\text{GW}/\mu\text{m}/\text{sr}$. There is no hot spot on Io that consistently exhibits this level of activity, and this cut-off therefore selects for transient events. These eruptions are typically vigorous, high-power events with significant short-wavelength emission. The majority of these were short-lived, exhibiting their peak brightness for only a few days before decaying. A few volcanoes are exceptions to this rule, producing thermal emission that is consistently present at a moderate level while also exhibiting infrequent brightenings; these volcanoes are Loki Patera, Pillan Patera, Marduk Fluctus, and Kurdalagon Patera. The first three of these were active throughout the period of observation, while Kurdalagon Patera was not detected before its eruption at the beginning of 2015 but was subsequently active and variable through 2018.

Table 2 lists these eighteen hot spots and the brightest L'-band intensity measured at each during our program. Note that only the single brightest detection is given even though some volcanoes had multiple large eruptions. The full timeline for each of these hot spots can be found in Table A.2. The events that occurred prior to the end of 2015 were presented in de Kleer and de Pater (2016a); our discussion here therefore focuses on eruptions detected since the beginning of 2016.

For volcanoes with detections at multiple wavelengths on a given night, we fit a Planck spectrum to estimate the temperature. All detections with measured temperatures above 800 K are given in Table 3; in total there are 32 such detections at 18 unique hot spots. These hot spots are not exactly the same set as the 18 sites where bright eruptions are seen, although there is significant overlap. While this is a small fraction of the total number of observations for which we were able to derive temperature estimates, it confirms previous findings that these high temperatures are common and widespread across a variety of volcanic styles and are not limited to outburst events (e.g. Carr

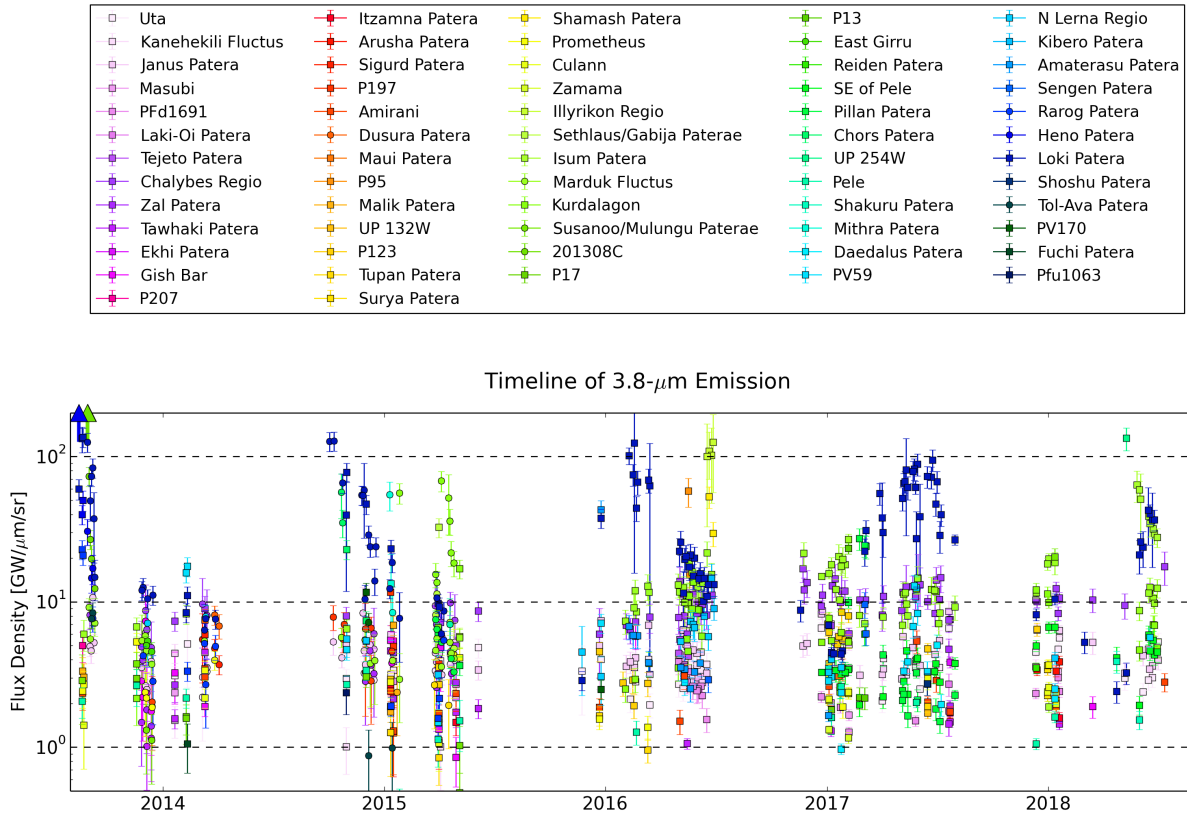


Figure 2. Timeline of Io’s volcanic activity from 2013-2018. All L’-band detections of thermal emission from volcanic centers are plotted, with each volcanic center in a different color. The gaps in the timeline correspond to periods when the Jupiter system was not observable from Maunakea. The timeline shows that there are multi-month intervals with no bright activity, and other intervals when several large eruptions took place.

1986; Lopes-Gautier et al. 1999). However, we note that Io’s active volcanoes likely exhibit a range of temperatures from near the magma temperature (~ 1500 K if the magma is basaltic) down to near the passive surface temperature (~ 125 K), and the temperatures recovered in a single temperature fit therefore do not directly represent any physical temperature (although they do serve as a lower limit on the eruption temperature). In fact, if the magma composition is the same at all of Io’s volcanoes, then the best-fit temperature instead reflects the proportion of high-temperature to low-temperature emitting areas, and high fitted temperatures are indicative of volcanic eruptions vigorous enough that sufficient area is exposed at very high temperatures to yield a short wavelength peak in thermal emission (e.g. Davies et al. 2010).

The temperatures in Table 3 are derived as in de Kleer and de Pater (2016a), using Markov Chain Monte Carlo simulations to determine the probability distribution for temperature and emitting area, from which the uncertainties are also derived. Measurements from all available wavelengths are used, incorporating uncertainties on the intensity measurements, and a maximum K-cont ($2.27 \mu\text{m}$) brightness limit of $7 \text{ GW}/\mu\text{m}/\text{sr}$ is imposed in the fitting when the hot spot was not detected at that wavelength.

The temperature estimates are derived from the intensity measurements given in Table A.2, which have been corrected for geometric foreshortening. However, in the case of a high emission angle observation of an event of significant vertical extent such as fire fountaining, the short-wavelength emission may arise primarily from the hot fountaining component that is not foreshortened, while the longer-wavelength emission arises from both the fountains and the resultant lava flows, which are foreshortened. Applying the foreshortening correction across all wavelengths may therefore inflate the derived short-wavelength emission and hence the temperature, so that temperatures derived from high emission angle observations should be viewed with caution.

3.1.1. Eruption at P95 (May 2016)

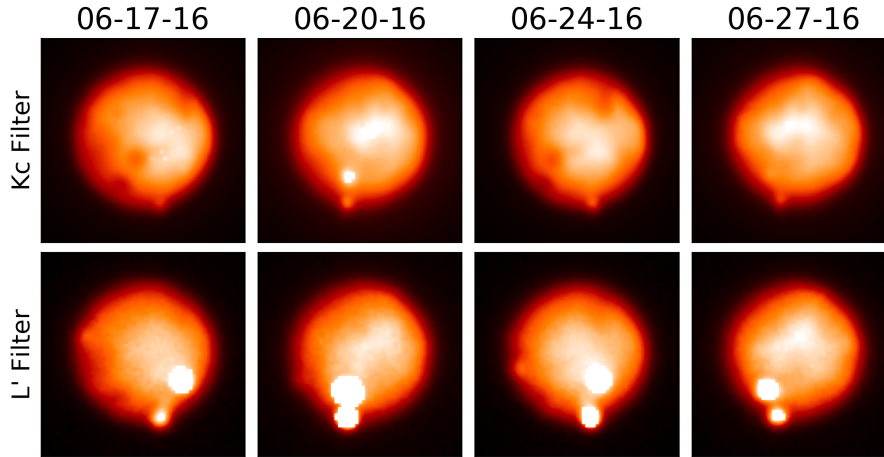


Figure 3. Near-infrared images from Gemini N of eruptions in Io’s southern hemisphere in 2016. The hot spot near the south pole is at a new site in the Illyrikon Regio. Despite the apparent similarity between all four L’ images, the viewing geometry changes significantly between observations: from left to right the central meridian longitudes are 249°; 138°; 233°; and 123° W. The mid-latitude hot spot is Marduk Fluctus on June 17 and 24, and is Shamash Patera on June 20 and 27.

In May 2016 a bright and short-lived eruption was detected at patera P95, near 10°S 128°W. The eruption was first detected on May 17 with a temperature around 1000 K. The second and final detection of the eruption occurred two days later on May 19, and the eruption had already declined significantly in brightness by this time. The latest non-detection of the site prior to the eruption was May 12, while the eruption had faded to below $I_{LP} \sim 5 \text{ GW}/\mu\text{m}/\text{sr}$ by May 24, and to below the detection limit even at optimal viewing geometry ($I_{LP} \sim 3 \text{ GW}/\mu\text{m}/\text{sr}$) by May 28. While high in both temperature and infrared emission, this event therefore was short-lived, detected only over a 3-night period and constrained to be active at a detectable level for less than 16 days.

3.1.2. Eruptions at Shamash Patera and in the Illyrikon Regio (June 2016)

A pair of dramatic eruptions occurred in the southern hemisphere at Shamash Patera (33°S 150°W) and in Illyrikon Regio near 71°S 180°W in June 2016. The eruption in Illyrikon Regio was first detected on June 17, and began no earlier than June 10. Shamash Patera was still not active as late as June 18, after the eruption at Illyrikon Regio had begun, but exhibited bright activity on June 20. The eruption at Shamash Patera had decayed and cooled somewhat by June 27, while the eruption in Illyrikon Regio stayed bright and hot through the end of June, after which we had no further observations until November. Figure 3 shows images of the eruptions at these volcanoes. The two volcanoes appear close in the images but are separated by over 1000 km of surface distance. The location of the hot spot in Illyrikon Regio is poorly constrained due to the high emission angle of all observations and we cannot conclusively match a surface feature at its location, but the positioning of a dark patera at 71°S 170°W is consistent with some of the thermal emission detections, whose best-fit longitudes fall in the range of 165-193°W. At 71°S, this is the most polar hot spot detected by our program.

3.1.3. Eruption at UP 254W (May 2018)

On May 10, 2018 a bright, high-temperature ($\sim 1000 \text{ K}$) eruption was detected at 37°S 254°W; a small patera at exactly this location is seen in spacecraft surface imaging (Williams et al. 2011a) and is a plausible source of the eruption. The hot spot was detected again on May 31 but had dimmed nearly to invisibility, and was not seen again. Although the hot spot location is close to the hot spot we refer to as “SE of Pele”, these hot spots are clearly distinct and are spatially resolved in the May 31 observations. No prior activity at this location has been documented.

3.1.4. Eruption at Isum Patera (May-June 2018)

Of the high-power events detected in 2016-2018, the most dramatic in both temperature and duration was an eruption at Isum Patera in May-June 2018. The event began prior to May 27 and exhibited temperatures around or above 1000 K for the subsequent month. The total emission decayed steadily over this period, suggesting that new magma was being erupted throughout but at a rate that decreased with time. Figures 4 and 5 show images of the eruption and plot its infrared timeline and the corresponding temperature fits.

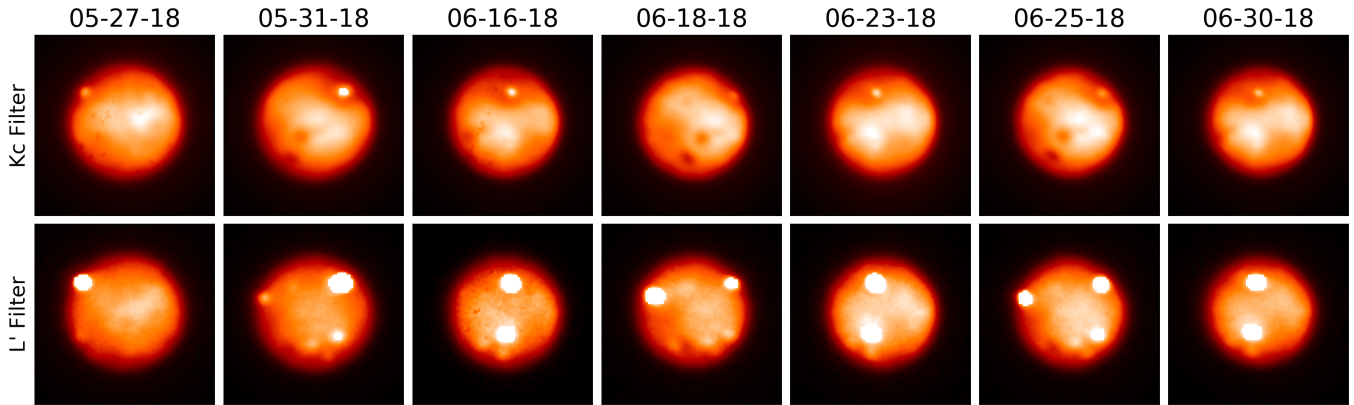


Figure 4. Near-infrared images from Gemini N of the eruption at Isum Patera in spring 2018. The eruption is the only hot spot visible in the K filter ($2.27 \mu\text{m}$), and is seen at a corresponding location in the L' images ($3.78 \mu\text{m}$). The bright hot spot south of Isum Patera is Marduk Fluctus.

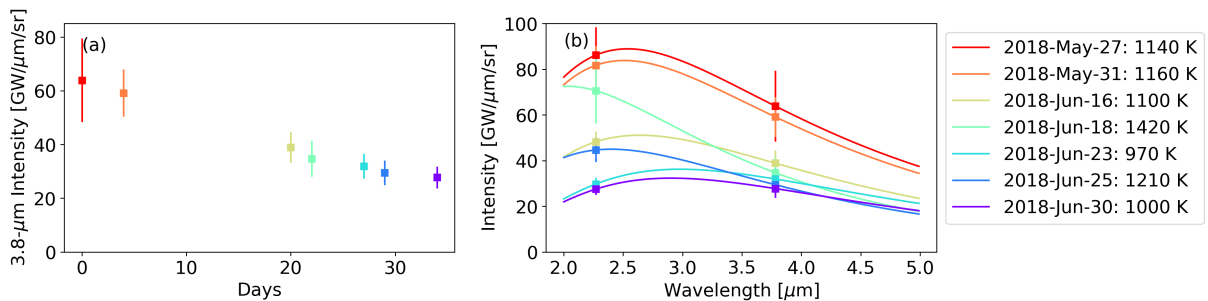


Figure 5. Eruption at Isum Patera in 2018. (a) Timeline of $3.8 \mu\text{m}$ intensity over a ~ 1 -month period; (b) Temperature fits to the 2.3 - and 3.8 - μm measured brightnesses. Temperatures may be over-estimated if lava fountaining is occurring, as discussed in the text.

3.2. Activity at new hot spots

Many of Io's most active hot spots today have exhibited persistent or episodic activity back to the *Voyager* and *Galileo* missions, nearly 40 years in some cases. However, the detection of new hot spots at locations where no thermal emission was previously seen is also common in the ground-based datasets (de Pater et al. 2016; Cantrall et al. 2018), including hot spots where no corresponding surface features are seen. The detection of these new hot spots improves our understanding of the distribution of active volcanic centers on Io's surface and of their heat flow.

Cantrall et al. (2018) identified 24 hot spots that had been detected in ground-based data and were not seen by *Galileo*, more than a quarter of the total number of hot spots seen in the ground-based dataset. The new data presented here bring the total number of hot spots seen in the ground-based adaptive optics datasets from 2001-2018 to 104, 29 of which were not seen by previous spacecraft missions. In the new data presented here, the hot spots where thermal emission had not been previously detected were: Ekhi Patera; the hot spot in Illyrikon Regio; an unknown location near 54°N 218°W ; the hot spot SE of Pele; and an unnamed patera near 37°S 254°W . Of these five, emission from Ekhi Patera and the unknown location at 218°W was detected only once and at low brightness; the hot spot SE of Pele was consistently detected from Dec 2016 through the end of 2018 though at a low level; and the hot spots in Illyrikon Regio and at 254°W were locations where bright eruptions took place.

Of the 75 hot spots detected in 2013-2018, about 1/3 of them were detected throughout the period of observation, 1/3 were detected only in 2013-2015, and 1/3 were detected only in 2016-2018. For the set of hot spots that were only detected during one of the two intervals of observation, the majority were detected less than half a dozen times. This characteristic, in combination with the fact that a substantial fraction of these hot spots were previously detected by *Galileo* or *Voyager*, suggests that despite the apparent turnover in activity between observing intervals, it is likely that nearly all hot spots have been geologically active throughout the period of space- and Earth-based observation, but

that they only output surface thermal emission sporadically, so that the set of hot spots detected in an observation period may depend heavily on the exact timing of the observations.

A clear exception to this is the category of hot spots where no previous thermal emission has been seen, no clear patera feature is present at the site of the emission, and yet the hot spot stays persistently active for years after the activity is first seen. In this dataset, the two most prominent examples are the hot spot in Chalybes Regio, and the hot spot SE of Pele. These appear to be locations where volcanic activity initiated since the *Galileo* mission.

Chalybes Regio is a northern region with extensive lava flow fields. Thermal emission was first detected from this location in 2010 (de Pater et al. 2014), and was attributed to PFu 2083, a small patera floor unit identified by Williams et al. (2011a) at 56°N 74°W. Thermal emission from this location was consistently detected in every observation we made between 2013 and 2018 that had appropriate viewing geometry. In many cases the emission appears spatially extended, indicative of multiple active areas that are not spatially resolved in the data.

The hot spot SE of Pele, located near 35°S 240°W, was first detected on Dec 23, 2016 and was thereafter detected through the end of our observation period in mid-2018. While there are many flows and paterae in this general area of Io's surface, there is no patera whose location provides a good match to the observed thermal emission.

3.3. Persistent volcanoes and periodicities

The sites that were most consistently detected during our campaign were Loki Patera (113 detections), Marduk Fluctus (87 detections), Janus Patera (84 detections), the hot spot in Chalybes Regio (80 detections), and Uta (57 detections). The first four of these were detected every time the viewing geometry was favorable. The hot spot at Uta does not appear to stay localized to the patera and may in fact be composed of multiple closely spaced volcanic centers not clearly resolved from one another. The timelines for these five hot spots are shown in Figure 6. The large number of observations of each of these hot spots provides a database of thermal brightness that may be used to fit models for volcanic activity style. In addition, the quantity and cadence of the images result in a dataset that is sensitive to periodicities in volcanic brightness on timescales from days to months. The tidal forcing that both powers the activity and deforms Io's crust is periodic, and the resultant activity may reflect these periodicities depending on the rheology and eruption mechanism.

We conducted a periodicity analysis on the five persistently active hot spots listed above by calculating Lomb-Scargle periodograms (Scargle 1982; Zechmeister and Kürster 2009) and comparing the periodogram peaks against significance levels derived by bootstrapping. These periodograms are shown, with significance levels indicated, in Figure 7, and the volcano intensity timeline is plotted phased on the period corresponding to the periodogram peak. The bootstrapping technique samples from the dataset randomly with replacement and computes the periodogram; the confidence levels correspond to the percentage of resampled datasets that show no peaks above the indicated level (Ivezić et al. 2014; VanderPlas 2018). Note that because the duration of Io's eruptions is typically longer than the interval between observations, confidence intervals derived from random resampling will lead to an apparent enhancement in the significance of observing cadence periodicities.

Nearly all hot spots show peaks near 0.997 days and 1.77 days, with weaker signals near 0.64 and 2.3 days (seen prominently in many of the periodograms in Figure 7), which correspond to Earth's sidereal day, Io's rotation period (sidereal period = 1.7691 days), and the periods corresponding to their beat frequencies ($\nu_{beat} = |\nu_1 - \nu_2|$). These periods reflect the observing cadence: the average interval between observations is a multiple of Earth's sidereal day, while repeat observations of a given hot spot are made (on average) at multiples of Io's rotation period. Io's rotation period as observed from Earth differs slightly from its sidereal period due to the relative motion of Earth and Jupiter, and is minimized at opposition when the motion of Earth relative to Jupiter is maximized perpendicular to the line of sight. This leads to Earth-apparent rotation periods in the range of 1.7680-1.7691 days.

A periodicity at Io's rotation period could also be an indication of a tidally modulated volcanic process, whereby the volcanic activity or thermal emission is controlled in part by diurnally varying tidal stresses. However, the periodicities near Io's rotation period in the dataset analyzed here do not show evidence for this effect. In particular, the peak periodogram power is at periods of 1.769-1.776 days, which match or slightly exceed Io's apparent rotation period but are a poorer match to Io's 1.7627 day anomalistic period, or time between successive perijoves, which is the relevant parameter for diurnal stresses and differs from the apparent rotation period due to the precession of Io's orbit. In order to further highlight the difference between the observed 1.77-day signal and Io's tidal forcing, the rightmost column in Figure 7 shows the brightness of each volcano as a function of Io's mean anomaly at the time of observation, demonstrating that there is no mean anomaly correlation even in hot spots that show a strong 1.77-day periodicity.

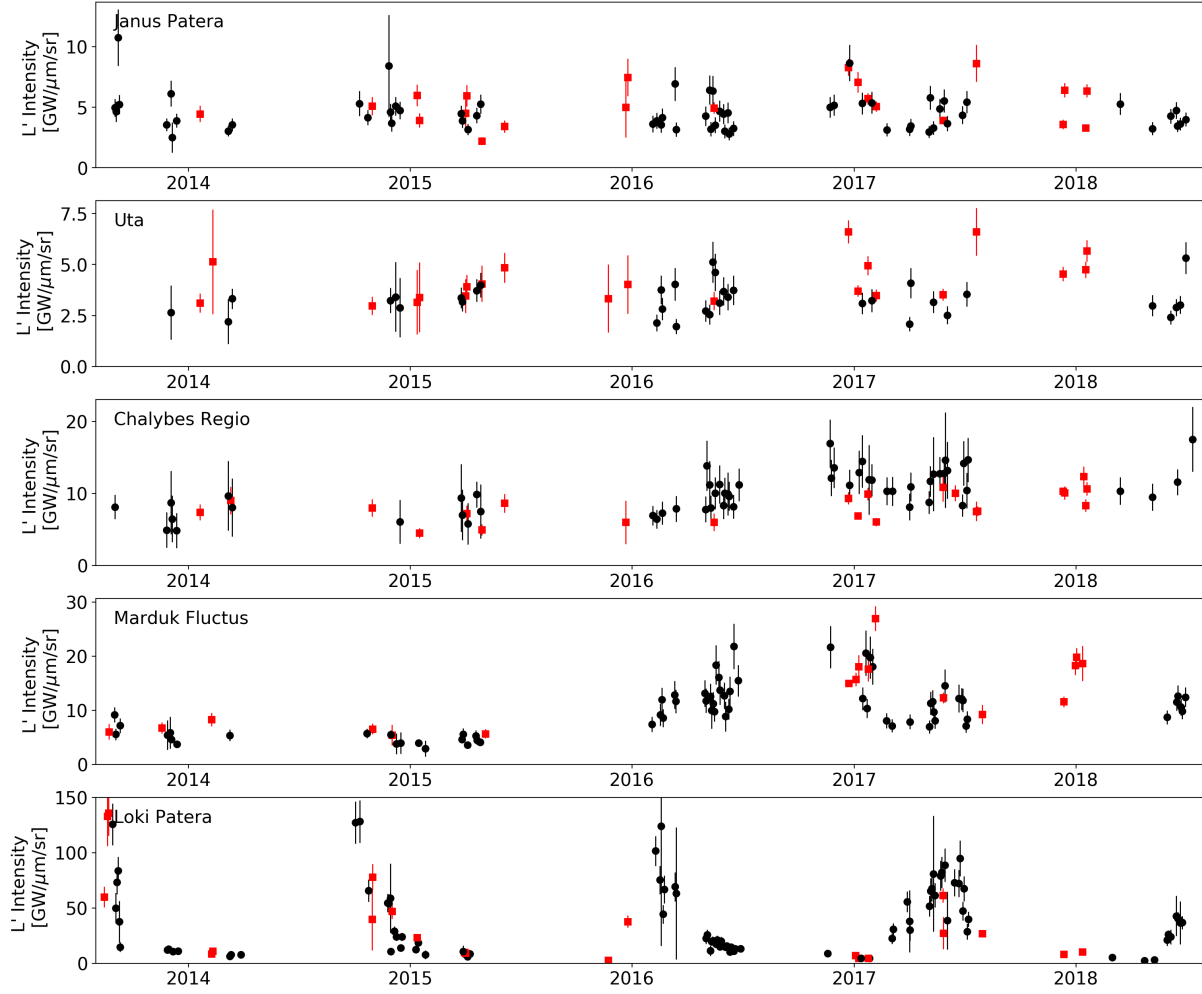


Figure 6. Activity timelines for five persistently active hot spots. Black circles and red squares indicate detections with Gemini N and Keck respectively.

The period of precession of Io’s longitude of perijove is ~ 1.5 years, so that on the timescale of a few months we see the same Ionian longitudes near a similar phase of Io’s orbit, which likely accounts for the prominence of both Earth’s and Io’s rotation periods in the periodograms. This can be seen in the middle column of Figure 7: all datapoints are color-coded by time (cycling from blue to red from early to late), and it is clear from the middle plot of the Chalybes Regio panel, for example, that the apparent periodicity likely arises from a combination of a long-term brightening and observing cadence biases. In essence, we are unable to rigorously distinguish between a scenario where a volcano is variable over an orbital period, and a scenario where it is variable over a longer timescale but observational effects caused apparent orbital-timescale periodicities.

This limitation could be entirely eliminated in a spacecraft dataset, where the observing cadence is less regular and the same hot spot can be viewed at a variety of mean anomalies within a time period that is short relative to the timescale for intrinsic variability of that volcano.

Only Loki Patera shows a statistically significant periodicity at a period other than the four discussed above. Over the time period of observation analyzed here, Loki Patera’s activity was periodic with a period of 465.63 days.

3.4. Hot spot spatial distribution

The distribution of hot spot number density with latitude and longitude is shown in Figure 8, and Figure 9 plots the location and brightness of all L’-band hot spot detections, updated from a similar figure based on the 2013-2015 data in de Kleer and de Pater (2016b). The longitudinal distribution has been corrected for the sensitivity of the

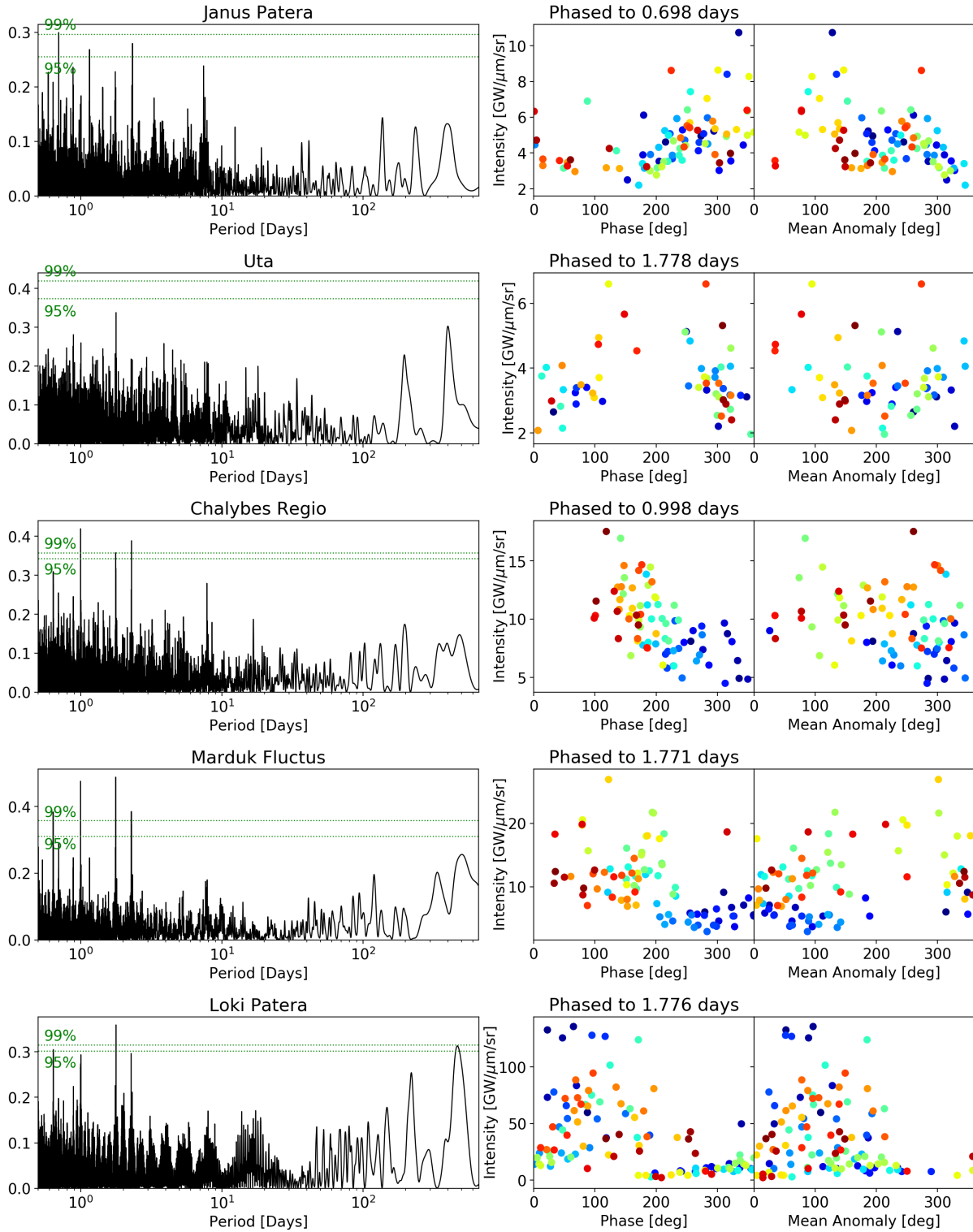


Figure 7. Generalized Lomb-Scargle periodograms for the five most consistently detected hot spots. The 99% and 95% significance levels are shown as dotted horizontal lines. The plots in the middle column show the data phased to the period corresponding to the peak in the periodogram, and the rightmost column shows the data as a function of Io's mean anomaly at the time of observation. The most prominent periodicities are near Io's and Earth's rotation periods (1 and 1.77 days), and their beat frequencies (periods near 0.6 and 2.3 days). The mean anomaly plots demonstrate that the 1.77-day periodicities are more consistent with being an observing cadence effect rather than a physical effect due to tidally modulated volcanism, which would exhibit a shorter period and a mean anomaly correlation. Within a given plot, the coloring of points is monotonic with time (blue=earliest; red=latest) to indicate the temporal ordering of the datapoints.

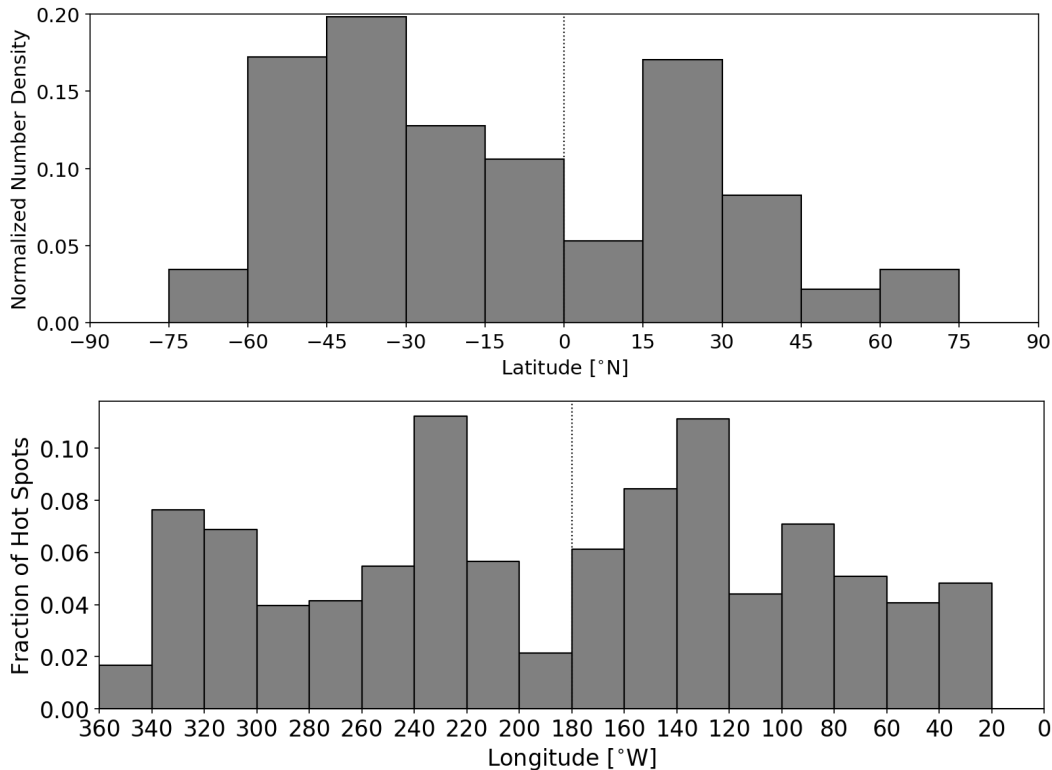


Figure 8. Distribution of detected hot spots in latitude and longitude. The longitude distribution is plotted as fraction of total hot spot number per longitude bin, using only hot spots that were detected at L' , and is corrected for observational biases. The latitude distribution is corrected for the surface area in each latitude bin and normalized but is not corrected for observational biases, which contribute to the dearth of hot spots at high latitudes.

observations to each longitude bin. The latitudinal distribution is not corrected because the latitudinal differences in the volcano brightness distribution or in topography are poorly constrained.

Our observations in 2013-2015 showed an apparent difference in the spatial distribution of bright, transient eruptions compared to persistent hot spots (de Kleer and de Pater 2016b). In particular, all nine of the volcanoes that hosted bright eruptions ($I_{max,Lp} > 30 \text{ GW}/\mu\text{m}/\text{sr}$) during those years are located on the trailing hemisphere. In the full dataset (2013-2018), 18 volcanoes exhibited bright eruptions, where bright is defined as $I_{max,Lp} > 20 \text{ GW}/\mu\text{m}/\text{sr}$. Note that this definition is effectively the same as in our previous paper because there were no volcanoes with detected $I_{max,Lp}$ between 20 and 30 $\text{GW}/\mu\text{m}/\text{sr}$ in 2013-2015. The threshold was lowered because the larger dataset now available indicates that no volcano persistently maintains a flux density level above 20 $\text{GW}/\mu\text{m}/\text{sr}$, and this cutoff is therefore sufficient to isolate bright transient events. Of these 18 volcanoes, every single one falls within a 180° band in longitude, from $128\text{-}308^\circ\text{W}$, despite the fact that our program had comparable sensitivity to events of this magnitude at all Ionian longitudes. Moreover, all but two of the eruptions occurred on Io's trailing hemisphere ($180\text{-}360^\circ\text{W}$); the probability of 16 or more eruptions occurring on the trailing hemisphere (given 18 eruptions total) is 0.00066 if volcanoes are randomly distributed in longitude.

Despite the distinctive distribution of the largest eruptions, there is no significant difference between the two hemispheres in terms of spatially and temporally averaged near-infrared brightness (provided that Loki Patera is excluded), nor in the number of active hot spots. The time-averaged volcanic L' -band intensity arises 47.5% and 52.5% from the leading and trailing hemispheres, respectively (excluding Loki Patera), while the number of hot spots detected at L' is identical between the two hemispheres (31 hot spots, excluding those detected only at longer wavelengths, to which only a subset of the data were sensitive).

In order to further explore whether any hemispheric-scale asymmetries are present in the distribution of the hot spots, we broaden this analysis from a comparison of just leading vs. trailing hemispheres by choosing all 180-degree longitude intervals and determining the fraction of hot spots that fall within each interval. While the leading and

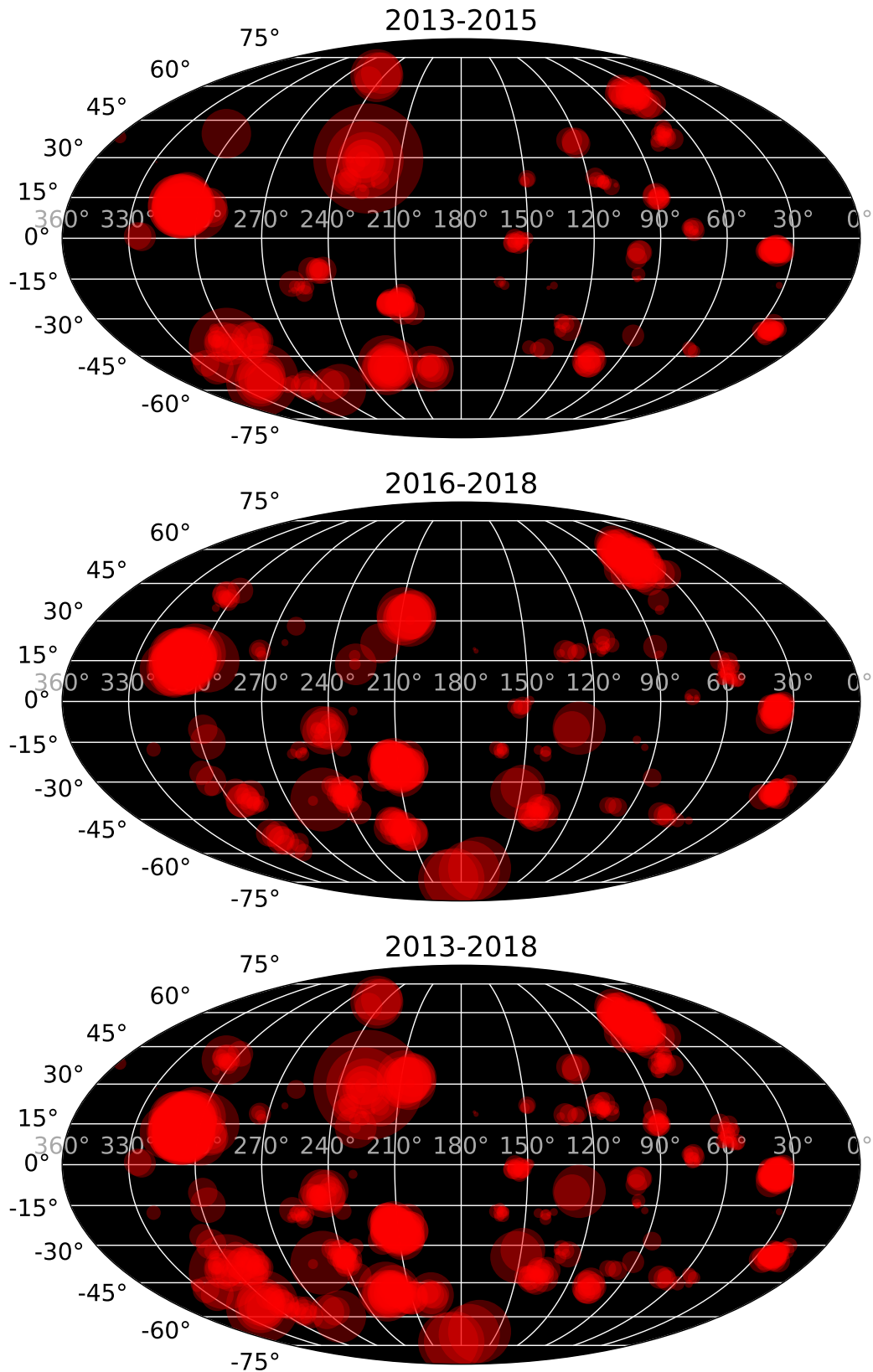


Figure 9. The spatial distribution of hot spot thermal emission detected on Io in 2013-2018. Each circle shows the location and brightness of a single hot spot detection, with circle size proportional to the log of the 3.8- μm intensity. All circles are semi-transparent, and high-opacity regions indicate multiple detections at the same location. The top and middle panels show the distribution in two distinct time periods (the 2013-2015 plot is identical to that given in de Kleer and de Pater 2016a), and the bottom panel shows the cumulative distribution from 2013-2018. The position uncertainties are typically a few degrees at low latitudes and higher towards the poles; much but not all of the apparent jitter in hot spot locations is within these uncertainties.

trailing hemispheres exhibit comparable time-averaged radiances and hot spot number, there is an asymmetry between the sub- and anti-jovian hemispheres with more hot spots and higher radiances on the anti-jovian hemisphere, despite the fact that this hemisphere had poorer coverage during our program. The hemisphere centered on 160°W maximizes both metrics, containing $\sim 60\%$ of the hot spots and $>70\%$ of the time averaged radiances. However, in artificial datasets where hot spots are randomly distributed in longitude, an asymmetry in hot spot number at this level is well within the expected range (i.e. within one σ of the median).

4. CONCLUSIONS

We present results from measurements of the thermal emission of Io’s volcanoes, derived from near-infrared imaging with adaptive optics at the Keck and Gemini N telescopes on 271 nights between August 2013 and the end of 2018. The first 100 nights of observations were presented in de Kleer and de Pater (2016a), while the 171 nights since the start of 2016 are presented here for the first time. Over the five years of the program to date, we made 980 detections of over 75 unique hot spots, with some hot spots detected more than 80 times and Loki Patera detected 113 times. We provide downloadable tables of hot spot brightnesses and observing details, and hope that these data products will serve as a resource for others in the community who will build on the analyses presented here.

Nearly all bright transient eruptions where temperature measurements were possible displayed temperatures above 800 K, confirming that eruptions at such high temperatures are common and are likely the rule rather than the exception. The detection of new hot spots that were not previously detected by spacecraft is a common occurrence. Adding the data presented here to that summarized by Cantrall et al. (2018), there have now been 104 distinct hot spots seen in the AO data from 2001-2018, 25-30 of which were not previously seen by spacecraft. It is likely that many of these hot spots have been active since before the *Galileo* and *Voyager* visits but were not emitting sufficient radiation during the visits to have been detected. However, some of the new hot spots have no corresponding surface feature and remain persistently active after they are first detected (e.g. Chalybes Regio and the hot spot SE of Pele), suggesting that activity recently initiated at these locations. We performed a periodicity search on the five most consistently detected hot spots (each detected 57-113 times) but did not detect any new periodicities beyond those introduced by the observing cadence. Spacecraft data would be needed to draw a robust conclusion about tidally modulated volcanism on diurnal timescales.

De Kleer and de Pater (2016b) noted that all bright, transient eruptions took place on Io’s trailing hemisphere. This trend continues through the additional 3 years of data presented here, and the probability of the observed asymmetry is 0.00066 if volcanoes are randomly distributed. Note that this asymmetry applies only to the character of the volcanism; the number and cumulative near-IR radiance is nearly identical between leading and trailing hemispheres.

This dataset now constitutes the largest set of unique detections of thermal emission from individual Ionian hot spots to date, permitting robust statistical analyses of properties such as the spatial distribution of hot spot activity, the variability and time-averaged power of numerous individual hot spots, and the occurrence rates of bright and/or high-temperature eruptions. These data, in combination with *Galileo*’s sensitivity to smaller, cooler hot spots and the multi-decadal time baseline provided by ground-based occultation data, are now providing a truly global, multi-wavelength picture of Io’s volcanic activity over a wide range of timescales.

The timing of our program coincided with intensive observations of the extended sodium cloud and the plasma torus by ground-based programs and by the *EXCEED/Hisaki* and *Juno* missions. The correlation of these datasets with our timeline of Io’s activity is already providing clues into the connections between different components of the jovian system (Yoshikawa et al. 2017; Koga et al. 2018; Morgenthaler et al. 2019), but our understanding of this system is far from complete. Continued coverage of Io’s volcanoes throughout these missions will be key to unraveling the sources of variability in the jovian neutral and plasma environment.

ACKNOWLEDGEMENTS

KdK is supported by the Heising-Simons Foundation through a *51 Pegasi b* postdoctoral fellowship, and this research was partially supported by the National Science Foundation grant AST-1313485 to UC Berkeley and a NASA Keck PI Data Award, administered by the NASA Exoplanet Science Institute. We are grateful to Roy and Frances Simperman for their support of the Keck Visiting Scholars program, which enabled KdK, EM, and CA to develop the Keck twilight program through which some of the data presented here were obtained. We thank G. Puniwai for acquiring several of the Keck observations. We thank P. Capak, J. Cohen, N. Hernitschek, D. Masters, and S.A. Stanford of the the Complete Calibration of the Color-Redshift Relation (C3R2; Masters et al. 2017) NASA Keck Key Strategic Mission

Support survey team for providing twilight observations on the nights of UT 2017 December 11-13. The work of DS and AGD was carried out at the Jet Propulsion Laboratory, California Institute of Technology, under a contract with NASA. Much of the data presented herein were obtained at the Gemini Observatory, which is operated by the Association of Universities for Research in Astronomy, Inc., under a cooperative agreement with the NSF on behalf of the Gemini partnership: the National Science Foundation (United States), National Research Council (Canada), CONICYT (Chile), Ministerio de Ciencia, Tecnología e Innovación Productiva (Argentina), Ministério da Ciência, Tecnologia e Inovação (Brazil), and Korea Astronomy and Space Science Institute (Republic of Korea). Some of the data presented herein were obtained at the W. M. Keck Observatory, which is operated as a scientific partnership among the California Institute of Technology, the University of California and the National Aeronautics and Space Administration. Some of the data was obtained at the W. M. Keck Observatory from telescope time allocated to the National Aeronautics and Space Administration through the agency's scientific partnership with the California Institute of Technology and the University of California. The Observatory was made possible by the generous financial support of the W. M. Keck Foundation. The authors wish to recognize and acknowledge the very significant cultural role and reverence that the summit of Maunakea has always had within the indigenous Hawaiian community. We are most fortunate to have the opportunity to conduct observations from this mountain.

Table 1. Overview of hot spots

Site	Lat °N	Lon °W	N_{det}	F_{filt}^a GW/ $\mu\text{m}/\text{sr}$	Filter ^a
Nusku Patera	-65.0	6.2	1	Narrowband	Only
Uta	-34.4	21.0	57	3.6	Lp
Kanehekili Fluctus	-17.0	34.5	8	1.2	Lp
Janus Patera	-3.9	37.4	84	4.7	Lp
UP 38W	-25.3	37.7	1	1.9	Ms
Pfu374	-24.3	49.7	3	1.0	Ms
Masubi	-42.9	53.7	9	2.4	Lp
PFd1691	9.4	58.3	22	2.5	Lp
Laki-Oi Patera	-44.6	59.7	4	3.9	Lp
Shamshu Patera	-8.3	61.5	1	1.1	Ms
Tejeto Patera	-42.9	68.7	4	4.4	Lp
Chalybes Regio	55.4	70.2	80	9.6	Lp
Zal Patera	37.9	74.6	24	2.9	Lp
Tawhaki Patera	2.5	75.6	19	2.1	Lp
Ekhi Patera	-28.4	86.7	1	3.8	Lp
Gish Bar	15.6	89.1	18	3.4	Lp
Aluna Patera	41.7	90.1	2	3.2	Ms
P207	-36.5	91.1	1	5.0	Lp
Shango Patera	33.5	95.6	3	1.8	Ms
Itzamna Patera	-15.0	99.0	9	1.6	Lp
Arusha Patera	-39.6	99.0	4	3.5	Lp
Sigurd Patera	-5.1	99.2	8	4.4	Lp
P197	-46.9	107.3	11	6.2	Lp
Amirani	20.5	113.2	27	2.6	Lp
Dusura Patera	36.4	121.1	3	7.5	Lp
Maui Patera	18.2	125.8	2	3.2	Lp
P95	-10.0	127.8	2	36.5	Lp
Malik Patera	-32.9	129.6	9	3.1	Lp
UP 132W	18.4	131.6	5	3.6	Lp
Thor	40.6	134.7	2	1.3	Ms
P123	-41.9	139.2	20	4.6	Lp
Tupan Patera	-18.0	140.5	10	1.6	Lp
Surya Patera	21.2	149.4	4	2.7	Lp
Shamash Patera	-33.2	150.5	2	41.3	Lp
Sobo Fluctus	12.9	152.8	1	Narrowband	Only
Prometheus	-1.5	153.3	22	2.8	Lp
Culann	-17.2	161.8	11	2.0	Lp
Zamama	18.5	173.2	3	1.2	Lp
Illyrikon Regio	-70.8	179.9	4	109.2	Lp
Sethlaus/Gabija Paterae	-50.0	198.1	6	11.6	Lp
Isum Patera	31.1	205.4	16	37.6	Lp
Marduk Fluctus	-23.7	211.1	87	10.5	Lp
Kurdalagon	-49.3	216.7	36	13.1	Lp
Unknown	53.6	217.8	1	Narrowband	Only
Susanoo/Mulungu Paterae	18.6	221.0	10	4.5	Lp
201308C	29.1	228.0	11	555.7	Lp
P17	-3.5	228.8	1	1.8	Lp
P13	13.9	229.0	4	9.2	Lp

Table 1 continued on next page

Table 1 (*continued*)

Site	Lat °N	Lon °W	N_{det}	\bar{F}_{filt}^a GW/ $\mu\text{m}/\text{sr}$	Filter ^a
East Girru	21.3	233.5	3	4.9	Lp
Reiden Patera	-18.0	234.4	2	3.5	Lp
Pyerun Patera	-57.7	237.1	1	3.9	Ms
SE of Pele	-34.5	239.5	30	3.9	Lp
Pillan Patera	-11.3	243.7	21	7.1	Lp
Chors Patera	65.1	245.6	5	30.6	Lp
UP 254W	-37.1	254.5	2	67.7	Lp
Pele	-18.2	255.2	19	2.2	Lp
Shakuru Patera	24.8	261.7	2	2.7	Lp
Mithra Patera	-58.0	265.6	4	25.4	Lp
Svarog Patera	-51.6	269.3	3	4.1	Ms
Daedalus Patera	18.7	273.9	5	2.5	Lp
PV59	-38.2	289.7	22	6.7	Lp
N Lerna Regio	-56.0	290.6	19	5.2	Lp
Kibero Patera	-12.5	297.1	2	11.7	Lp
Amaterasu Patera	38.8	304.3	13	7.6	Lp
Sengen Patera	-29.8	305.1	4	5.2	Lp
Rarog Patera	-39.2	305.4	14	29.3	Lp
Heno Patera	-55.6	307.5	7	70.3	Lp
Loki Patera	12.6	307.5	113	38.3	Lp
Shoshu Patera	-17.6	322.9	1	2.7	Lp
Tol-Ava Patera	0.7	326.5	4	4.4	Lp
PV170	-47.9	327.8	3	7.1	Lp
Fuchi Patera	28.3	328.7	1	1.0	Lp
Surt	44.4	334.1	2	1.2	Ms
Pfu1063	41.7	357.7	3	1.7	Lp
Paive Patera	-42.9	358.3	2	0.9	Ms

^aThe mean observed flux density \bar{F}_{filt} is given in the Lp filter if data were available in this filter, and in the Ms filter if no Lp detections were made. If no detections were made in either broadband filter, detection in narrowband only is indicated.

Table 2. Bright eruptions^a, 2013-2018

Site	Date of Peak [UT]	Lat [°N]	Lon [°W]	$I_{max,Lp}$ [GW/ $\mu\text{m}/\text{sr}$]	Reference
Heno Patera	08-15-2013	-56	308	270±70	c
Rarog Patera	08-15-2013	-39	305	325±80	c
Loki Patera ^b	08-22-2013	13	308	136±20	c
201308C	08-29-2013	29	228	>500	d
Chors Patera	10-22-2014	65	246	57±19	e
Mithra Patera	01-10-2015	-58	266	55±12	e
Sethlaus/Gabija Paterae	04-01-2015	-50	198	33±5	e
Kurdalagon ^b	04-05-2015	-49	217	68±11	e
Amaterasu Patera	12-25-2015	39	304	43±6	e
P95	05-17-2016	-10	128	58±13	
Shamash Patera	06-20-2016	-33	151	53±9	
Illyrikon Regio	06-27-2016	-71	180	125±69	
P13	02-05-2017	14	229	23±2	
Marduk Fluctus ^b	02-05-2017	-24	211	27±2	
Pillan Patera ^b	02-23-2017	-11	244	27±5	
Susanoo/Mulungu Paterae	01-12-2018	19	221	20±3	
UP 254W	05-10-2018	-37	252	134±24	
Isum Patera	05-27-2018	31	205	64±16	

^aAll eruptions detected with $I_{max,Lp} > 20$ GW/ $\mu\text{m}/\text{sr}$ during this time period.

^bNearly all bright eruptions were transient events at sites where activity was not otherwise detected. Exceptions are: Pillan Patera, Loki Patera, and Marduk Fluctus, which were persistently active but exhibited spikes in activity; and Kurdalagon Patera, which was not detected prior to its first eruption but remained detectable afterwards.

^cde Pater et al. (2014)

^dde Kleer et al. (2014)

^ede Kleer and de Pater (2016a)

Table 3. High-temperature eruptions^a, 2013-2018

Site	Date [UT]	μ	T ^b [K]	Reference
Shamash Patera	2016-Jun-20	0.81	1000±110	
	2016-Jun-27	0.74	850±80	
Culann	2017-Jun-16	0.81	860±140	
UP 254W	2018-May-10	0.63	960±100	
PV170	2014-Dec-02	0.42	850±40	c
Isum Patera	2018-May-27	0.48	1200±220	
	2018-May-31	0.70	1180±120	
	2018-Jun-16	0.84	1120±100	
	2018-Jun-18	0.43	1440±410	
	2018-Jun-23	0.85	980±70	
	2018-Jun-25	0.62	1230±280	
	2018-Jun-30	0.85	1010±80	
PFd1691	2018-Jan-19	0.98	830±80	
Rarog Patera	2013-Aug-15	0.60	1300±200	d
	2014-Feb-10	0.78	890±120	c
	2015-Mar-31	0.76	950±60	c
PV59	2014-Oct-31	0.59	950±200	c
P95	2016-May-17	0.39	1020±180	
Kurdalagon Patera	2015-Jan-26	0.54	1200±150	c
	2015-Mar-31	0.26	820±110	c
	2015-Apr-05	0.57	1300±200	c
Tawhaki Patera	2014-Mar-11	0.54	900±170	c
	2018-Jan-19	0.97	800±90	
P197	2014-Mar-11	0.67	1000±250	c
N Lerna Regio	2014-Dec-02	0.50	820±180	c
	2015-Mar-31	0.54	940±120	c
Reiden Patera	2017-Dec-12	0.90	1170±100	
	201308C	2014-Dec-02	0.64	850±160
SE of Pele	2017-Dec-12	0.79	950±160	
P123	2015-Jan-11	0.74	820±160	c
Illyrikon Regio	2016-Jun-20	0.24	1210±690	
	2016-Jun-27	0.17	1060±340	

^aAll eruptions detected with T>800 K during this period.

^bTemperatures are derived from intensities corrected for geometric foreshortening, and may be overestimated in observations with high emission angle (μ) if fire fountaining is producing a substantial fraction of the short-wavelength emission.

^cde Kleer and de Pater (2016a)

^dde Pater et al. (2014)

^ede Kleer et al. (2014)

REFERENCES

- Cantrall, C., de Kleer, K., de Pater, I., et al. Variability and geologic associations of volcanic activity on Io in 2001-2016. *Icarus* 312, 267-294 (2018).
- Carlson, R.W., Weissman, P.R., Smythe, W.D., Mahoney, J.C. Near-Infrared Mapping Spectrometer experiment on Galileo. *Space Sci Rev* 60, 457-502 (1992).
- Carr, M.H. Silicate volcanism on Io. *JGR* 91, 3521-3532 (1986).
- Davies, A.G. *Volcanism on Io: a Comparison with Earth*, Cam. Univ. Press (2007).
- Davies, A.G., Keszthelyi, L.P., Harris, A.J.L. The thermal signature of volcanic eruptions on Io and Earth. *J. Volc. Geo. Res.* 194, 75-99 (2010).
- Davies, A.G., Veeder, G.J., Matson, D.L., Johnson, T.V. Io: Charting thermal emission variability with the Galileo NIMS Io Thermal Emission Database (NITED): Loki Patera. *GeoRL* 39, L01201, p. 1-6 (2012).
- Davies, A.G., Davies, R.L., Veeder, G.J., et al. Discovery of a powerful, transient, explosive thermal event at Marduk Fluctus, Io, in *Galileo* NIMS data. *GRL* 45, 2926-2933 (2018).
- de Kleer, K., de Pater, I., Davies, A.G., et al. Near-infrared monitoring of Io and detection of a violent outburst on 29 August 2013. *Icarus* 242, 352-364 (2014).
- de Kleer, K., de Pater, I. Time variability of Io's volcanic activity from near-IR adaptive optics observations on 100 nights in 2013-2015. *Icarus* 280, 378-404 (2016a).
- de Kleer, K., de Pater, I. Spatial distribution of Io's volcanic activity from near-IR adaptive optics observations on 100 nights in 2013-2015. *Icarus* 280, 405-414 (2016b).
- de Pater, I., Davies, A.G., Ádámkóvics, M., Ciardi, D.R. Two new, rare, high-effusion outburst eruptions at Rarog and Heno Paterae on Io. *Icarus* 242, 365-378 (2014).
- de Pater, I., Davies, A.G., Marchis, F. Keck observations of eruptions on Io in 2003-2005. *Icarus* 274, 284-296 (2016).
- Gaskell, R.W., Synnott, S.P., McEwen, A.S., Schaber, G.G. Large-scale topography of Io - Implications for internal structure and heat transfer. *GRL* 15, 581-584 (1988). item[]Hodapp, K.W., Jensen, J.B., Irwin, E.M., et al. The Gemini near-infrared imager (NIRI). *PASP* 115, 1388-1406 (2003).
- Koga, R., Tsuchiya, F., Kagitani, M., et al. The time variation of atomic oxygen emission around Io during a volcanic event observed with Hisaki/EXCEED. *Icarus* 299, 300-307 (2018).
- Lopes-Gautier, R., McEwen, A.S., Smythe, W.B., et al. Active volcanism on Io: Global distribution and variations in activity. *Icarus* 140, 243-264 (1999).
- Hamilton, C.W. et al. Spatial distribution of volcanoes on Io: Implications for tidal heating and magma ascent. *Earth Planet Sci Lett* 361, 272-286 (2013).
- Ivezić, Ž., Connolly, A.J., VanderPlas, J.T., Gray, A. *Statistics, Data Mining, and Machine Learning in Astronomy*, Princeton Series in Modern Observational Astronomy, pp. 140-144 (2014).
- Johnson, T.V., Veeder, G.J., Matson, D.L. et al. Io: Evidence for silicate volcanism in 1986. *Science* 242, 1280-1283 (1988).
- Marchis, F., de Pater, I., Davies, A.G. et al. High-resolution Keck adaptive optics imaging of violent volcanic activity on Io. *Icarus* 160, 124-131 (2002).
- Masters, D.C., Stern, D.K., Cohen, J.G. et al. The Complete Calibration of the Color-Redshift Relation (C3R2) Survey: Survey Overview and Data Release 1. *ApJ*, 841, 111, 10pp (2017).

- Morgenthaler, J.P., Rathbun, J.A., Schmidt, C.A., Baumgardner, J., Schneider, N.M. Large volcanic event on Io inferred from jovian sodium nebula brightening. *ApJ Lett* 871, article id. L 23, 6pp (2019).
- Rathbun, J.A., Spencer, J.R. Ground-based observations of time variability of multiple active volcanoes on Io. *Icarus* 209, 625-630 (2010).
- Rathbun, J.A., Howell, R.R., Spencer, J.R. Active volcanoes on Io: Putting ground-based observations of Jupiter occultations into the PDS. 49th LPSC #2083 (2018).
- Scargle, J.D. Studies in astronomical time series analysis. II - Statistical aspects of spectral analysis of unevenly spaced data. *ApJ* 263, 835-853 (1982).
- Segatz, M. et al. Tidal dissipation, surface heat flow, and figure of viscoelastic models of Io. *Icarus* 75, 187-206 (1988).
- Spencer, J.R., Shure, M.A., Ressler, M.E., et al. Discovery of hotspots on Io using disk-resolved infrared imaging. *Nature* 348, 618-621 (1990).
- Tsang, C.C.C., Rathbun, J.A., Spencer, J.R., Hesman, B.E., Abramov, O. Io's hot spots in the near-infrared detected by LEISA during the New Horizons flyby, *JGR Planets*, 119, 2222-2238 (2014).
- VanderPlas, J.T. Understanding the Lomb-Scargle Periodogram. *ApJ Supp.*, 236:16, 28pp (2018).
- Veeder, G.J., Matson, D.L., Johnson, T.V., Blaney, D.L., Goguen, J.D. Io's heat flow from infrared radiometry: 1983-1993. *JGR Planets* 99 (E8), 17095-17162 (1994).
- Veeder, G.J., Davies, A.G., Matson, D.L., Johnson, T.V., Williams, D.A. and Radebaugh, J. Io: Volcanic thermal sources and global heat flow. *Icarus* 219, 701-722 (2012).
- Veeder, G.J., et al., 2015. Io: Heat flow from small volcanic features. *Icarus* 245, 379-410.
- Williams, D.A. et al. Geologic map of Io, USGS Scientific Investigations Map 3168, scale 1:15,000,000 (2011a).
- Williams, D.A., Keszthelyi, L.P., Crown, D.A. Volcanism on Io: New insights from global geologic mapping. *Icarus* 214, 91-112 (2011b).
- Wizinowich, P., Acton, D.S., Shelton, et al. First light adaptive optics images from the Keck II telescope: A new era in high angular resolution imagery. *PASP* 112, 315-319 (2000).
- Yoshikawa, I., Suzuki, F., Hikida, R., et al. Volcanic activity on Io and its influence on the dynamics of the jovian magnetosphere observed by EXCEED/Hisaki in 2015. *Earth, Planets and Space-Frontier Letter* 69, 110, 11pp (2017).
- Zechmeister, M. and Kürster, M., 2009. The generalized Lomb-Scargle periodogram. *A&A* 496, 577-584 (2009).

APPENDIX

A. TABLES

Table A.1 provides details on the observations, and Table A.2 provides the measured intensities for all hot spot detections in 2013-2018, corrected for geometric foreshortening. Both Tables A.1 and A.2 are available for download.

Table A.1. Observations

Date ^a	Tel/Inst	Lon ^b	Lat ^b	Distance ^b
UT		°W	°N	AU
2013-08-15	Keck/NIRC2	337.0	2.0	5.85
2013-08-20	Keck/NIRC2	275.0	2.0	5.79
2013-08-21	Keck/NIRC2	115.0	2.0	5.78
2013-08-22	Keck/NIRC2	319.0	2.0	5.77
2013-08-23	Keck/NIRC2	161.0	2.0	5.76
2013-08-29	Gemini N/NIRI	305.7	1.9	5.69
2013-08-30	Gemini N/NIRI	146.2	1.9	5.68
2013-09-01	Gemini N/NIRI	192.7	1.9	5.65
2013-09-02	Gemini N/NIRI	36.4	1.9	5.65
2013-09-03	Gemini N/NIRI	241.4	1.9	5.63
2013-09-04	Gemini N/NIRI	79.4	1.9	5.62
2013-09-05	Gemini N/NIRI	285.2	1.9	5.61
2013-09-06	Gemini N/NIRI	129.2	1.9	5.59
2013-09-07	Gemini N/NIRI	334.4	1.9	5.58
2013-09-09	Gemini N/NIRI	24.2	1.9	5.55
2013-09-10	Gemini N/NIRI	226.0	1.9	5.54
2013-11-18	Keck/NIRC2	221.3	1.6	4.53
2013-11-26	Gemini N/NIRI	54.3	1.6	4.44
2013-11-27	Gemini N/NIRI	257.7	1.6	4.43
2013-11-28	Gemini N/NIRI	101.3	1.6	4.42
2013-11-29	Gemini N/NIRI	306.9	1.6	4.41
2013-12-02	Gemini N/NIRI	154.6	1.6	4.38
2013-12-03	Gemini N/NIRI	25.4	1.6	4.37
2013-12-04	Gemini N/NIRI	202.4	1.6	4.36
2013-12-05	Gemini N/NIRI	81.0	1.6	4.35
2013-12-06	Gemini N/NIRI	273.1	1.6	4.34
2013-12-12	Gemini N/NIRI	72.3	1.6	4.29
2013-12-13	Gemini N/NIRI	231.2	1.6	4.29
2013-12-14	Gemini N/NIRI	118.9	1.6	4.28
2013-12-15	Gemini N/NIRI	320.4	1.6	4.28
2014-01-20	Keck/NIRC2	34.2	1.6	4.25
2014-02-08	Keck/NIRC2	274.0	1.6	4.39
2014-02-10	Keck/NIRC2	318.1	1.6	4.41
2014-03-07	Gemini N/NIRI	35.7	1.6	4.74
2014-03-10	Gemini N/NIRI	257.7	1.6	4.78
2014-03-11	Keck/NIRC2	131.8	1.6	4.79
2014-03-11	Gemini N/NIRI	98.9	1.6	4.79
2014-03-12	Gemini N/NIRI	302.4	1.6	4.81
2014-03-14	Gemini N/NIRI	23.6	1.6	4.85
2014-03-27	Gemini N/NIRI	129.1	1.6	5.05
2014-03-28	Gemini N/NIRI	337.0	1.6	5.07
2014-04-03	Gemini N/NIRI	105.8	1.6	5.16
2014-10-03	Gemini N/NIRI	307.5	0.2	5.82
2014-10-09	Gemini N/NIRI	86.8	0.2	5.74
2014-10-10	Gemini N/NIRI	290.8	0.1	5.73
2014-10-22	Gemini N/NIRI	209.8	0.0	5.55
2014-10-23	Gemini N/NIRI	55.8	0.0	5.54
2014-10-24	Gemini N/NIRI	258.4	0.0	5.53
2014-10-25	Gemini N/NIRI	95.0	0.0	5.51
2014-10-27	Gemini N/NIRI	145.8	0.0	5.48
2014-10-30	Keck/NIRC2	39.0	0.0	5.44
2014-10-31	Keck/NIRC2	241.8	0.0	5.42
2014-11-25	Gemini N/NIRI	283.9	-0.1	5.03
2014-11-27	Gemini N/NIRI	334.2	-0.1	5.0
2014-11-28	Gemini N/NIRI	153.1	-0.1	4.99

Table A.1 continued on next page

Table A.1 (continued)

Date ^a	Tel/Inst	Lon ^b	Lat ^b	Distance ^b
UT		°W	°N	AU
2014-11-29	Gemini N/NIRI	22.1	-0.1	4.97
2014-11-30	Gemini N/NIRI	227.9	-0.1	4.95
2014-12-01	Gemini N/NIRI	71.0	-0.1	4.94
2014-12-02	Keck/NIRC2	275.7	-0.1	4.92
2014-12-06	Gemini N/NIRI	329.3	-0.2	4.87
2014-12-08	Gemini N/NIRI	50.0	-0.2	4.84
2014-12-09	Gemini N/NIRI	249.7	-0.2	4.82
2014-12-10	Gemini N/NIRI	97.6	-0.2	4.81
2014-12-15	Gemini N/NIRI	40.0	-0.2	4.74
2014-12-16	Gemini N/NIRI	247.0	-0.2	4.73
2014-12-18	Gemini N/NIRI	293.3	-0.2	4.7
2015-01-10	Gemini N/NIRI	296.0	-0.2	4.46
2015-01-11	Keck/NIRC2	137.7	-0.2	4.44
2015-01-12	Keck/NIRC2	338.5	-0.2	4.44
2015-01-13	Gemini N/NIRI	134.0	-0.2	4.32
2015-01-14	Gemini N/NIRI	327.6	-0.2	4.43
2015-01-15	Gemini N/NIRI	230.7	-0.2	4.42
2015-01-16	Keck/NIRC2	74.3	-0.2	4.41
2015-01-22	Gemini N/NIRI	153.6	-0.2	4.38
2015-01-26	Gemini N/NIRI	249.7	-0.2	4.36
2015-03-25	Gemini N/NIRI	149.4	-0.0	4.66
2015-03-26	Gemini N/NIRI	29.1	-0.0	4.68
2015-03-27	Gemini N/NIRI	213.2	-0.0	4.69
2015-03-28	Gemini N/NIRI	41.8	-0.0	4.71
2015-03-29	Gemini N/NIRI	244.2	-0.0	4.72
2015-03-31	Keck/NIRC2	291.5	-0.0	4.74
2015-04-01	Keck/NIRC2	134.9	-0.0	4.75
2015-04-02	Keck/NIRC2	339.1	-0.0	4.77
2015-04-04	Keck/NIRC2	27.9	-0.0	4.80
2015-04-05	Gemini N/NIRI	250.6	-0.0	4.81
2015-04-06	Gemini N/NIRI	70.3	-0.0	4.83
2015-04-09	Gemini N/NIRI	322.0	-0.0	4.87
2015-04-17	Gemini N/NIRI	149.0	-0.0	4.99
2015-04-19	Gemini N/NIRI	197.3	-0.0	5.02
2015-04-20	Gemini N/NIRI	39.8	-0.0	5.04
2015-04-21	Gemini N/NIRI	243.6	-0.0	5.03
2015-04-22	Gemini N/NIRI	88.7	-0.0	5.07
2015-04-26	Gemini N/NIRI	206.4	-0.0	5.13
2015-04-27	Gemini N/NIRI	23.8	-0.0	5.15
2015-04-29	Keck/NIRC2	72.9	-0.0	5.18
2015-05-05	Keck/NIRC2	213.5	-0.0	5.27
2015-06-05	Keck/NIRC2	38.9	-0.1	5.75
2015-11-23	Keck/NIRC2	327.2	-1.5	5.65
2015-12-22	Keck/NIRC2	328.5	-1.8	5.15
2015-12-25	Keck/NIRC2	106.5	-1.8	5.19
2016-01-30	Gemini N/NIRI	124.5	-1.9	4.65
2016-02-03	Gemini N/NIRI	220.1	-1.9	4.60
2016-02-04	Gemini N/NIRI	65.2	-1.9	4.60
2016-02-09	Gemini N/NIRI	323.6	-1.9	4.56
2016-02-11	Gemini N/NIRI	44.4	-1.9	4.54
2016-02-15	Gemini N/NIRI	122.0	-1.9	4.51
2016-02-16	Gemini N/NIRI	299.5	-1.9	4.50
2016-02-17	Gemini N/NIRI	144.5	-1.9	4.49
2016-02-18	Gemini N/NIRI	18.2	-1.9	4.49
2016-02-19	Gemini N/NIRI	206.6	-1.9	4.48
2016-02-20	Gemini N/NIRI	51.4	-1.9	4.48
2016-02-21	Gemini N/NIRI	257.1	-1.9	4.47
2016-02-23	Gemini N/NIRI	296.4	-1.9	4.46
2016-03-11	Gemini N/NIRI	156.0	-1.9	4.43
2016-03-12	Gemini N/NIRI	336.6	-1.9	4.44
2016-03-13	Gemini N/NIRI	199.0	-1.8	4.43
2016-03-14	Gemini N/NIRI	27.8	-1.8	4.44
2016-04-30	Gemini N/NIRI	201.4	-1.6	4.81
2016-05-01	Gemini N/NIRI	45.0	-1.6	4.83
2016-05-02	Gemini N/NIRI	250.7	-1.6	4.84

Table A.1 continued on next page

Table A.1 (*continued*)

Date ^a	Tel/Inst	Lon ^b	Lat ^b	Distance ^b
UT		°W	°N	AU
2016-05-03	Gemini N/NIRI	94.1	-1.6	4.86
2016-05-04	Gemini N/NIRI	299.5	-1.6	4.87
2016-05-08	Gemini N/NIRI	30.3	-1.6	4.93
2016-05-09	Gemini N/NIRI	238.2	-1.6	4.94
2016-05-10	Gemini N/NIRI	77.1	-1.6	4.95
2016-05-11	Gemini N/NIRI	281.0	-1.6	4.97
2016-05-12	Gemini N/NIRI	132.8	-1.6	4.98
2016-05-13	Gemini N/NIRI	343.2	-1.5	5.00
2016-05-14	Gemini N/NIRI	201.4	-1.5	5.01
2016-05-15	Keck/NIRC2	35.5	-1.5	5.03
2016-05-16	Gemini N/NIRI	218.5	-1.5	5.04
2016-05-17	Gemini N/NIRI	61.3	-1.5	5.06
2016-05-18	Gemini N/NIRI	264.0	-1.5	5.07
2016-05-19	Gemini N/NIRI	125.6	-1.5	5.09
2016-05-20	Gemini N/NIRI	314.4	-1.5	5.11
2016-05-23	Gemini N/NIRI	203.5	-1.5	5.15
2016-05-24	Gemini N/NIRI	47.8	-1.5	5.17
2016-05-25	Gemini N/NIRI	261.6	-1.5	5.18
2016-05-27	Gemini N/NIRI	299.1	-1.5	5.21
2016-05-28	Gemini N/NIRI	140.3	-1.5	5.23
2016-05-31	Gemini N/NIRI	35.4	-1.5	5.28
2016-06-01	Gemini N/NIRI	234.0	-1.5	5.29
2016-06-02	Gemini N/NIRI	78.5	-1.5	5.31
2016-06-03	Gemini N/NIRI	281.5	-1.5	5.32
2016-06-04	Gemini N/NIRI	125.6	-1.5	5.34
2016-06-05	Gemini N/NIRI	329.2	-1.5	5.36
2016-06-07	Gemini N/NIRI	27.9	-1.5	5.39
2016-06-08	Gemini N/NIRI	218.5	-1.5	5.40
2016-06-09	Gemini N/NIRI	62.2	-1.5	5.42
2016-06-10	Gemini N/NIRI	264.3	-1.5	5.43
2016-06-12	Gemini N/NIRI	313.8	-1.5	5.46
2016-06-16	Gemini N/NIRI	45.3	-1.5	5.53
2016-06-17	Gemini N/NIRI	249.0	-1.5	5.43
2016-06-18	Gemini N/NIRI	92.7	-1.5	5.56
2016-06-19	Gemini N/NIRI	296.9	-1.5	5.57
2016-06-20	Gemini N/NIRI	138.3	-1.5	5.58
2016-06-24	Gemini N/NIRI	232.6	-1.5	5.65
2016-06-25	Gemini N/NIRI	76.4	-1.5	5.66
2016-06-27	Gemini N/NIRI	122.9	-1.5	5.69
2016-06-28	Gemini N/NIRI	326.9	-1.5	5.71
2016-11-18	Gemini N/NIRI	323.4	-2.4	6.14
2016-11-22	Gemini N/NIRI	55.1	-2.5	6.10
2016-11-23	Gemini N/NIRI	257.1	-2.5	6.09
2016-11-24	Gemini N/NIRI	103.3	-2.5	6.07
2016-11-29	Gemini N/NIRI	38.4	-2.5	6.02
2016-12-22	Keck/NIRC2	39.5	-2.7	5.69
2016-12-23	Keck/NIRC2	240.0	-2.7	5.67
2016-12-24	Gemini N/NIRI	85.6	-2.7	5.66
2017-01-02	Gemini N/NIRI	114.2	-2.8	5.51
2017-01-03	Keck/NIRC2	314.1	-2.8	5.50
2017-01-04	Keck/NIRC2	156.0	-2.8	5.48
2017-01-07	Keck/NIRC2	31.9	-2.8	5.44
2017-01-08	Keck/NIRC2	253.8	-2.8	5.42
2017-01-09	Gemini N/NIRI	99.9	-2.8	5.40
2017-01-12	Gemini N/NIRI	333.8	-2.8	5.36
2017-01-14	Gemini N/NIRI	37.1	-2.9	5.32
2017-01-15	Gemini N/NIRI	236.9	-2.9	5.30
2017-01-18	Gemini N/NIRI	115.6	-2.9	5.26
2017-01-20	Gemini N/NIRI	148.1	-2.9	5.23
2017-01-22	Gemini N/NIRI	220.5	-2.9	5.19
2017-01-23	Gemini N/NIRI	53.0	-2.9	5.18
2017-01-23	Keck/NIRC2	69.3	-2.9	5.18
2017-01-24	Keck/NIRC2	274.6	-2.9	5.16
2017-01-25	Gemini N/NIRI	113.9	-2.9	5.15
2017-01-26	Gemini N/NIRI	317.6	-2.9	5.13

Table A.1 continued on next page

Table A.1 (continued)

Date ^a	Tel/Inst	Lon ^b	Lat ^b	Distance ^b
UT		°W	°N	AU
2017-01-27	Gemini N/NIRI	149.0	-2.9	5.11
2017-01-30	Gemini N/NIRI	49.8	-2.9	5.07
2017-01-31	Gemini N/NIRI	256.6	-2.9	5.50
2017-02-05	Keck/NIRC2	194.2	-3.0	4.97
2017-02-06	Keck/NIRC2	37.6	-3.0	4.96
2017-02-23	Gemini N/NIRI	229.9	-3.0	4.73
2017-02-24	Gemini N/NIRI	62.4	-3.0	4.73
2017-03-04	Gemini N/NIRI	246.5	-3.0	4.64
2017-03-05	Gemini N/NIRI	97.1	-3.0	4.63
2017-03-06	Gemini N/NIRI	298.4	-3.0	4.62
2017-03-29	Gemini N/NIRI	312.5	-3.0	4.47
2017-04-02	Gemini N/NIRI	26.0	-3.0	4.46
2017-04-03	Gemini N/NIRI	233.1	-3.0	4.45
2017-04-04	Gemini N/NIRI	67.3	-3.0	4.45
2017-05-04	Gemini N/NIRI	63.5	-2.8	4.55
2017-05-05	Gemini N/NIRI	253.7	-2.8	4.55
2017-05-06	Gemini N/NIRI	76.4	-2.8	4.56
2017-05-07	Gemini N/NIRI	272.2	-2.8	4.57
2017-05-09	Gemini N/NIRI	328.2	-2.8	4.59
2017-05-10	Gemini N/NIRI	162.7	-2.8	4.59
2017-05-11	Gemini N/NIRI	23.6	-2.8	4.61
2017-05-12	Gemini N/NIRI	207.0	-2.8	4.61
2017-05-14	Gemini N/NIRI	256.3	-2.8	4.63
2017-05-22	Gemini N/NIRI	83.8	-2.7	4.72
2017-05-23	Gemini N/NIRI	287.3	-2.7	4.73
2017-05-24	Gemini N/NIRI	129.5	-2.7	4.74
2017-05-25	Gemini N/NIRI	334.2	-2.7	4.75
2017-05-27	Gemini N/NIRI	20.5	-2.7	4.78
2017-05-27	Keck/NIRC2	19.5	-2.7	4.78
2017-05-28	Keck/NIRC2	222.9	-2.7	4.79
2017-05-29	Gemini N/NIRI	68.6	-2.7	4.80
2017-05-30	Gemini N/NIRI	272.3	-2.7	4.81
2017-05-31	Gemini N/NIRI	117.3	-2.7	4.82
2017-06-03	Gemini N/NIRI	32.0	-2.7	4.87
2017-06-15	Gemini N/NIRI	288.3	-2.6	5.03
2017-06-16	Keck/NIRC2	130.1	-2.6	5.05
2017-06-22	Gemini N/NIRI	273.4	-2.6	5.14
2017-06-23	Gemini N/NIRI	115.5	-2.6	5.15
2017-06-24	Gemini N/NIRI	320.1	-2.6	5.17
2017-06-27	Gemini N/NIRI	210.5	-2.6	5.21
2017-06-28	Gemini N/NIRI	53.6	-2.6	5.23
2017-06-29	Gemini N/NIRI	257.8	-2.6	5.24
2017-06-30	Gemini N/NIRI	100.7	-2.6	5.26
2017-07-01	Gemini N/NIRI	305.7	-2.6	5.28
2017-07-04	Gemini N/NIRI	202.3	-2.6	5.32
2017-07-05	Gemini N/NIRI	37.0	-2.6	5.34
2017-07-06	Gemini N/NIRI	243.6	-2.6	5.35
2017-07-07	Gemini N/NIRI	84.2	-2.6	5.37
2017-07-08	Gemini N/NIRI	287.9	-2.6	5.39
2017-07-09	Gemini N/NIRI	130.4	-2.6	5.40
2017-07-10	Gemini N/NIRI	336.0	-2.6	5.42
2017-07-21	Keck/NIRC2	50.1	-2.5	5.59
2017-07-23	Keck/NIRC2	95.5	-2.5	5.61
2017-07-31	Keck/NIRC2	282.9	-2.5	5.73
2017-12-11	Keck/NIRC2	50.1	-3.0	6.19
2017-12-12	Keck/NIRC2	252.4	-3.0	6.18
2017-12-13	Keck/NIRC2	94.6	-3.0	6.17
2017-12-31	Keck/NIRC2	157.0	-3.1	5.95
2018-01-02	Keck/NIRC2	201.5	-3.1	5.93
2018-01-10	Keck/NIRC2	30.3	-3.1	5.82
2018-01-11	Keck/NIRC2	223.5	-3.1	5.80
2018-01-12	Keck/NIRC2	283.1	-3.1	5.78
2018-01-14	Keck/NIRC2	125.0	-3.2	5.76
2018-01-17	Keck/NIRC2	17.7	-3.2	5.72
2018-01-19	Keck/NIRC2	62.2	-3.2	5.69

Table A.1 continued on next page

Table A.1 (*continued*)

Date ^a	Tel/Inst	Lon ^b	Lat ^b	Distance ^b
UT		°W	°N	AU
2018-03-02	Gemini N/NIRI	319.0	-3.3	5.02
2018-03-15	Gemini N/NIRI	84.4	-3.4	4.82
2018-03-17	Gemini N/NIRI	132.6	-3.4	4.78
2018-04-24	Gemini N/NIRI	283.7	-3.4	4.43
2018-04-25	Gemini N/NIRI	133.9	-3.4	4.43
2018-05-07	Gemini N/NIRI	51.7	-3.3	4.40
2018-05-10	Gemini N/NIRI	289.4	-3.3	4.40
2018-05-27	Gemini N/NIRI	150.3	-3.3	4.44
2018-05-31	Gemini N/NIRI	240.3	-3.3	4.46
2018-06-02	Gemini N/NIRI	283.8	-3.2	4.47
2018-06-06	Gemini N/NIRI	18.7	-3.2	4.50
2018-06-15	Gemini N/NIRI	18.9	-3.2	4.58
2018-06-16	Gemini N/NIRI	214.9	-3.2	4.58
2018-06-17	Gemini N/NIRI	61.1	-3.2	4.60
2018-06-18	Gemini N/NIRI	264.8	-3.2	4.61
2018-06-22	Gemini N/NIRI	21.7	-3.1	4.65
2018-06-23	Gemini N/NIRI	200.5	-3.1	4.66
2018-06-25	Gemini N/NIRI	249.0	-3.1	4.68
2018-06-30	Gemini N/NIRI	203.9	-3.1	4.74
2018-07-01	Gemini N/NIRI	29.6	-3.1	4.76
2018-07-12	Gemini N/NIRI	106.6	-3.1	4.90

^a Data from 2013-08-15 to 2013-08-23 were previously published in de Pater et al. (2014); and data from 2013-2015 were previously published in de Kleer and de Pater (2016a).

^b Sub-observer latitude and longitude, and Earth-Io distance, from JPL Horizons.

Table A.2. Hot Spot Intensities^a

Hot Spot	Date	Lat	Lon	K-cont	H ₂ O	PAH	L'	Bra-cont	Bra	Ms
				$\lambda = 2.27 \mu\text{m}$	$3.06 \mu\text{m}$	$3.29 \mu\text{m}$	$3.78 \mu\text{m}$	$3.99 \mu\text{m}$	$4.05 \mu\text{m}$	$4.67 \mu\text{m}$
	[UT]	[°N]	[°W]	[GW/ $\mu\text{m}/\text{sr}$]						
Nusku Patara	2017-May-27	-65.0±1.1	6.2±1.9							4.0±1.0
	Average	-65.0	6.2							
Uta	2013-Dec-03	-33.8±2.0	20.1±2.1				2.7±1.3			
	2014-Jan-20	-34.9±0.8	20.9±0.8			1.6±0.2	3.1±0.5			5.4±0.8
	2014-Feb-10	-34.1±0.5	23.4±2.1				5.1±2.6			4.6±0.9
	2014-Mar-07	-34.9±2.0	25.9±2.2				2.2±1.1			
	2014-Mar-14	-34.7±2.0	24.8±2.1				3.3±0.5			
	2014-Oct-30	-33.7±0.8	21.2±0.8				3.0±0.4			5.8±0.9
	2014-Nov-29	-35.5±2.1	20.6±2.1				3.2±0.6			
	2014-Dec-08	-34.1±1.6	19.1±2.5				3.4±1.7			
	2014-Dec-15	-34.2±1.8	19.6±2.3				2.9±1.4			
	2015-Jan-12	-35.4±1.0	22.6±1.8				3.2±1.6			4.9±0.7
	2015-Jan-16	-34.1±1.0	21.0±1.8				3.4±1.7			4.6±0.7
	2015-Mar-26	-37.0±2.0	22.1±2.2				3.4±0.5			
	2015-Mar-28	-34.6±1.8	25.3±2.3				3.2±0.5			
	2015-Apr-02	-33.5±0.6	23.9±1.3				3.5±0.8			4.7±0.7
	2015-Apr-04	-33.9±0.5	24.8±0.5				3.9±0.6			6.1±0.9
	2015-Apr-20	-34.6±1.9	27.2±2.2				3.7±0.6			
	2015-Apr-27	-35.8±2.0	24.4±2.1				4.0±0.6			
	2015-Apr-29	-34.7±0.7	23.4±1.2				4.1±0.9			5.4±0.8
	2015-Jun-05	-32.2±0.7	23.5±0.9			3.3±0.5	4.8±0.7			7.1±1.1
	2015-Nov-23	-35.5±0.7	21.3±1.9				3.3±1.7			5.2±0.8
	2015-Dec-25	-34.6±0.6	22.7±1.9				4.0±1.4			6.1±0.9
	2016-Feb-11	-32.3±1.3	18.1±1.8				2.1±0.4			
	2016-Feb-18	-31.9±1.2	18.2±1.3				3.8±0.7			
	2016-Feb-20	-32.3±1.3	22.2±1.9				2.8±0.5			
	2016-Mar-12	-35.9±1.3	19.6±2.8				4.0±0.8			

Table A.2 continued on next page

Table A.2 (continued)

Hot Spot	Date	Lat	Lon	K-cont	H ₂ O	PAH	L'	Br α -cont	Br α	Ms
				$\lambda = 2.27 \mu\text{m}$	$3.06 \mu\text{m}$	$3.29 \mu\text{m}$	$3.78 \mu\text{m}$	$3.99 \mu\text{m}$	$4.05 \mu\text{m}$	$4.67 \mu\text{m}$
	[UT]	[°N]	[°W]				[GW/ $\mu\text{m}/\text{sr}$]			
	2016-Mar-14	-32.7 \pm 1.2	20.9 \pm 1.3				2.0 \pm 0.4			
	2016-May-01	-32.0 \pm 1.4	19.5 \pm 1.9				2.7 \pm 0.5			
	2016-May-08	-32.8 \pm 1.4	24.1 \pm 1.5				2.5 \pm 0.5			
	2016-May-13	-34.7 \pm 1.4	22.2 \pm 2.8				5.1 \pm 1.0			
	2016-May-15	-35.4 \pm 0.5	23.5 \pm 1.7			2.6 \pm 0.4	3.2 \pm 0.5			5.4 \pm 0.8
	2016-May-17	-33.3 \pm 1.4	21.0 \pm 2.6				4.6 \pm 0.9			
	2016-May-24	-31.5 \pm 1.4	22.2 \pm 2.0				3.1 \pm 0.6			
	2016-May-31	-32.0 \pm 1.5	21.9 \pm 1.7				3.7 \pm 0.7			
	2016-Jun-07	-34.7 \pm 1.5	24.0 \pm 1.6				3.4 \pm 0.6			
	2016-Jun-16	-34.9 \pm 1.6	18.5 \pm 2.3				3.7 \pm 0.7			
	2016-Dec-22	-35.3 \pm 1.1	20.1 \pm 1.2			3.3 \pm 0.5	6.6 \pm 1.0	7.8 \pm 1.2	9.7 \pm 1.5	7.5 \pm 1.1
	2017-Jan-03	-34.4 \pm 0.9	17.9 \pm 1.5						8.0 \pm 1.4	8.9 \pm 1.3
	2017-Jan-07	-35.6 \pm 1.2	20.4 \pm 1.5				3.7 \pm 0.6	5.3 \pm 0.8	6.6 \pm 1.5	7.0 \pm 1.0
	2017-Jan-14	-33.6 \pm 1.5	19.6 \pm 1.9				3.1 \pm 0.5			
	2017-Jan-23	-34.7 \pm 0.7	20.6 \pm 1.5				5.0 \pm 0.7			
	2017-Jan-30	-36.5 \pm 1.5	19.1 \pm 2.3				3.2 \pm 0.6			
	2017-Feb-06	-35.6 \pm 1.0	19.2 \pm 0.6				3.5 \pm 0.5	4.5 \pm 0.7	4.7 \pm 0.7	7.3 \pm 1.1
	2017-Apr-02	-31.5 \pm 1.2	19.7 \pm 1.3				2.1 \pm 0.4			
	2017-Apr-04	-34.4 \pm 1.3	21.0 \pm 2.6				4.1 \pm 0.7			
	2017-May-11	-33.1 \pm 1.3	20.3 \pm 1.3				3.2 \pm 0.5			
	2017-May-27	-34.4 \pm 0.8	24.7 \pm 0.8		1.1 \pm 0.2	2.1 \pm 0.3	3.5 \pm 0.5	7.0 \pm 1.2	9.8 \pm 2.4	8.3 \pm 1.2
	2017-Jun-03	-34.0 \pm 1.4	22.6 \pm 1.6				2.5 \pm 0.4			
	2017-Jul-05	-34.7 \pm 1.5	21.3 \pm 1.9				3.5 \pm 0.6			
	2017-Jul-21	-35.8 \pm 0.5	25.7 \pm 0.7				6.6 \pm 1.2	7.9 \pm 1.2		8.3 \pm 1.2
	2017-Dec-11	-33.9 \pm 0.4	20.6 \pm 0.3				4.5 \pm 0.7			
	2018-Jan-17	-33.8 \pm 0.7	19.6 \pm 0.8				4.7 \pm 0.7			
	2018-Jan-19	-36.0 \pm 0.3	16.8 \pm 0.0				5.7 \pm 0.9			9.1 \pm 1.4
	2018-May-07	-35.8 \pm 1.3	22.0 \pm 2.0				3.0 \pm 0.5			
	2018-Jun-06	-31.0 \pm 1.2	19.7 \pm 1.3				2.4 \pm 0.4			
	2018-Jun-15	-32.5 \pm 1.3	20.0 \pm 1.3				2.9 \pm 0.4			
	2018-Jun-22	-30.1 \pm 1.2	17.9 \pm 1.3				3.0 \pm 0.5			
	2018-Jul-01	-33.1 \pm 1.3	21.3 \pm 1.5				5.3 \pm 0.8			
	Average	-34.4	21.0							
Kanehekili Fluctus	2014-Jan-20	-17.3 \pm 0.7	32.3 \pm 1.1				1.5 \pm 0.4			3.3 \pm 0.5
	2014-Oct-30	-19.1 \pm 1.2	30.9 \pm 0.7				1.0 \pm 0.4			1.5 \pm 0.2
	2015-Jan-16	-16.6 \pm 1.8	31.3 \pm 2.3							1.4 \pm 0.7
	2015-Apr-02	-15.7 \pm 0.8	34.4 \pm 1.9							1.4 \pm 0.5
	2015-Apr-04	-17.6 \pm 0.9	35.2 \pm 0.5				1.0 \pm 0.5			2.0 \pm 0.3
	2015-Apr-29	-15.2 \pm 1.0	36.5 \pm 1.2							1.4 \pm 0.5
	2015-Jun-05	-16.1 \pm 1.5	34.5 \pm 0.6							1.3 \pm 0.4
	2017-May-27	-17.7 \pm 0.8	34.5 \pm 0.3					1.7 \pm 0.3	2.4 \pm 0.6	
	Average	-17.0	34.5							
Janus Patera	2013-Sep-02	-4.5 \pm 1.4	37.0 \pm 1.4				5.0 \pm 0.7			
	2013-Sep-04	-4.4 \pm 1.7	36.2 \pm 2.4				4.6 \pm 0.8			
	2013-Sep-07	-4.6 \pm 1.4	37.3 \pm 3.5				11 \pm 2			
	2013-Sep-09	-5.0 \pm 1.3	36.5 \pm 1.4				5.2 \pm 0.8			
	2013-Nov-26	-4.8 \pm 1.1	37.9 \pm 1.1				3.5 \pm 0.5			
	2013-Dec-03	-4.0 \pm 1.0	37.7 \pm 1.1				6.1 \pm 1.1			
	2013-Dec-05	-4.4 \pm 1.7	38.0 \pm 2.4				2.5 \pm 1.2			
	2013-Dec-12	-5.3 \pm 1.8	34.1 \pm 2.3				3.9 \pm 0.6			
	2014-Jan-20	-4.8 \pm 0.5	38.0 \pm 0.7		3.5 \pm 0.5	4.2 \pm 0.6	4.4 \pm 0.7			4.7 \pm 0.7
	2014-Mar-07	-3.7 \pm 1.1	39.7 \pm 1.1				3.0 \pm 0.5			
	2014-Mar-14	-3.9 \pm 1.2	39.0 \pm 1.2				3.6 \pm 0.5			
	2014-Oct-09	-3.8 \pm 1.6	39.6 \pm 2.4				5.3 \pm 1.0			
	2014-Oct-23	-3.2 \pm 1.3	40.5 \pm 1.4				4.1 \pm 0.6			
	2014-Oct-30	-4.8 \pm 0.4	36.6 \pm 0.4				5.1 \pm 0.8			4.8 \pm 0.7
	2014-Nov-27	-4.3 \pm 1.2	39.2 \pm 3.4				8.4 \pm 4.2			
	2014-Nov-29	-4.3 \pm 1.2	37.4 \pm 1.3				4.6 \pm 0.7			
	2014-Dec-01	-4.8 \pm 1.8	37.8 \pm 2.3				3.7 \pm 0.7			
	2014-Dec-08	-5.0 \pm 1.2	35.6 \pm 1.2				5.1 \pm 0.8			
	2014-Dec-15	-5.4 \pm 1.1	36.9 \pm 1.1				4.7 \pm 0.7			
	2015-Jan-12	-4.8 \pm 0.6	34.6 \pm 1.5			5.0 \pm 0.7	6.0 \pm 0.9			5.7 \pm 0.9
	2015-Jan-16	-4.5 \pm 0.4	37.0 \pm 0.8				3.9 \pm 0.6			4.5 \pm 0.7

Table A.2 continued on next page

Table A.2 (continued)

Hot Spot	Date	Lat	Lon	K-cont	H ₂ O	PAH	L'	Br α -cont	Br α	Ms
				$\lambda = 2.27 \mu\text{m}$	$3.06 \mu\text{m}$	$3.29 \mu\text{m}$	$3.78 \mu\text{m}$	$3.99 \mu\text{m}$	$4.05 \mu\text{m}$	$4.67 \mu\text{m}$
	[UT]	[°N]	[°W]				[GW/ $\mu\text{m}/\text{sr}$]			
	2015-Mar-26	-3.7±1.1	38.5±1.2				4.5±0.7			
	2015-Mar-28	-4.9±1.1	41.3±1.1				3.9±0.6			
	2015-Apr-02	-4.4±0.6	40.8±1.3				4.5±1.2			4.4±0.7
	2015-Apr-04	-4.1±0.4	40.9±0.5				5.9±0.9			5.7±0.9
	2015-Apr-06	-3.6±1.9	40.3±2.2				3.2±0.5			
	2015-Apr-20	-5.5±1.2	39.8±1.2				4.3±0.6			
	2015-Apr-27	-4.6±1.2	41.8±1.3				5.3±0.8			
	2015-Apr-29	-4.4±0.5	39.5±0.8				2.2±0.3			2.2±0.3
	2015-Jun-05	-2.8±0.5	38.7±0.7			2.1±0.3	3.4±0.5			3.3±0.5
	2015-Dec-22	-3.5±0.7	36.5±2.0				5.0±2.5			7.4±1.3
	2015-Dec-25	-3.6±0.9	37.3±2.0				7.5±1.5			6.5±1.0
	2016-Feb-04	-5.8±1.1	38.0±1.3				3.6±0.7			
	2016-Feb-11	-5.1±1.1	33.7±1.1				3.9±0.7			
	2016-Feb-18	-1.6±1.1	34.8±1.1				3.5±0.7			
	2016-Feb-20	-0.7±1.1	37.2±1.1				4.1±0.8			
	2016-Mar-12	-2.5±1.1	36.1±2.3				6.9±1.4			
	2016-Mar-14	-1.6±1.1	35.8±1.1				3.2±0.6			
	2016-May-01	-1.3±1.2	37.1±1.2				4.3±0.8			
	2016-May-08	-2.0±1.2	40.4±1.2				6.4±1.2			
	2016-May-10	-1.4±1.2	38.1±1.5				3.2±0.6			
	2016-May-13	-2.6±1.2	36.4±2.2				6.4±1.2			
	2016-May-15	-6.1±0.7	39.5±0.8			5.0±0.7	4.9±0.7			5.1±0.8
	2016-May-17	-2.4±1.2	39.9±1.3				3.5±0.7			
	2016-May-24	-1.0±1.2	38.7±1.3				4.7±0.9			
	2016-May-31	-1.0±1.3	36.4±1.3				4.4±0.8			
	2016-Jun-02	-1.0±1.3	33.3±1.8				3.0±0.6			
	2016-Jun-07	-2.8±1.3	39.3±1.3				4.5±0.8			
	2016-Jun-09	-3.0±1.3	39.8±1.4				2.8±0.5			
	2016-Jun-16	-4.2±1.3	36.4±1.4				3.2±0.6			
	2016-Nov-22	-2.9±1.5	35.5±1.6				5.0±0.8			
	2016-Nov-29	-3.7±1.5	34.5±1.5				5.2±0.9			
	2016-Dec-22	-5.7±0.3	36.9±0.6			6.2±0.9	8.3±1.2	8.9±1.3	11±2	6.9±1.0
	2016-Dec-24	-3.0±1.4	39.6±2.0				8.7±1.5			
	2017-Jan-07	-5.1±0.6	37.0±0.6		4.2±0.6	5.9±0.9	7.1±1.1	7.5±1.1	9.0±1.9	7.1±1.1
	2017-Jan-14	-0.5±1.3	34.4±1.3				5.3±0.9			
	2017-Jan-23	-5.4±0.8	38.3±0.3		3.0±0.5	4.5±0.7	5.7±0.9			
	2017-Jan-30	-3.1±1.2	35.7±1.3				5.4±0.9			
	2017-Feb-06	-5.0±0.6	35.7±1.1		3.3±0.5		5.1±0.8	6.3±0.9	6.1±0.9	6.6±1.0
	2017-Feb-24	-1.2±1.2	34.2±1.3				3.1±0.5			
	2017-Apr-02	-2.3±1.1	36.3±1.1				3.2±0.5			
	2017-Apr-04	-1.9±1.1	36.5±1.2				3.5±0.6			
	2017-May-04	-1.5±1.1	39.2±1.2				3.0±0.5			
	2017-May-06	-1.3±1.1	37.9±1.4				5.8±1.0			
	2017-May-11	-0.7±1.1	35.9±1.1				3.3±0.6			
	2017-May-22	-1.4±1.2	38.6±1.6				4.9±0.8			
	2017-May-27	-4.8±0.5	40.6±0.8		2.6±0.4	3.9±0.7	3.9±0.6	7.3±1.2	9.6±2.3	5.9±0.9
	2017-May-29	-2.5±1.2	37.1±1.4				5.5±0.9			
	2017-Jun-03	-1.0±1.2	38.8±1.2				3.7±0.6			
	2017-Jun-28	-4.8±1.3	39.9±1.3				4.4±0.7			
	2017-Jul-05	-2.3±1.3	39.4±1.3				5.4±0.9			
	2017-Jul-21	-6.6±0.6	40.0±0.6		2.9±0.4	5.0±0.8	8.6±1.5	8.3±1.3		7.6±1.1
	2017-Jul-23	-5.1±0.6	41.5±1.2						6.9±1.0	
	2017-Dec-11	-5.5±0.3	37.4±0.3				3.6±0.5			
	2017-Dec-13	-5.5±1.0	38.0±0.2				6.4±1.0			8.0±1.2
	2018-Jan-17	-4.3±0.6	36.2±0.7				3.3±0.5			
	2018-Jan-19	-5.3±0.2	36.0±0.8			6.1±0.9	6.3±1.0			7.1±1.1
	2018-Mar-15	-1.2±1.2	34.7±1.8				5.3±0.9			
	2018-May-07	-3.9±1.1	37.9±1.1				3.2±0.5			
	2018-Jun-06	-4.2±1.1	37.4±1.2				4.3±0.6			
	2018-Jun-15	-0.5±1.1	36.5±1.2				4.7±0.7			
	2018-Jun-17	-2.6±1.1	36.5±1.2				3.5±0.5			
	2018-Jun-22	-0.9±1.1	37.4±1.2				3.6±0.5			
	2018-Jul-01	-3.3±1.1	37.0±1.2				4.0±0.6			

Table A.2 continued on next page

Table A.2 (continued)

Hot Spot	Date	Lat	Lon	K-cont	H ₂ O	PAH	L'	Br α -cont	Br α	Ms
				$\lambda = 2.27 \mu\text{m}$	$3.06 \mu\text{m}$	$3.29 \mu\text{m}$	$3.78 \mu\text{m}$	$3.99 \mu\text{m}$	$4.05 \mu\text{m}$	$4.67 \mu\text{m}$
	[UT]	[°N]	[°W]				[GW/ $\mu\text{m}/\text{sr}$]			
	Average	-3.9	37.4							
UP 38W	2018-Jan-19	-25.3 \pm 0.7	37.7 \pm 0.9							1.9 \pm 0.3
	Average	-25.3	37.7							
Pfu374	2014-Jan-20	-23.7 \pm 1.0	47.7 \pm 0.5							1.3 \pm 0.4
	2015-Jan-16	-25.7 \pm 0.7	49.7 \pm 0.7							0.94 \pm 0.47
	2015-Apr-29	-24.3 \pm 0.5	52.4 \pm 1.5							1.0 \pm 0.4
	Average	-24.3	49.7							
Masubi	2014-Jan-20	-42.9 \pm 0.7	52.5 \pm 1.3				2.4 \pm 0.4			3.4 \pm 0.5
	2015-Jan-16	-42.5 \pm 1.5	54.9 \pm 1.4				2.9 \pm 0.4			3.1 \pm 0.5
	2015-Apr-04	-41.4 \pm 1.6	56.5 \pm 2.4							2.5 \pm 0.4
	2015-Apr-29	-41.6 \pm 1.2	56.8 \pm 0.9				2.7 \pm 0.4			2.9 \pm 0.4
	2015-Jun-05	-42.7 \pm 1.3	54.8 \pm 1.6							3.0 \pm 0.5
	2016-Dec-22	-44.1 \pm 0.8	50.8 \pm 1.0							2.5 \pm 0.4
	2017-Jan-07	-45.2 \pm 0.9	51.6 \pm 0.4						3.4 \pm 0.5	3.0 \pm 0.5
	2017-Feb-06	-45.4 \pm 0.9	52.0 \pm 0.8				1.7 \pm 0.3	2.2 \pm 0.3	1.6 \pm 0.2	2.8 \pm 0.4
	2018-Jan-19	-43.7 \pm 0.8	53.7 \pm 1.0							3.0 \pm 0.4
	Average	-42.9	53.7							
PFd1691	2016-May-01	12.2 \pm 1.2	57.2 \pm 1.3				3.9 \pm 0.7			
	2016-May-03	15.0 \pm 1.2	60.7 \pm 1.6				4.3 \pm 0.8			
	2016-May-08	11.9 \pm 1.2	58.8 \pm 1.6				3.6 \pm 0.7			
	2016-May-10	14.7 \pm 1.3	56.8 \pm 1.4				3.7 \pm 0.7			
	2016-May-15	8.6 \pm 0.7	61.0 \pm 0.3				2.8 \pm 0.5			4.4 \pm 0.7
	2016-May-17	10.6 \pm 1.2	58.5 \pm 1.2				3.3 \pm 0.6			
	2016-May-24	13.5 \pm 1.3	59.2 \pm 1.4				2.6 \pm 0.5			
	2016-May-31	12.8 \pm 1.3	55.1 \pm 1.5				2.5 \pm 0.5			
	2016-Jun-02	7.6 \pm 1.3	54.6 \pm 1.5				2.5 \pm 0.5			
	2016-Jun-07	10.2 \pm 1.3	58.8 \pm 1.7				2.6 \pm 0.5			
	2016-Jun-09	10.4 \pm 1.3	59.2 \pm 1.3				2.3 \pm 0.4			
	2016-Jun-16	6.7 \pm 1.3	54.5 \pm 1.4				1.6 \pm 0.3			
	2016-Dec-22	7.1 \pm 0.6	56.9 \pm 0.3				2.2 \pm 0.3	2.5 \pm 0.4	2.7 \pm 0.4	2.6 \pm 0.4
	2017-Jan-07	8.4 \pm 0.7	57.2 \pm 1.4				2.0 \pm 0.3	2.0 \pm 0.3	2.1 \pm 0.5	2.6 \pm 0.4
	2017-Jan-23	10.5 \pm 0.6	60.5 \pm 0.6				1.9 \pm 0.3			
	2017-Feb-06	8.8 \pm 0.3	57.4 \pm 0.7				1.3 \pm 0.2	1.2 \pm 0.2	1.2 \pm 0.2	1.9 \pm 0.3
	2017-May-27	9.9 \pm 0.8	61.7 \pm 0.1				1.5 \pm 0.2	2.7 \pm 0.5	3.0 \pm 0.7	2.6 \pm 0.4
	2017-Jul-21	7.6 \pm 0.6	61.6 \pm 0.6				1.8 \pm 0.3			
	2017-Jul-23	8.7 \pm 0.6	60.1 \pm 0.1				1.9 \pm 0.3		2.1 \pm 0.3	
	2017-Dec-11	8.3 \pm 1.3	57.2 \pm 0.0				2.4 \pm 0.4			
	2018-Jan-17	8.3 \pm 0.6	54.4 \pm 0.9				3.0 \pm 0.5			
	2018-Jan-19	8.5 \pm 0.6	58.0 \pm 0.9				2.4 \pm 0.4			2.3 \pm 0.3
	Average	9.4	58.3			2.8 \pm 0.4				
Laki-Oi Patera	2016-May-15	-46.4 \pm 0.8	60.7 \pm 1.5							4.0 \pm 0.6
	2017-May-27	-43.9 \pm 0.6	57.5 \pm 1.1					3.8 \pm 0.6	4.8 \pm 1.2	5.1 \pm 0.8
	2017-Jul-21	-45.2 \pm 2.3	58.6 \pm 0.9				2.7 \pm 0.5	3.3 \pm 0.5		4.0 \pm 0.6
	2017-Jul-23	-42.0 \pm 0.8	62.5 \pm 1.5						2.8 \pm 0.4	
	Average	-44.6	59.7							
Shamshu Patera	2017-May-27	-8.3 \pm 0.2	61.5 \pm 2.0						2.2 \pm 0.5	1.2 \pm 0.2
	Average	-8.3	61.5							
Tejeto Patera	2016-May-01	-44.0 \pm 1.6	65.9 \pm 2.4				4.4 \pm 0.9			
	2016-May-03	-42.6 \pm 1.5	71.5 \pm 2.2				5.5 \pm 1.1			
	2016-May-10	-42.1 \pm 1.6	68.4 \pm 1.8				3.6 \pm 0.7			
	2016-May-17	-43.1 \pm 1.6	68.9 \pm 2.0				4.2 \pm 0.8			
	Average	-42.9	68.7							
Chalybes Regio	2013-Sep-02	52.0 \pm 2.2	63.4 \pm 4.3				8.1 \pm 1.7			
	2013-Nov-26	54.5 \pm 1.8	65.8 \pm 2.6				4.9 \pm 2.5			
	2013-Dec-03	56.6 \pm 1.9	69.0 \pm 6.0				8.7 \pm 4.4			
	2013-Dec-05	57.3 \pm 1.9	66.8 \pm 2.6				6.5 \pm 3.2			
	2013-Dec-12	56.3 \pm 2.0	66.5 \pm 2.2				4.8 \pm 2.4			
	2014-Jan-20	55.7 \pm 2.2	66.6 \pm 3.0		4.3 \pm 0.6	6.4 \pm 1.0	7.4 \pm 1.1			9.7 \pm 1.4
	2014-Mar-07	56.6 \pm 2.1	75.8 \pm 5.9				9.7 \pm 4.8			
	2014-Mar-11	58.4 \pm 1.7	71.8 \pm 4.7				9.0 \pm 1.9			8.2 \pm 2.2
	2014-Mar-14	51.9 \pm 1.9	68.8 \pm 5.6				8.1 \pm 4.0			
	2014-Oct-30	57.9 \pm 1.0	67.2 \pm 1.7				8.0 \pm 1.2			11 \pm 2

Table A.2 continued on next page

Table A.2 (continued)

Hot Spot	Date	Lat	Lon	K-cont	H ₂ O	PAH	L'	Br α -cont	Br α	Ms
				$\lambda = 2.27 \mu\text{m}$	$3.06 \mu\text{m}$	$3.29 \mu\text{m}$	$3.78 \mu\text{m}$	$3.99 \mu\text{m}$	$4.05 \mu\text{m}$	$4.67 \mu\text{m}$
	[UT]	[°N]	[°W]				[GW/ $\mu\text{m}/\text{sr}$]			
	2014-Dec-15	54.8±2.1	65.4±3.9				6.1±3.0			
	2015-Jan-16	55.6±1.1	64.8±1.3				4.5±0.7			7.7±1.2
	2015-Mar-26	57.2±2.2	72.3±7.0				9.4±4.7			
	2015-Mar-28	55.1±2.1	75.7±4.9				7.0±3.5			
	2015-Apr-01	56.1±0.8	77.5±2.8							6.2±0.9
	2015-Apr-04	54.9±0.9	68.0±1.9				7.2±1.1			11±2
	2015-Apr-06	56.9±2.2	75.1±2.6				5.8±2.9			
	2015-Apr-20	54.0±2.1	73.2±4.9				9.9±1.8			
	2015-Apr-27	51.0±2.0	67.5±5.8				7.5±3.8			
	2015-Apr-29	55.4±1.5	70.1±1.5			4.0±0.6	5.0±0.8			7.9±1.2
	2015-Jun-05	55.0±1.0	68.5±1.9			9.5±1.4	8.7±1.3			11±2
	2015-Dec-22	59.3±1.4	57.6±2.8				6.0±3.0			14±2
	2016-Feb-04	54.9±2.1	67.2±2.2				6.9±1.4			
	2016-Feb-11	54.4±2.1	61.4±3.1				6.4±1.3			
	2016-Feb-20	61.2±2.6	71.8±4.7				7.3±1.6			
	2016-Mar-14	57.3±2.3	62.1±5.5				7.9±1.8			
	2016-May-01	59.9±2.7	71.4±5.6				7.8±1.8			
	2016-May-03	63.0±3.0	68.2±4.9				14±3			
	2016-May-08	59.7±2.8	72.5±9.1				11±3			
	2016-May-10	59.8±2.7	69.2±2.8				8.0±1.7			
	2016-May-15	50.7±0.8	65.9±1.4			7.8±1.2	6.0±1.2			9.6±1.4
	2016-May-17	62.1±3.0	70.5±4.1				10±2			
	2016-May-24	61.2±3.0	71.4±6.1				11±3			
	2016-May-31	56.1±2.6	63.3±5.2				8.3±1.8			
	2016-Jun-02	59.6±2.9	65.9±3.3				10±2			
	2016-Jun-07	57.8±2.9	71.2±9.3				9.9±3.0			
	2016-Jun-09	58.4±2.8	74.7±4.0				9.6±2.0			
	2016-Jun-16	53.2±2.4	63.0±3.7				8.1±1.7			
	2016-Jun-25	56.2±2.7	73.9±2.5				11±2			
	2016-Nov-22	57.2±3.2	64.7±4.0				17±3			
	2016-Nov-24	50.1±2.6	70.9±4.3				12±3			
	2016-Nov-29	54.9±3.0	63.7±5.4				14±3			
	2016-Dec-22	49.0±1.4	63.4±1.6			10±2	9.3±1.4	10.0±1.5	10±2	11±2
	2016-Dec-24	54.5±2.7	70.3±3.2				11±2			
	2017-Jan-04	50.8±1.2	80.0±4.2							6.9±1.5
	2017-Jan-07	50.9±1.9	64.2±3.8			9.2±1.4	6.9±1.0	8.2±1.2	8.0±1.7	9.8±1.6
	2017-Jan-09	56.8±2.9	66.0±5.1				13±3			
	2017-Jan-14	61.2±3.4	66.5±7.9				14±4			
	2017-Jan-23	50.8±1.7	74.3±0.4		7.4±1.1	7.9±1.2	9.9±1.5			
	2017-Jan-25	57.8±3.2	63.3±7.8				12±5			
	2017-Jan-30	55.3±2.5	66.4±3.7				12±2			
	2017-Feb-06	50.6±1.3	64.6±2.8		3.6±0.5		6.0±0.9	7.0±1.1	7.2±1.1	11±2
	2017-Feb-24	58.4±2.5	62.4±2.4				10±2			
	2017-Mar-05	54.8±2.3	70.1±3.5				10±2			
	2017-Apr-02	54.9±2.3	66.4±6.0				8.1±1.8			
	2017-Apr-04	56.6±2.2	70.5±2.3				11±2			
	2017-May-04	54.4±2.1	76.1±2.8				8.7±1.6			
	2017-May-06	57.3±2.3	73.5±2.1				12±2			
	2017-May-11	59.5±3.0	74.4±13.0				13±5			
	2017-May-22	54.4±2.2	76.9±2.2				13±2			
	2017-May-27	51.3±1.2	72.1±3.6		8.9±1.3	7.8±1.4	11±2	14±3	21±6	16±2
	2017-May-29	53.3±2.2	73.0±2.3				13±2			
	2017-May-31	56.7±2.9	62.3±7.9				15±7			
	2017-Jun-03	59.1±2.9	75.3±9.6				13±4			
	2017-Jun-16	50.9±1.0	84.8±2.4				10±2			
	2017-Jun-28	52.8±2.4	70.2±3.4				8.3±1.5			
	2017-Jun-30	57.4±2.8	72.3±4.5				14±3			
	2017-Jul-05	57.0±2.9	71.9±7.0				10±2			
	2017-Jul-07	59.3±3.0	66.1±3.9				15±3			
	2017-Jul-21	46.8±1.7	75.6±1.1			6.7±1.0	7.5±1.3			13±2
	2017-Jul-23	48.3±0.7	78.8±1.4			7.9±1.2	7.6±1.1	9.6±1.4	14±2	16±2
	2017-Dec-11	46.4±0.7	72.7±0.2				10±2			
	2017-Dec-13	49.0±0.3	77.0±0.8				10±2			17±3

Table A.2 continued on next page

Table A.2 (continued)

Hot Spot	Date	Lat	Lon	K-cont	H ₂ O	PAH	L'	Bra-cont	Bra α	Ms
				$\lambda = 2.27 \mu\text{m}$	$3.06 \mu\text{m}$	$3.29 \mu\text{m}$	$3.78 \mu\text{m}$	$3.99 \mu\text{m}$	$4.05 \mu\text{m}$	$4.67 \mu\text{m}$
	[UT]	[°N]	[°W]				[GW/ $\mu\text{m}/\text{sr}$]			
	2018-Jan-14	49.3 \pm 1.5	82.1 \pm 3.6				12 \pm 2		11 \pm 2	25 \pm 4
	2018-Jan-17	48.7 \pm 1.1	59.6 \pm 2.6				8.3 \pm 1.3			
	2018-Jan-19	48.9 \pm 0.8	73.7 \pm 1.6			13 \pm 2	11 \pm 2			22 \pm 3
	2018-Mar-15	54.0 \pm 2.3	71.6 \pm 2.6				10 \pm 2			
	2018-May-07	55.5 \pm 2.3	79.9 \pm 4.3				9.5 \pm 1.9			
	2018-Jun-17	50.3 \pm 2.0	77.8 \pm 2.7				12 \pm 2			
	2018-Jul-12	60.5 \pm 3.1	69.8 \pm 5.9				18 \pm 5			
	Average	55.4	70.2							
Zal Patera	2013-Nov-26	38.8 \pm 1.7	71.6 \pm 2.4				1.5 \pm 0.7			
	2013-Nov-28	37.8 \pm 1.6	72.6 \pm 2.4				4.0 \pm 2.0			
	2013-Dec-05	41.2 \pm 1.9	72.3 \pm 2.2				1.8 \pm 0.9			
	2013-Dec-12	39.3 \pm 2.0	72.3 \pm 2.1				1.4 \pm 0.7			
	2014-Jan-20	37.6 \pm 0.8	73.6 \pm 1.0				2.7 \pm 0.6			5.0 \pm 0.7
	2014-Oct-30	37.0 \pm 1.8	76.6 \pm 2.3							4.2 \pm 0.6
	2014-Dec-01	38.6 \pm 2.0	73.5 \pm 2.1				2.8 \pm 1.4			
	2014-Dec-08	37.3 \pm 1.7	69.8 \pm 2.4				4.6 \pm 0.7			
	2014-Dec-10	41.3 \pm 1.6	71.1 \pm 2.4				3.7 \pm 1.8			
	2014-Dec-15	40.7 \pm 1.5	71.1 \pm 2.7				3.2 \pm 1.6			
	2015-Jan-11	37.6 \pm 1.0	78.6 \pm 2.8							6.2 \pm 0.9
	2015-Jan-16	38.4 \pm 1.1	73.8 \pm 1.1				2.2 \pm 0.3			5.0 \pm 0.7
	2015-Mar-28	36.5 \pm 1.4	78.7 \pm 2.7				2.6 \pm 1.3			
	2015-Apr-01	38.5 \pm 0.7	77.3 \pm 1.9							4.7 \pm 0.7
	2015-Apr-04	36.7 \pm 1.3	78.5 \pm 2.6							5.5 \pm 0.8
	2015-Apr-20	38.3 \pm 1.6	73.4 \pm 2.8				4.5 \pm 2.3			
	2015-Apr-22	35.4 \pm 2.0	78.7 \pm 2.2				3.2 \pm 0.5			
	2015-Apr-29	39.5 \pm 0.8	75.6 \pm 0.8				2.8 \pm 0.6			5.0 \pm 0.8
	2015-Jun-05	37.9 \pm 1.3	74.9 \pm 1.6							3.2 \pm 0.5
	2016-Dec-22	33.4 \pm 0.8	74.3 \pm 1.3							2.4 \pm 0.4
	2017-Jan-07	34.2 \pm 0.7	76.4 \pm 1.0							1.7 \pm 0.2
	2017-May-27	36.6 \pm 1.7	76.2 \pm 1.6						4.9 \pm 1.2	3.9 \pm 0.6
	2017-Jul-21	38.0 \pm 1.1	76.8 \pm 0.4				4.7 \pm 0.8	7.4 \pm 1.1		
	2017-Jul-23	34.2 \pm 0.8	79.1 \pm 0.9				1.9 \pm 0.3			
	Average	37.9	74.6							
Tawhaki Patera	2013-Aug-21	3.6 \pm 0.6	78.1 \pm 0.8							2.0 \pm 0.3
	2013-Dec-05	2.5 \pm 1.0	73.4 \pm 1.0				1.0 \pm 0.5			
	2013-Dec-12	2.5 \pm 1.0	74.4 \pm 1.0				1.2 \pm 0.6			
	2013-Dec-14	2.8 \pm 1.7	75.1 \pm 2.4				1.9 \pm 1.0			
	2014-Jan-20	2.1 \pm 0.6	74.1 \pm 0.9				1.6 \pm 0.2			2.0 \pm 0.5
	2014-Mar-11	3.7 \pm 0.9	75.1 \pm 1.8				4.5 \pm 0.7			3.5 \pm 0.5
	2015-Jan-11	2.7 \pm 0.8	74.8 \pm 1.9				4.6 \pm 2.3			3.9 \pm 0.6
	2015-Jan-16	4.2 \pm 0.6	76.3 \pm 0.6							1.4 \pm 0.7
	2015-Apr-01	3.7 \pm 0.6	76.5 \pm 1.3				3.5 \pm 1.2			3.4 \pm 0.5
	2015-Apr-29	3.1 \pm 0.5	76.8 \pm 0.6			1.5 \pm 0.2	1.7 \pm 0.4			2.0 \pm 0.3
	2015-Jun-05	4.3 \pm 1.3	77.2 \pm 1.6				1.9 \pm 0.3			
	2016-May-15	1.5 \pm 0.5	75.6 \pm 0.6				1.1 \pm 0.2			
	2017-Jan-07	1.6 \pm 0.8	73.8 \pm 1.6				1.3 \pm 0.2		2.0 \pm 0.3	1.3 \pm 0.2
	2017-Jan-23	1.6 \pm 1.0	75.6 \pm 0.2		1.9 \pm 0.3	2.8 \pm 0.4	3.2 \pm 0.5			
	2017-Feb-06	1.5 \pm 1.7	72.3 \pm 0.8						1.0 \pm 0.2	1.0 \pm 0.15
	2017-Jul-21	1.1 \pm 0.3	76.7 \pm 0.9				1.4 \pm 0.3	1.8 \pm 0.3		
	2017-Jul-23	1.7 \pm 0.3	77.4 \pm 0.8				1.5 \pm 0.2	1.7 \pm 0.3		
	2018-Jan-14	1.0 \pm 0.6	79.6 \pm 0.9						2.2 \pm 0.3	
	2018-Jan-19	0.7 \pm 0.6	73.7 \pm 0.1				1.4 \pm 0.2			1.3 \pm 0.2
	Average	2.5	75.6							
Ekhi Patera	2017-Jul-23	-28.4 \pm 1.1	86.7 \pm 1.4		3.2 \pm 0.5	3.8 \pm 0.6	3.9 \pm 0.6	3.8 \pm 0.6	4.5 \pm 0.7	3.8 \pm 0.6
	Average	-28.4	86.7							
Gish Bar	2013-Nov-26	14.5 \pm 1.7	87.9 \pm 2.4				2.9 \pm 1.4			
	2013-Nov-28	15.7 \pm 1.1	87.0 \pm 1.2				2.2 \pm 1.1			
	2013-Dec-03	15.4 \pm 1.1	90.2 \pm 3.5				7.4 \pm 3.7			
	2013-Dec-05	15.8 \pm 1.1	87.3 \pm 1.1				2.4 \pm 1.2			
	2013-Dec-12	14.5 \pm 1.1	86.1 \pm 1.2				1.8 \pm 0.9			
	2014-Jan-20	15.2 \pm 0.5	89.5 \pm 0.9				3.3 \pm 1.3			5.5 \pm 0.9
	2014-Mar-11	16.1 \pm 1.1	90.5 \pm 1.7				1.9 \pm 0.3			2.0 \pm 0.3
	2015-Jan-11	14.5 \pm 1.0	89.3 \pm 1.8				5.4 \pm 0.8			4.9 \pm 0.7

Table A.2 continued on next page

Table A.2 (continued)

Hot Spot	Date	Lat	Lon	K-cont	H ₂ O	PAH	L'	Bra-cont	Bra α	Ms
				$\lambda = 2.27 \mu\text{m}$	$3.06 \mu\text{m}$	$3.29 \mu\text{m}$	$3.78 \mu\text{m}$	$3.99 \mu\text{m}$	$4.05 \mu\text{m}$	$4.67 \mu\text{m}$
	[UT]	[°N]	[°W]				[GW/ $\mu\text{m}/\text{sr}$]			
	2015-Jan-13	14.2 \pm 1.5	89.6 \pm 2.5				3.8 \pm 1.9			
	2015-Jan-16	14.7 \pm 0.6	88.7 \pm 0.4				5.4 \pm 0.8			7.9 \pm 1.2
	2015-Apr-01	16.1 \pm 1.2	91.9 \pm 1.2				1.3 \pm 0.5			2.0 \pm 0.3
	2015-Apr-04	15.9 \pm 1.3	90.7 \pm 2.6				4.9 \pm 2.4			
	2015-Apr-29	15.2 \pm 0.3	89.8 \pm 0.7				0.85 \pm 0.32			1.4 \pm 0.5
	2016-Feb-20	20.1 \pm 1.2	89.0 \pm 1.9				5.8 \pm 1.1			
	2017-Jan-07	15.5 \pm 0.6	82.6 \pm 0.8						1.9 \pm 0.3	
	2017-Feb-06	16.2 \pm 0.1	86.4 \pm 1.7						1.5 \pm 0.2	2.8 \pm 0.4
	2017-Jul-23	16.1 \pm 0.6	89.6 \pm 1.1						2.2 \pm 0.3	
	2018-Mar-15	16.9 \pm 1.2	88.2 \pm 1.2				1.9 \pm 0.3			
	Average	15.6	89.1							
Aluna Patera	2015-Jan-11	41.5 \pm 1.3	91.6 \pm 2.6							4.6 \pm 0.7
	2015-Jan-16	42.0 \pm 2.2	88.7 \pm 2.0							1.8 \pm 0.3
	Average	41.7	90.1							
P207	2013-Aug-21	-36.5 \pm 1.2	91.1 \pm 0.8				5.0 \pm 1.2			8.0 \pm 1.2
	Average	-36.5	91.1							
Shango Patera	2013-Aug-21	33.5 \pm 0.7	100.0 \pm 0.9							2.2 \pm 0.3
	2014-Jan-20	32.0 \pm 1.1	92.9 \pm 1.7							2.6 \pm 0.5
	2015-Apr-29	34.2 \pm 1.5	95.6 \pm 1.4							0.85 \pm 0.39
	Average	33.5	95.6							
Itzamna Patera	2015-Jan-11	-13.2 \pm 1.0	98.7 \pm 1.2				2.7 \pm 0.4			2.7 \pm 0.4
	2015-Jan-16	-14.4 \pm 0.4	98.0 \pm 0.5				1.3 \pm 0.6			1.4 \pm 0.7
	2015-Apr-01	-14.4 \pm 0.8	100.6 \pm 0.9				1.1 \pm 0.4			1.0 \pm 0.4
	2015-Apr-29	-15.0 \pm 0.5	99.0 \pm 1.0				1.5 \pm 0.3			1.3 \pm 0.5
	2017-Jul-21	-17.6 \pm 0.6	104.3 \pm 1.3					3.7 \pm 0.6		
	2017-Jul-23	-14.0 \pm 0.9	99.2 \pm 1.1				1.7 \pm 0.3	1.9 \pm 0.3	2.6 \pm 0.4	1.7 \pm 0.3
	2017-Dec-31	-18.4 \pm 0.7	94.7 \pm 1.9						3.0 \pm 0.4	
	2018-Jan-14	-15.5 \pm 0.6	100.1 \pm 0.8						1.9 \pm 0.3	
	2018-Jan-19	-16.8 \pm 0.6	94.8 \pm 0.9				1.6 \pm 0.2			
	Average	-15.0	99.0							
Arusha Patera	2017-Dec-13	-39.2 \pm 2.1	99.6 \pm 0.6				3.4 \pm 0.5			7.3 \pm 1.1
	2017-Dec-31	-40.5 \pm 1.2	98.4 \pm 0.7						3.9 \pm 0.6	9.9 \pm 1.5
	2018-Jan-14	-39.1 \pm 0.3	102.6 \pm 1.4				3.3 \pm 0.5		4.5 \pm 0.7	9.0 \pm 1.3
	2018-Jan-19	-39.9 \pm 1.5	96.6 \pm 1.3				3.9 \pm 0.6			6.3 \pm 0.9
	Average	-39.6	99.0							
Sigurd Patera	2014-Mar-07	-5.1 \pm 1.2	98.9 \pm 3.0				5.5 \pm 2.8			
	2014-Mar-11	-5.0 \pm 0.6	99.6 \pm 0.5				6.0 \pm 1.2			11 \pm 2
	2014-Mar-27	-7.3 \pm 1.2	100.6 \pm 1.5				4.8 \pm 0.7			
	2014-Apr-03	-5.0 \pm 1.2	100.9 \pm 1.2				3.7 \pm 0.6			
	2015-Jan-11	-5.7 \pm 0.6	97.5 \pm 0.8							2.3 \pm 0.3
	2015-Jan-16	-5.2 \pm 0.6	95.5 \pm 0.7							0.89 \pm 0.45
	2015-Apr-01	-3.5 \pm 0.4	101.5 \pm 1.1							1.1 \pm 0.4
	2015-Apr-29	-4.3 \pm 0.5	96.0 \pm 0.5							1.0 \pm 0.4
	Average	-5.1	99.2							
P197	2014-Mar-11	-44.2 \pm 1.2	110.6 \pm 1.7				3.5 \pm 0.5			1.5 \pm 0.2
	2014-Oct-09	-44.4 \pm 1.9	107.7 \pm 3.0				7.9 \pm 1.5			
	2014-Oct-25	-47.8 \pm 2.0	105.6 \pm 2.6				5.5 \pm 1.1			
	2014-Oct-27	-45.1 \pm 1.9	109.4 \pm 3.5				7.0 \pm 1.5			
	2014-Dec-01	-46.6 \pm 1.7	104.4 \pm 3.6				6.5 \pm 3.3			
	2014-Dec-10	-48.5 \pm 1.8	105.9 \pm 2.3				6.6 \pm 1.3			
	2015-Jan-11	-46.9 \pm 0.7	107.3 \pm 0.7				12 \pm 2			13 \pm 2
	2015-Jan-13	-49.2 \pm 1.6	107.4 \pm 2.7				4.6 \pm 2.3			
	2015-Jan-16	-46.9 \pm 0.9	106.8 \pm 1.4				4.9 \pm 0.7			6.9 \pm 1.0
	2015-Apr-01	-48.3 \pm 1.0	109.7 \pm 1.1				3.7 \pm 0.6			4.2 \pm 0.6
	2015-Apr-29	-44.1 \pm 1.2	103.2 \pm 1.7							2.5 \pm 0.4
	Average	-46.9	107.3							
Amirani	2013-Aug-21	21.0 \pm 1.5	114.6 \pm 1.2				2.4 \pm 0.6			3.9 \pm 0.6
	2013-Aug-23	22.4 \pm 1.4	115.9 \pm 2.6							3.9 \pm 0.6
	2013-Dec-14	19.5 \pm 1.1	112.3 \pm 1.1				2.1 \pm 1.0			
	2014-Mar-11	21.5 \pm 0.4	116.2 \pm 0.5				3.1 \pm 0.5			3.5 \pm 0.5
	2014-Dec-01	18.8 \pm 1.5	109.8 \pm 2.5				3.3 \pm 1.6			
	2014-Dec-10	20.8 \pm 1.2	112.6 \pm 1.4				2.9 \pm 1.4			

Table A.2 continued on next page

Table A.2 (continued)

Hot Spot	Date	Lat	Lon	K-cont	H ₂ O	PAH	L'	Bra-cont	Bra	Ms
				$\lambda = 2.27 \mu\text{m}$	$3.06 \mu\text{m}$	$3.29 \mu\text{m}$	$3.78 \mu\text{m}$	$3.99 \mu\text{m}$	$4.05 \mu\text{m}$	$4.67 \mu\text{m}$
	[UT]	[°N]	[°W]				[GW/ $\mu\text{m}/\text{sr}$]			
	2015-Jan-11	20.5±1.5	113.3±0.5				2.4±0.4			4.7±0.7
	2015-Jan-16	19.5±1.0	107.5±1.6				1.3±0.6			3.3±0.5
	2015-Apr-01	21.3±1.3	117.8±1.1				1.7±0.3			2.8±0.4
	2015-Apr-22	22.4±1.7	116.5±2.4				4.2±0.6			
	2015-Apr-29	20.7±0.7	113.2±1.0				2.3±0.6			4.1±0.6
	2015-Dec-22	21.6±0.6	112.5±0.5				1.9±0.3			4.8±0.7
	2016-May-03	20.5±1.3	112.0±1.5				1.5±0.3			
	2016-May-10	23.9±1.4	112.8±2.1				3.1±0.6			
	2017-Jan-04	19.7±0.6	113.3±1.9				2.6±0.4	4.1±0.6	4.0±0.6	4.0±0.6
	2017-Jan-07	18.4±1.2	109.2±0.1						4.6±0.7	6.7±1.0
	2017-Feb-05	18.3±0.9	117.4±3.8						6.3±4.4	
	2017-May-29	22.6±1.4	112.4±2.4				5.4±1.0			
	2017-Jun-16	19.6±0.6	118.3±0.6				2.1±0.3			
	2017-Jun-30	21.4±1.4	113.2±1.5				2.9±0.5			
	2017-Jul-21	15.6±0.2	110.8±0.0							6.6±1.0
	2017-Jul-23	18.9±1.0	113.3±0.9				1.8±0.3	2.8±0.4	3.3±0.5	3.3±0.5
	2017-Dec-13	17.5±0.7	109.8±0.8							3.0±0.4
	2017-Dec-31	19.0±0.0	116.3±1.8						2.6±0.4	4.8±0.7
	2018-Jan-14	18.1±1.3	114.8±0.7				1.9±0.3		3.2±0.5	5.0±0.7
	2018-Jan-19	20.2±0.7	110.5±1.3							6.5±1.0
	2018-Jul-12	20.7±1.3	109.0±1.3				2.8±0.4			
	Average	20.5	113.2							
Dusura Patera	2014-Mar-11	36.4±0.6	121.1±0.9				7.5±1.3			6.4±1.0
	2014-Mar-27	35.4±1.5	121.0±1.6				8.1±1.2			
	2014-Apr-03	36.8±1.7	124.0±2.4				6.9±1.3			
	Average	36.4	121.1							
Maui Patera	2017-Jan-20	18.6±1.4	124.9±1.6				3.1±0.5			
	2017-Jan-27	17.7±1.4	126.6±1.6				3.5±0.6			
	Average	18.2	125.8							
P95	2016-May-17	-9.7±0.4	126.2±1.4	56±11			58±13			
	2016-May-19	-10.2±1.2	129.4±1.3				15±3			
	Average	-10.0	127.8							
Malik Patera	2013-Aug-21	-32.2±0.5	127.6±1.4				3.3±0.8			3.9±0.6
	2013-Aug-23	-31.0±0.9	130.2±1.3				3.0±0.7			2.7±0.4
	2014-Mar-11	-33.6±0.6	129.9±0.6							1.3±0.6
	2015-Jan-11	-32.9±1.6	127.3±1.1				1.7±0.3			1.7±0.3
	2015-Jan-16	-33.5±0.9	125.9±1.8				6.9±1.0			6.6±1.0
	2015-Jan-22	-34.7±1.7	129.6±2.4				2.4±1.2			
	2015-Apr-01	-32.4±1.0	132.0±0.8				1.5±0.3			1.9±0.3
	2015-Apr-29	-35.1±1.2	130.3±2.7							3.2±0.5
	2018-Jan-14	-30.9±0.7	128.0±0.7						1.0±0.2	
	Average	-32.9	129.6							
UP 132W	2017-Jan-04	18.8±0.9	129.8±1.1		3.3±0.5	3.1±0.5	3.8±0.6	4.3±0.6	3.7±0.6	3.9±0.6
	2017-Feb-05	18.4±0.9	131.6±0.8				5.4±0.8			5.3±0.8
	2017-Jun-16	17.7±0.6	133.7±0.6				1.7±0.3			
	2017-Jul-23	19.9±0.7	131.0±0.9						1.7±0.2	
	2018-Jan-14	17.4±0.7	134.7±0.7						0.83±0.12	
	Average	18.4	131.6							
Thor	2015-Jan-11	41.6±2.0	133.0±2.1							1.5±0.7
	2015-Apr-01	39.5±1.5	136.4±1.4							1.2±0.4
	Average	40.6	134.7							
P123	2015-Jan-11	-42.0±1.2	138.6±1.4			2.5±0.4	2.9±0.4			2.6±0.4
	2015-Apr-01	-41.2±0.7	143.4±0.9				2.7±0.4			2.7±0.4
	2015-Dec-22	-41.8±1.1	135.4±1.3				4.6±0.7			7.8±1.2
	2016-Jan-30	-42.1±1.5	135.2±1.9				2.8±0.5			
	2016-Feb-15	-42.4±1.4	136.8±1.9				2.9±0.6			
	2016-Feb-17	-41.1±1.4	139.4±1.5				1.9±0.4			
	2016-Mar-11	-41.2±1.4	139.7±1.8				2.7±0.5			
	2017-Jan-02	-39.7±1.7	134.2±2.5				7.1±1.2			
	2017-Jan-04	-42.7±1.1	142.0±1.2		3.9±0.6	3.8±0.6	6.2±0.9	7.2±1.1	5.9±0.9	8.2±1.2
	2017-Jan-18	-39.8±1.6	136.5±2.4				5.1±0.9			
	2017-Jan-20	-39.4±1.6	138.9±1.8				5.8±1.0			

Table A.2 continued on next page

Table A.2 (continued)

Hot Spot	Date	Lat	Lon	K-cont	H ₂ O	PAH	L'	Br α -cont	Br α	Ms
				$\lambda = 2.27 \mu\text{m}$	$3.06 \mu\text{m}$	$3.29 \mu\text{m}$	$3.78 \mu\text{m}$	$3.99 \mu\text{m}$	$4.05 \mu\text{m}$	$4.67 \mu\text{m}$
	[UT]	[°N]	[°W]				[GW/ $\mu\text{m}/\text{sr}$]			
	2017-Jan-25	-42.8 \pm 1.6	134.7 \pm 2.5				8.5 \pm 1.5			
	2017-Jan-27	-40.4 \pm 1.6	139.0 \pm 1.8				5.5 \pm 0.9			
	2017-Feb-05	-43.4 \pm 0.6	141.3 \pm 0.9				8.0 \pm 1.2	7.1 \pm 1.1	5.4 \pm 0.8	10 \pm 2
	2017-Jun-16	-42.4 \pm 0.2	145.2 \pm 0.1			2.9 \pm 0.4	4.8 \pm 0.7			
	2017-Jul-23	-41.4 \pm 0.3	139.5 \pm 0.0						5.3 \pm 0.8	6.7 \pm 1.0
	2017-Dec-13	-44.7 \pm 1.3	138.2 \pm 1.0				6.5 \pm 1.0			9.0 \pm 1.3
	2017-Dec-31	-44.6 \pm 1.9	142.0 \pm 1.1				3.4 \pm 0.5		2.9 \pm 0.4	6.9 \pm 1.0
	2018-Jan-02	-42.2 \pm 0.7	143.9 \pm 2.5					5.3 \pm 0.8	3.2 \pm 0.5	7.8 \pm 1.5
	2018-Jan-14	-41.7 \pm 1.6	142.2 \pm 0.9				2.4 \pm 0.4		2.9 \pm 0.4	4.7 \pm 0.7
	Average	-41.9	139.2							
Tupan Patera	2015-Jan-11	-18.2 \pm 0.8	139.2 \pm 0.7				1.3 \pm 0.6			1.6 \pm 0.2
	2015-Apr-01	-17.7 \pm 1.0	143.7 \pm 1.0				0.85 \pm 0.3			1.3 \pm 0.4
	2015-Dec-22	-17.4 \pm 1.0	136.9 \pm 1.2				1.7 \pm 0.2			3.5 \pm 0.5
	2016-Mar-11	-15.1 \pm 1.1	139.9 \pm 1.2				0.96 \pm 0.18			
	2017-Jan-04	-18.3 \pm 0.6	140.4 \pm 1.1				2.1 \pm 0.3	2.4 \pm 0.4	2.6 \pm 0.4	2.9 \pm 0.4
	2017-Jun-16	-17.8 \pm 0.5	144.0 \pm 0.6				1.9 \pm 0.3			
	2017-Jul-23	-19.4 \pm 0.6	141.4 \pm 1.1						2.4 \pm 0.4	
	2017-Dec-31	-20.0 \pm 0.8	140.4 \pm 1.9				2.3 \pm 0.3		2.7 \pm 0.4	3.3 \pm 0.5
	2018-Jan-02	-17.1 \pm 0.7	142.2 \pm 1.7						2.6 \pm 0.4	
	2018-Jan-14	-18.4 \pm 1.3	140.7 \pm 1.0				2.1 \pm 0.3		3.7 \pm 0.6	3.3 \pm 0.5
	Average	-18.0	140.5							
Surya Patera	2015-Mar-25	21.5 \pm 1.2	148.7 \pm 1.2				2.7 \pm 1.3			
	2015-Apr-01	21.9 \pm 0.9	148.8 \pm 0.7				3.6 \pm 0.5			6.6 \pm 1.0
	2015-Apr-17	21.0 \pm 1.3	150.0 \pm 1.3				2.0 \pm 1.0			
	2015-May-05	20.6 \pm 1.0	151.1 \pm 2.8							5.0 \pm 0.8
	Average	21.2	149.4							
Shamash Patera	2016-Jun-20	-34.6 \pm 0.4	151.9 \pm 0.5	51 \pm 8			53 \pm 9			
	2016-Jun-27	-31.9 \pm 2.4	149.1 \pm 3.9	18 \pm 3			30 \pm 6			
	Average	-33.2	150.5							
Sobo Fluctus	2018-Jan-14	12.9 \pm 0.6	152.8 \pm 0.8						1.0 \pm 0.2	
	Average	12.9	152.8							
Prometheus	2013-Aug-21	-0.0 \pm 0.6	150.3 \pm 0.5				2.4 \pm 0.6			3.5 \pm 0.5
	2013-Aug-23	0.0 \pm 0.9	152.9 \pm 0.4				2.7 \pm 0.6			3.8 \pm 0.6
	2013-Nov-18	-1.5 \pm 1.2	154.2 \pm 2.7				5.3 \pm 0.8			
	2013-Dec-02	-1.1 \pm 1.0	152.8 \pm 1.0				2.4 \pm 1.2			
	2013-Dec-04	-1.2 \pm 1.7	156.5 \pm 2.4				2.2 \pm 1.1			
	2013-Dec-14	-2.2 \pm 1.8	154.3 \pm 2.3				1.9 \pm 0.9			
	2014-Mar-11	-1.3 \pm 0.4	155.2 \pm 1.3				3.4 \pm 0.5			3.9 \pm 0.6
	2014-Mar-27	-1.8 \pm 1.2	156.8 \pm 1.4				4.0 \pm 0.6			
	2015-Jan-11	-2.3 \pm 0.7	152.4 \pm 0.4				2.8 \pm 0.4			3.9 \pm 0.6
	2015-Apr-01	-1.1 \pm 0.5	155.9 \pm 0.5				1.5 \pm 0.2			2.2 \pm 0.3
	2015-Apr-26	-1.5 \pm 1.6	156.4 \pm 2.5				4.3 \pm 2.2			
	2015-May-05	-0.0 \pm 0.6	155.8 \pm 1.3				4.1 \pm 0.6			4.4 \pm 0.7
	2015-Dec-22	-0.8 \pm 1.3	151.3 \pm 1.3				1.6 \pm 0.2			3.7 \pm 0.6
	2016-Mar-11	0.0 \pm 1.1	150.1 \pm 1.1				1.4 \pm 0.3			
	2017-Jan-04	-2.1 \pm 0.6	153.1 \pm 0.8				3.1 \pm 0.5	3.8 \pm 0.6	3.3 \pm 0.5	3.9 \pm 0.6
	2017-Jan-27	0.3 \pm 1.2	149.1 \pm 1.2				1.9 \pm 0.3			
	2017-Feb-05	-2.1 \pm 0.9	151.8 \pm 1.6				2.3 \pm 0.4	2.8 \pm 0.4	2.3 \pm 0.3	4.1 \pm 0.6
	2017-Jun-16	-1.7 \pm 0.5	155.7 \pm 0.6				3.0 \pm 0.4			
	2017-Jul-23	-2.8 \pm 0.0	153.0 \pm 1.3					2.8 \pm 0.4	5.0 \pm 0.7	
	2017-Dec-31	-2.9 \pm 0.8	153.6 \pm 1.5				3.7 \pm 0.5		3.7 \pm 0.6	5.7 \pm 0.9
	2018-Jan-02	-1.5 \pm 0.7	152.3 \pm 0.9				3.7 \pm 0.6	4.4 \pm 0.7	3.5 \pm 0.5	5.5 \pm 0.8
	2018-Jan-14	-2.4 \pm 1.5	153.6 \pm 1.1						2.9 \pm 0.4	4.4 \pm 0.7
	Average	-1.5	153.3							
Culann	2013-Aug-23	-16.5 \pm 0.4	161.6 \pm 0.9				1.4 \pm 0.7			2.1 \pm 0.3
	2014-Mar-11	-16.0 \pm 0.4	162.0 \pm 0.5				2.2 \pm 0.3			1.9 \pm 0.3
	2015-Jan-11	-17.2 \pm 0.4	159.8 \pm 0.5				1.9 \pm 0.3			2.3 \pm 0.3
	2015-Apr-01	-16.0 \pm 0.5	164.6 \pm 1.1				1.1 \pm 0.4			1.7 \pm 0.2
	2015-May-05	-14.7 \pm 1.0	169.4 \pm 1.8							2.1 \pm 0.3
	2017-Jan-04	-17.2 \pm 0.6	161.0 \pm 0.7				2.1 \pm 0.3	2.2 \pm 0.3	1.9 \pm 0.3	2.4 \pm 0.4
	2017-Feb-05	-17.4 \pm 0.9	160.5 \pm 0.7				2.4 \pm 0.4	2.5 \pm 0.4	2.1 \pm 0.3	3.1 \pm 0.5
	2017-Jun-16	-17.1 \pm 0.6	163.7 \pm 0.3			2.8 \pm 0.4	2.7 \pm 0.4			

Table A.2 continued on next page

Table A.2 (continued)

Hot Spot	Date	Lat	Lon	K-cont	H ₂ O	PAH	L'	Br α -cont	Br α	Ms
				$\lambda = 2.27 \mu\text{m}$	$3.06 \mu\text{m}$	$3.29 \mu\text{m}$	$3.78 \mu\text{m}$	$3.99 \mu\text{m}$	$4.05 \mu\text{m}$	$4.67 \mu\text{m}$
	[UT]	[°N]	[°W]				[GW/ $\mu\text{m}/\text{sr}$]			
	2017-Dec-31	-18.8 \pm 1.1	160.5 \pm 0.8				2.4 \pm 0.4		2.3 \pm 0.4	3.2 \pm 0.5
	2018-Jan-02	-17.8 \pm 0.7	161.8 \pm 2.1				2.6 \pm 0.4	2.5 \pm 0.4	2.1 \pm 0.3	3.2 \pm 0.5
	2018-Jan-14	-19.1 \pm 0.8	162.1 \pm 2.1				2.0 \pm 0.3		2.4 \pm 0.4	2.8 \pm 0.4
	Average	-17.2	161.8							
Zamama	2017-Jan-04	18.5 \pm 1.1	173.0 \pm 1.0				1.3 \pm 0.2	1.8 \pm 0.3	1.2 \pm 0.2	1.7 \pm 0.3
	2017-Feb-05	19.4 \pm 1.3	173.8 \pm 1.0				1.2 \pm 0.2	1.4 \pm 0.2	1.1 \pm 0.2	1.9 \pm 0.3
	2017-Dec-31	16.8 \pm 0.7	173.2 \pm 0.7							1.4 \pm 0.2
	Average	18.5	173.2							
Ilyrikon Regio	2016-Jun-17	-73.2 \pm 0.8	192.8 \pm 3.3	200 \pm 190			100 \pm 70			
	2016-Jun-20	-68.8 \pm 0.3	173.0 \pm 2.6	180 \pm 70			110 \pm 40			
	2016-Jun-24	-72.7 \pm 1.1	186.8 \pm 10.7	310 \pm 260			100 \pm 50			
	2016-Jun-27	-67.2 \pm 2.9	164.9 \pm 11.3	94 \pm 21			130 \pm 70			
	Average	-70.8	179.9							
Sethlaus/Gabija Paterae	2015-Mar-27	-50.0 \pm 1.7	195.5 \pm 2.4				8.1 \pm 1.5			
	2015-Mar-29	-51.4 \pm 1.8	197.9 \pm 4.7				11 \pm 3			
	2015-Apr-01	-50.2 \pm 0.9	198.0 \pm 2.4		27 \pm 5	22 \pm 4	33 \pm 5			28 \pm 4
	2015-Apr-19	-50.0 \pm 2.0	198.1 \pm 2.2				7.2 \pm 1.3			
	2015-Apr-26	-49.6 \pm 1.9	199.7 \pm 2.2				4.8 \pm 2.4			
	2015-May-05	-48.5 \pm 1.6	198.8 \pm 1.0		6.0 \pm 0.9	3.9 \pm 0.6	5.8 \pm 0.9			9.3 \pm 1.4
	Average	-50.0	198.1							
Isum Patera	2015-May-05	31.9 \pm 0.4	209.2 \pm 0.5							1.9 \pm 0.3
	2016-Dec-23	31.0 \pm 0.8	203.5 \pm 1.2							2.7 \pm 0.4
	2017-Jan-04	29.3 \pm 1.4	201.2 \pm 2.0					3.9 \pm 0.6	3.1 \pm 0.5	2.9 \pm 0.4
	2017-Jan-08	30.4 \pm 1.0	204.5 \pm 1.8						1.9 \pm 0.3	2.1 \pm 0.3
	2017-Feb-05	27.2 \pm 0.6	204.3 \pm 0.6						2.0 \pm 0.3	
	2017-May-28	31.1 \pm 0.9	209.6 \pm 1.1					2.0 \pm 0.3	2.3 \pm 0.3	2.0 \pm 0.3
	2017-Dec-31	27.4 \pm 0.6	202.7 \pm 0.4						3.1 \pm 0.5	4.6 \pm 0.7
	2018-Jan-02	30.1 \pm 1.0	205.2 \pm 1.7				1.9 \pm 0.3	2.8 \pm 0.4	2.9 \pm 0.4	3.2 \pm 0.5
	2018-May-27	32.5 \pm 0.6	208.7 \pm 2.2	86 \pm 13			64 \pm 16			
	2018-May-31	30.3 \pm 1.8	205.6 \pm 3.0	82 \pm 12			59 \pm 9			
	2018-Jun-02	30.5 \pm 1.1	209.0 \pm 6.9				51 \pm 25			
	2018-Jun-16	32.2 \pm 1.2	204.3 \pm 0.7	48 \pm 7			39 \pm 6			
	2018-Jun-18	31.5 \pm 1.0	206.9 \pm 2.0	71 \pm 14			35 \pm 7			
	2018-Jun-23	31.4 \pm 0.6	205.9 \pm 0.7	30 \pm 4			32 \pm 5			
	2018-Jun-25	31.6 \pm 2.0	206.0 \pm 0.5	45 \pm 7			29 \pm 5			
	2018-Jun-30	33.5 \pm 0.0	204.3 \pm 1.3	28 \pm 4			28 \pm 4			
	Average	31.1	205.4							
Marduk Fluctus	2013-Aug-20	-24.8 \pm 0.8	211.1 \pm 2.8							5.7 \pm 0.9
	2013-Aug-23	-22.7 \pm 0.8	207.4 \pm 1.4				6.0 \pm 1.4			7.5 \pm 1.1
	2013-Sep-01	-26.5 \pm 1.6	208.0 \pm 1.8				9.2 \pm 1.4			
	2013-Sep-03	-21.0 \pm 1.7	207.9 \pm 2.4				5.6 \pm 1.1			
	2013-Sep-10	-22.8 \pm 1.5	209.1 \pm 1.7				7.1 \pm 1.3			
	2013-Nov-18	-24.4 \pm 0.6	208.5 \pm 0.6		3.4 \pm 0.5	4.8 \pm 0.7	6.7 \pm 1.0			9.2 \pm 1.4
	2013-Nov-27	-27.9 \pm 1.3	203.3 \pm 2.9				5.4 \pm 2.7			
	2013-Dec-02	-22.5 \pm 1.2	209.1 \pm 2.9				5.8 \pm 2.9			
	2013-Dec-04	-23.4 \pm 1.1	210.0 \pm 1.2				4.6 \pm 0.7			
	2013-Dec-13	-23.7 \pm 1.9	210.7 \pm 2.2				3.7 \pm 0.6			
	2014-Feb-08	-23.8 \pm 1.1	213.3 \pm 2.0				8.3 \pm 1.2			6.5 \pm 1.0
	2014-Mar-10	-24.0 \pm 1.5	215.1 \pm 2.5				5.4 \pm 1.0			
	2014-Oct-22	-24.7 \pm 1.5	208.6 \pm 1.5				5.7 \pm 0.9			
	2014-Oct-31	-23.2 \pm 0.8	210.0 \pm 0.5				6.5 \pm 1.0			9.0 \pm 1.4
	2014-Nov-30	-25.0 \pm 1.3	208.0 \pm 1.6				5.5 \pm 0.8			
	2014-Dec-02	-23.5 \pm 0.9	213.2 \pm 1.5				5.4 \pm 1.9			8.4 \pm 1.3
	2014-Dec-09	-23.5 \pm 1.5	207.9 \pm 2.5				3.8 \pm 1.9			
	2014-Dec-16	-25.4 \pm 1.5	206.8 \pm 2.5				4.0 \pm 2.0			
	2015-Jan-11	-23.7 \pm 0.8	205.5 \pm 2.8							7.6 \pm 1.1
	2015-Jan-15	-23.5 \pm 1.1	212.2 \pm 1.4				4.0 \pm 0.6			
	2015-Jan-26	-23.8 \pm 1.5	211.0 \pm 2.5				2.9 \pm 1.5			
	2015-Mar-27	-24.8 \pm 1.2	211.1 \pm 1.2				4.6 \pm 0.7			
	2015-Mar-29	-25.7 \pm 1.6	211.1 \pm 2.4				5.6 \pm 1.1			
	2015-Apr-01	-22.2 \pm 0.7	217.4 \pm 6.1							8.5 \pm 6.1
	2015-Apr-05	-23.4 \pm 1.6	215.9 \pm 2.4				3.6 \pm 0.7			

Table A.2 continued on next page

Table A.2 (continued)

Hot Spot	Date	Lat	Lon	K-cont	H ₂ O	PAH	L'	Br α -cont	Br α	Ms
				$\lambda = 2.27 \mu\text{m}$	$3.06 \mu\text{m}$	$3.29 \mu\text{m}$	$3.78 \mu\text{m}$	$3.99 \mu\text{m}$	$4.05 \mu\text{m}$	$4.67 \mu\text{m}$
	[UT]	[°N]	[°W]				[GW/ $\mu\text{m}/\text{sr}$]			
	2015-Apr-19	-24.7±1.3	215.2±1.6				5.3±1.0			
	2015-Apr-21	-24.3±1.7	215.4±2.4				4.4±0.8			
	2015-Apr-26	-23.9±1.3	215.7±1.5				4.1±0.6			
	2015-May-05	-23.7±0.5	214.4±1.0		4.3±0.6	3.6±0.5	5.7±0.8			11±2
	2016-Feb-03	-22.5±1.2	210.6±1.3				7.4±1.4			
	2016-Feb-17	-22.7±1.2	206.1±3.6				9.1±2.1			
	2016-Feb-19	-23.6±1.1	205.4±1.2				12±2			
	2016-Feb-21	-23.2±1.2	211.0±2.1				8.6±1.7			
	2016-Mar-11	-23.7±1.2	209.1±2.7				13±3			
	2016-Mar-13	-24.2±1.1	209.8±1.3				12±2			
	2016-Apr-30	-20.9±1.2	209.2±1.3				13±2			
	2016-May-02	-22.0±1.3	215.5±1.9				12±2			
	2016-May-09	-21.2±1.3	211.4±1.6				13±2			
	2016-May-11	-22.3±1.3	212.0±4.4				9.9±3.3			
	2016-May-14	-20.6±1.3	214.2±1.5				11±2			
	2016-May-16	-23.4±1.3	210.5±1.4				9.7±1.8			
	2016-May-18	-21.4±1.3	215.1±2.5				18±4			
	2016-May-23	-22.5±1.3	213.9±1.5				16±3			
	2016-May-25	-24.4±1.4	215.2±2.5				14±3			
	2016-Jun-01	-20.2±1.3	214.5±1.6				13±2			
	2016-Jun-03	-21.1±1.4	214.2±4.4				8.8±2.7			
	2016-Jun-08	-20.1±1.4	212.7±1.4				10±2			
	2016-Jun-10	-20.2±1.4	214.4±2.7				13±3			
	2016-Jun-17	-25.3±1.5	212.3±2.3				22±4			
	2016-Jun-24	-25.7±1.5	212.0±1.9				15±3			
	2016-Nov-23	-20.9±1.6	211.9±2.7				22±4			
	2016-Dec-23	-24.7±0.3	210.8±0.6			12±2	15±2	15±2	13±2	27±4
	2017-Jan-04	-26.3±0.9	206.7±1.8		7.6±1.1	9.4±1.4	16±2	15±2	12±2	20±3
	2017-Jan-08	-25.9±0.9	208.7±1.0		10±2	18±3	18±3	16±2	13±2	27±5
	2017-Jan-15	-20.4±1.4	205.1±1.9				12±2			
	2017-Jan-20	-24.6±1.4	205.1±3.7				21±4			
	2017-Jan-22	-23.1±1.3	206.0±1.5				10±2			
	2017-Jan-24	-26.4±0.5	208.2±0.5			15±2	18±3			25±4
	2017-Jan-27	-24.4±1.4	205.1±3.5				20±4			
	2017-Jan-31	-25.4±1.4	206.7±2.7				18±3			
	2017-Feb-05	-27.3±0.6	208.2±0.9		15±2	22±3	27±4	25±4	22±3	33±5
	2017-Feb-23	-24.6±1.2	211.5±1.5				8.1±1.4			
	2017-Mar-04	-22.3±1.2	211.9±1.8				7.1±1.2			
	2017-Apr-03	-21.0±1.1	209.4±1.4				7.9±1.3			
	2017-May-05	-22.3±1.2	212.8±1.9				6.9±1.2			
	2017-May-07	-21.5±1.2	215.3±2.7				11±2			
	2017-May-10	-22.9±1.2	210.5±2.4				12±2			
	2017-May-12	-23.9±1.2	213.2±1.3				9.7±1.6			
	2017-May-14	-25.0±1.2	213.4±2.1				8.0±1.4			
	2017-May-28	-24.9±0.7	215.5±0.4		5.6±0.8	8.5±1.3	12±2	18±3	15±2	20±3
	2017-May-30	-21.4±1.3	211.5±3.2				15±3			
	2017-Jun-22	-23.6±1.4	214.4±3.4				12±3			
	2017-Jun-27	-24.1±1.3	212.2±1.4				12±2			
	2017-Jun-29	-25.6±1.4	209.2±2.7				12±2			
	2017-Jul-04	-20.6±1.3	208.7±1.5				7.1±1.2			
	2017-Jul-06	-20.9±1.4	214.4±1.8				8.4±1.4			
	2017-Jul-31	-27.9±1.3	218.2±2.9				9.2±1.8		6.3±1.0	18±3
	2017-Dec-12	-24.6±0.8	212.6±0.9			8.5±1.3	12±2			
	2017-Dec-31	-26.5±0.9	208.5±2.0		11±2	13±2	18±3		17±3	27±4
	2018-Jan-02	-26.8±1.2	209.7±0.3		10±2	16±2	20±3	23±3	18±3	28±4
	2018-Jan-12	-25.3±0.7	214.3±1.3				19±3			27±4
	2018-May-31	-26.2±1.2	212.8±1.6				8.7±1.3			
	2018-Jun-16	-24.9±1.2	210.2±1.2				12±2			
	2018-Jun-18	-23.2±1.2	214.2±2.4				13±2			
	2018-Jun-23	-25.4±1.2	212.6±1.4				11±2			
	2018-Jun-25	-24.6±1.2	214.0±1.8				9.8±1.5			
	2018-Jun-30	-22.1±1.2	210.1±1.3				12±2			
	Average	-23.7	211.1							

Table A.2 continued on next page

Table A.2 (continued)

Hot Spot	Date	Lat	Lon	K-cont	H ₂ O	PAH	L'	Bra-cont	Bra α	Ms
				$\lambda = 2.27 \mu\text{m}$	$3.06 \mu\text{m}$	$3.29 \mu\text{m}$	$3.78 \mu\text{m}$	$3.99 \mu\text{m}$	$4.05 \mu\text{m}$	$4.67 \mu\text{m}$
	[UT]	[°N]	[°W]				[GW/ $\mu\text{m}/\text{sr}$]			
Kurdalagon	2013-Nov-18	-45.3±1.1	214.9±1.0				2.2±0.8			2.2±0.3
	2015-Jan-26	-48.6±1.1	219.4±2.0	81±12			56±9			
	2015-Mar-27	-50.0±1.9	219.4±2.3				15±3			
	2015-Mar-29	-49.6±1.7	223.8±2.5				14±3			
	2015-Mar-31	-50.0±0.9	224.5±2.3		11±3	9.6±1.8	6.7±2.2			12±6
	2015-Apr-05	-47.7±1.2	223.7±2.0	120±20			68±11			
	2015-Apr-17	-50.4±2.1	224.2±2.0				52±23			
	2015-Apr-19	-50.0±1.9	224.4±3.6				36±7			
	2015-Apr-21	-49.7±1.9	223.3±2.7				22±4			
	2015-Apr-26	-49.6±1.9	223.7±2.9				19±4			
	2015-May-05	-48.4±2.1	222.3±1.1		12±2	12±2	17±3			32±5
	2016-Feb-03	-49.3±1.6	216.6±1.8				2.5±0.5			
	2016-Feb-19	-48.6±1.6	210.3±1.8				2.9±0.6			
	2016-Mar-13	-48.5±1.5	213.9±2.3				3.8±0.7			
	2016-Apr-30	-45.2±1.6	214.1±2.2				3.5±0.7			
	2016-May-14	-47.0±1.7	217.3±2.5				5.6±1.1			
	2016-May-16	-49.3±1.8	215.8±1.9				4.6±0.9			
	2016-May-18	-48.5±1.8	218.0±4.4				11±3			
	2016-May-23	-45.7±1.7	218.1±2.4				8.9±1.7			
	2016-May-25	-48.4±1.8	220.8±4.0				14±3			
	2016-Jun-01	-45.8±1.8	220.2±2.3				8.8±1.7			
	2016-Jun-08	-45.1±1.8	217.7±1.9				5.8±1.1			
	2016-Dec-23	-48.7±0.8	216.8±1.5				5.3±0.8	5.7±0.8	4.5±0.7	8.8±1.3
	2017-Jan-04	-50.0±0.7	208.3±2.0				7.7±1.2	7.2±1.1	4.8±0.7	7.7±1.2
	2017-Jan-08	-50.5±1.5	214.7±2.0				5.4±1.0	5.6±0.8	5.1±0.8	9.5±1.4
	2017-Jan-22	-45.5±1.7	214.2±1.9				2.4±0.4			
	2017-Jan-24	-53.0±0.9	212.8±3.6				6.1±1.1			
	2017-Feb-05	-49.9±1.1	213.3±1.1				5.3±0.8	5.8±0.9	5.7±0.9	9.6±1.4
	2017-Dec-12	-51.3±1.0	209.8±0.2			13±2	12±2			
	2017-Dec-31	-51.7±2.0	210.3±2.1				11±2		9.1±1.4	17±2
	2018-Jan-02	-51.5±2.2	213.6±0.5		4.7±0.7	8.1±1.2	9.9±1.5	12±2	9.1±1.4	15±2
	2018-May-31	-50.4±1.6	214.7±2.7				4.7±0.7			
	2018-Jun-16	-46.7±1.5	211.9±1.7				5.7±0.9			
2018-Jun-23	-50.8±1.7	215.3±2.5				7.0±1.1				
2018-Jun-25	-50.1±1.7	218.0±3.1				6.9±1.1				
2018-Jun-30	-45.3±1.5	214.8±2.0				4.8±0.7				
	Average	-49.3	216.7							
Unknown	2018-Jan-02	53.6±0.6	217.8±1.2					2.9±0.4	2.3±0.3	
	Average	53.6	217.8							
Susanoo/Mulungu Paterae	2013-Aug-20	17.0±0.7	226.0±2.4				2.9±1.4			6.1±0.9
	2013-Aug-23	18.2±1.1	221.8±2.7							5.9±0.9
	2013-Nov-18	21.5±1.1	218.2±1.0		0.62±0.09	1.8±0.3	3.8±0.7			7.8±1.2
	2013-Dec-04	20.0±1.9	221.2±2.2				1.3±0.7			
	2013-Dec-13	18.9±2.0	220.8±2.1				1.1±0.6			
	2014-Feb-08	18.4±1.2	225.7±1.3				1.6±0.6			1.8±0.3
	2014-Oct-31	20.6±0.8	220.6±1.0							1.1±0.5
	2015-May-05	16.6±1.0	223.3±1.4				0.49±0.17			0.93±0.33
	2018-Jan-02	14.5±0.7	220.5±0.7					1.6±0.2		
	2018-Jan-12	21.4±1.4	218.1±4.0			21±3	20±3			19±3
	Average	18.6	221.0							
201308C	2013-Aug-29	29.6±1.7	225.7±9.2				>500			
	2013-Aug-30	29.1±1.7	227.2±6.1				360 ⁺⁸²⁰ ₋₂₀₀			
	2013-Sep-01	29.1±1.6	226.9±2.6				73±11			
	2013-Sep-03	28.6±1.5	227.5±1.8				27±4			
	2013-Sep-05	29.5±1.6	227.6±3.9				20±5			
	2013-Sep-10	28.4±1.5	228.0±1.6				12±2			
	2013-Nov-18	29.4±0.9	228.2±0.5		1.2±0.2	2.4±0.4	3.0±0.5			4.4±0.7
	2014-Feb-08	29.2±1.0	234.5±1.2				1.6±0.4			1.8±0.3
	2014-Oct-31	31.5±0.9	231.4±1.0							1.8±0.3
	2014-Dec-02	27.4±0.8	230.3±1.4				3.0±0.5			2.5±0.4
	2015-May-05	28.1±0.7	232.4±1.1				1.0±0.4			1.5±0.3
	Average	29.1	228.0							

Table A.2 continued on next page

Table A.2 (continued)

Hot Spot	Date	Lat	Lon	K-cont	H ₂ O	PAH	L'	Br α -cont	Br α	Ms
				$\lambda = 2.27 \mu\text{m}$	$3.06 \mu\text{m}$	$3.29 \mu\text{m}$	$3.78 \mu\text{m}$	$3.99 \mu\text{m}$	$4.05 \mu\text{m}$	$4.67 \mu\text{m}$
	[UT]	[°N]	[°W]				[GW/ $\mu\text{m}/\text{sr}$]			
P17	2017-Jan-08	-3.5 \pm 0.9	228.8 \pm 0.4				1.8 \pm 0.3	1.6 \pm 0.2	1.3 \pm 0.2	
	Average	-3.5	228.8							
P13	2017-Feb-05	13.6 \pm 0.6	228.4 \pm 0.8		9.0 \pm 1.3	15 \pm 2	23 \pm 4	23 \pm 3	21 \pm 3	34 \pm 5
	2017-Feb-23	13.6 \pm 1.2	228.7 \pm 1.2				2.2 \pm 0.4			
	2017-Mar-04	16.8 \pm 1.2	229.3 \pm 1.3				2.2 \pm 0.4			
	2017-May-28	14.1 \pm 1.1	234.6 \pm 0.1					1.1 \pm 0.2	1.0 \pm 0.2	1.9 \pm 0.3
	Average	13.9	229.0							
East Girru	2013-Dec-04	21.3 \pm 1.7	232.1 \pm 2.4				5.0 \pm 0.8			
	2013-Dec-06	20.2 \pm 1.6	234.7 \pm 2.4				5.4 \pm 1.0			
	2013-Dec-13	22.3 \pm 1.1	233.5 \pm 1.1				4.6 \pm 0.7			
	Average	21.3	233.5							
Reiden Patara	2017-Dec-12	-17.0 \pm 0.7	234.9 \pm 1.2			6.0 \pm 0.9	3.5 \pm 0.5			
	2018-Jan-02	-18.9 \pm 2.1	234.0 \pm 1.2		2.7 \pm 0.4	2.6 \pm 0.4				4.1 \pm 0.6
	Average	-18.0	234.4							
Pyerun Patara	2013-Nov-18	-57.7 \pm 1.9	237.1 \pm 2.3							4.0 \pm 0.6
	Average	-57.7	237.1							
SE of Pele	2016-Dec-23	-34.0 \pm 1.8	240.0 \pm 1.6			3.0 \pm 0.4	3.3 \pm 0.5	2.6 \pm 0.4	2.5 \pm 0.4	5.8 \pm 0.9
	2017-Jan-08	-35.1 \pm 1.0	238.9 \pm 0.8		3.6 \pm 0.5	4.5 \pm 0.7	4.2 \pm 0.6	3.9 \pm 0.6	3.0 \pm 0.5	5.9 \pm 1.0
	2017-Jan-15	-30.6 \pm 1.4	232.5 \pm 1.5				3.4 \pm 0.6			
	2017-Jan-22	-34.0 \pm 1.5	236.6 \pm 1.9				2.6 \pm 0.4			
	2017-Jan-24	-36.4 \pm 1.0	239.8 \pm 1.8			3.9 \pm 0.6	3.2 \pm 0.5			5.2 \pm 0.8
	2017-Jan-31	-36.4 \pm 1.5	240.0 \pm 1.9				3.3 \pm 0.6			
	2017-Feb-05	-36.9 \pm 1.5	235.6 \pm 1.1				3.4 \pm 0.5	3.9 \pm 0.6	3.1 \pm 0.5	5.8 \pm 0.9
	2017-Feb-23	-36.7 \pm 1.4	238.8 \pm 1.6				2.0 \pm 0.3			
	2017-Mar-04	-41.9 \pm 1.4	235.2 \pm 1.7				6.0 \pm 1.0			
	2017-Apr-03	-30.9 \pm 1.2	236.4 \pm 1.3				2.2 \pm 0.4			
	2017-May-05	-34.2 \pm 1.3	239.0 \pm 1.6				2.4 \pm 0.4			
	2017-May-07	-31.2 \pm 1.3	244.2 \pm 1.8				2.9 \pm 0.5			
	2017-May-12	-34.5 \pm 1.3	240.0 \pm 2.3				4.6 \pm 0.8			
	2017-May-14	-33.4 \pm 1.3	242.8 \pm 1.5				2.3 \pm 0.4			
	2017-May-28	-35.1 \pm 1.0	242.2 \pm 0.8		2.6 \pm 0.4	3.0 \pm 0.4	4.0 \pm 0.6	5.8 \pm 0.9	4.6 \pm 0.7	6.6 \pm 1.0
	2017-May-30	-31.6 \pm 1.3	239.8 \pm 2.1				4.1 \pm 0.7			
	2017-Jun-27	-34.3 \pm 1.5	237.9 \pm 2.3				3.3 \pm 0.6			
	2017-Jun-29	-38.4 \pm 1.6	238.0 \pm 2.1				3.8 \pm 0.7			
	2017-Jul-06	-34.2 \pm 1.5	238.4 \pm 1.6				2.8 \pm 0.5			
	2017-Jul-31	-38.7 \pm 0.6	241.0 \pm 1.1				3.8 \pm 0.6		3.1 \pm 0.5	8.0 \pm 1.2
	2017-Dec-12	-35.5 \pm 0.6	239.3 \pm 1.7			5.6 \pm 0.8	5.0 \pm 0.7			
	2018-Jan-02	-35.1 \pm 1.7	237.2 \pm 1.2			4.7 \pm 0.7	6.7 \pm 1.0	7.4 \pm 1.1	6.6 \pm 1.0	14 \pm 2
	2018-Jan-12	-36.3 \pm 3.0	239.8 \pm 2.4				6.7 \pm 1.0			13 \pm 2
	2018-Apr-24	-32.9 \pm 1.3	236.8 \pm 2.6				4.1 \pm 0.8			
	2018-May-31	-34.5 \pm 1.2	243.3 \pm 1.4				4.2 \pm 0.6			
	2018-Jun-16	-36.2 \pm 1.3	240.1 \pm 2.0				5.9 \pm 0.9			
	2018-Jun-18	-31.4 \pm 1.3	244.4 \pm 1.6				4.6 \pm 0.7			
	2018-Jun-23	-32.3 \pm 1.3	240.7 \pm 2.5				5.4 \pm 0.8			
	2018-Jun-25	-35.3 \pm 1.3	240.1 \pm 1.5				4.3 \pm 0.6			
	2018-Jun-30	-33.1 \pm 1.3	237.4 \pm 2.3				4.5 \pm 0.7			
	Average	-34.5	239.5							
Pillan Patara	2015-Mar-27	-11.8 \pm 1.1	243.2 \pm 1.5				7.6 \pm 1.1			
	2015-Mar-29	-12.1 \pm 1.1	245.4 \pm 1.2				6.5 \pm 1.0			
	2015-Mar-31	-11.4 \pm 0.4	248.7 \pm 1.3			3.1 \pm 0.5	6.2 \pm 0.9			15 \pm 2
	2015-Apr-05	-11.3 \pm 1.2	245.4 \pm 1.2				5.3 \pm 0.8			
	2015-Apr-21	-12.1 \pm 1.2	244.6 \pm 1.2				4.1 \pm 0.6			
	2015-Apr-26	-11.8 \pm 1.6	244.4 \pm 2.4				3.3 \pm 0.6			
	2015-May-05	-11.1 \pm 0.6	245.3 \pm 0.8				3.7 \pm 0.5			11 \pm 2
	2017-Feb-05	-12.2 \pm 0.7	240.1 \pm 0.8		4.4 \pm 0.7	8.9 \pm 1.3	9.9 \pm 1.5	9.3 \pm 1.4	8.8 \pm 1.3	11 \pm 2
	2017-Feb-23	-11.5 \pm 1.2	242.6 \pm 1.2				27 \pm 5			
	2017-Mar-04	-9.5 \pm 1.1	240.8 \pm 1.1				24 \pm 4			
	2017-Mar-06	-9.3 \pm 1.2	243.7 \pm 2.1				24 \pm 4			
	2017-Apr-03	-8.1 \pm 1.1	239.6 \pm 1.1				4.3 \pm 0.7			
	2017-May-05	-10.1 \pm 1.1	243.7 \pm 1.1				2.1 \pm 0.4			
	2017-May-07	-9.6 \pm 1.1	245.6 \pm 1.3				2.3 \pm 0.4			
	2017-May-14	-11.3 \pm 1.1	243.6 \pm 1.2				1.6 \pm 0.3			

Table A.2 continued on next page

Table A.2 (continued)

Hot Spot	Date	Lat	Lon	K-cont	H ₂ O	PAH	L'	Bra-cont	Bra α	Ms
				$\lambda = 2.27 \mu\text{m}$	$3.06 \mu\text{m}$	$3.29 \mu\text{m}$	$3.78 \mu\text{m}$	$3.99 \mu\text{m}$	$4.05 \mu\text{m}$	$4.67 \mu\text{m}$
	[UT]	[°N]	[°W]				[GW/ $\mu\text{m}/\text{sr}$]			
	2017-May-28	-10.8 \pm 0.7	245.2 \pm 0.5				3.3 \pm 0.5	5.7 \pm 0.9	5.1 \pm 0.8	9.1 \pm 1.4
	2017-May-30	-7.5 \pm 1.2	239.2 \pm 1.5				2.1 \pm 0.4			
	2017-Jun-29	-12.7 \pm 1.3	242.0 \pm 1.4				1.8 \pm 0.3			
	2017-Jul-06	-9.2 \pm 1.3	237.6 \pm 1.3				1.5 \pm 0.3			
	2017-Jul-31	-14.1 \pm 2.9	245.8 \pm 0.8				2.3 \pm 0.3			7.1 \pm 1.1
	2018-Jan-12	-10.9 \pm 0.6	243.9 \pm 0.9							3.8 \pm 0.6
	Average	-11.3	243.7							
Chors Patara	2014-Oct-22	65.1 \pm 3.5	245.6 \pm 12.0				57 \pm 19			
	2014-Oct-24	65.1 \pm 3.4	245.3 \pm 4.3				35 \pm 8			
	2014-Oct-31	66.4 \pm 2.6	243.8 \pm 1.2				23 \pm 3			53 \pm 8
	2014-Dec-02	63.0 \pm 1.0	248.5 \pm 1.5				7.4 \pm 1.1			14 \pm 2
	2015-Mar-31	66.3 \pm 1.6	254.5 \pm 4.7							3.0 \pm 1.5
	Average	65.1	245.6							
UP 254W	2018-May-10	-36.8 \pm 1.2	251.9 \pm 0.3	120 \pm 20			130 \pm 20			
	2018-May-31	-37.3 \pm 1.3	257.0 \pm 1.8				2.0 \pm 0.3			
	Average	-37.1	254.5							
Pele	2013-Aug-20	-17.4 \pm 0.4	255.1 \pm 1.6				2.1 \pm 0.5			3.3 \pm 0.5
	2013-Nov-18	-18.1 \pm 0.9	251.6 \pm 0.8		0.72 \pm 0.11	1.0 \pm 0.2	2.7 \pm 0.8			3.7 \pm 0.6
	2014-Feb-08	-17.6 \pm 0.6	257.3 \pm 0.4				2.2 \pm 0.3			2.5 \pm 0.4
	2014-Oct-31	-18.1 \pm 0.7	253.1 \pm 0.4				2.7 \pm 0.4			3.3 \pm 0.5
	2014-Dec-02	-20.3 \pm 1.6	253.6 \pm 0.5		1.1 \pm 0.2		3.4 \pm 0.5			4.6 \pm 0.7
	2015-Jan-26	-19.2 \pm 2.0	255.2 \pm 2.1				0.34 \pm 0.17			
	2015-Mar-31	-19.4 \pm 0.7	260.2 \pm 2.5		0.8 \pm 0.12	1.1 \pm 0.2	1.1 \pm 0.4			1.7 \pm 0.3
	2015-Apr-19	-16.7 \pm 1.2	258.2 \pm 3.6				7.0 \pm 3.5			
	2015-May-05	-19.2 \pm 1.0	257.9 \pm 1.8				1.5 \pm 0.6			
	2015-Nov-23	-17.3 \pm 0.7	256.7 \pm 2.9							4.1 \pm 0.7
	2016-Feb-21	-18.2 \pm 1.1	253.2 \pm 1.1				1.3 \pm 0.2			
	2016-Dec-23	-17.8 \pm 1.1	253.7 \pm 0.6						2.5 \pm 0.4	2.5 \pm 0.4
	2017-Jan-03	-17.8 \pm 0.6	255.4 \pm 1.8				3.5 \pm 0.5		7.2 \pm 1.1	6.4 \pm 1.0
	2017-Jan-08	-18.2 \pm 0.7	253.4 \pm 1.1				1.6 \pm 0.4	1.6 \pm 0.2	2.3 \pm 0.4	2.9 \pm 0.7
	2017-Jan-24	-19.4 \pm 0.4	254.2 \pm 0.7				2.6 \pm 0.4			3.2 \pm 0.5
	2017-May-28	-19.2 \pm 1.2	259.0 \pm 0.6			0.92 \pm 0.14	2.0 \pm 0.3	3.4 \pm 0.5	3.6 \pm 0.5	3.2 \pm 0.5
	2017-Jul-31	-19.9 \pm 0.8	256.7 \pm 0.9					2.0 \pm 0.3	2.3 \pm 0.3	
	2017-Dec-12	-18.6 \pm 0.7	254.6 \pm 0.7				1.1 \pm 0.2			
	2018-Jan-12	-19.3 \pm 0.0	256.0 \pm 1.0				1.6 \pm 0.2			2.4 \pm 0.4
	Average	-18.2	255.2							
Shakuru Patara	2018-Apr-24	27.9 \pm 1.3	260.3 \pm 1.6				3.9 \pm 0.7			
	2018-May-31	21.7 \pm 1.2	263.2 \pm 1.5				1.5 \pm 0.2			
	Average	24.8	261.7							
Mithra Patara	2015-Jan-10	-59.8 \pm 2.1	264.3 \pm 4.4				55 \pm 12			
	2015-Jan-12	-57.7 \pm 0.8	269.6 \pm 6.0				13 \pm 8			20 \pm 8
	2015-Jan-15	-57.3 \pm 1.9	263.5 \pm 4.9				8.5 \pm 4.2			
	2015-Mar-31	-58.3 \pm 0.9	266.9 \pm 1.8							3.1 \pm 0.5
	Average	-58.0	265.6							
Svarog Patara	2016-Dec-23	-52.9 \pm 1.0	269.3 \pm 1.9							5.1 \pm 0.8
	2017-Jan-08	-51.0 \pm 0.0	266.6 \pm 0.3							2.5 \pm 0.4
	2017-May-28	-51.6 \pm 0.8	275.5 \pm 2.7							4.9 \pm 0.7
	Average	-51.6	269.3							
Daedalus Patara	2016-May-11	19.1 \pm 1.3	274.7 \pm 1.3				2.8 \pm 0.5			
	2017-Jan-24	18.7 \pm 0.1	274.9 \pm 1.3				0.97 \pm 0.15			2.1 \pm 0.3
	2017-Jul-01	18.7 \pm 1.4	273.9 \pm 1.8				5.0 \pm 0.9			
	2017-Jul-08	16.8 \pm 1.4	272.3 \pm 1.5				2.0 \pm 0.3			
	2018-Jan-12	18.1 \pm 0.0	273.3 \pm 0.3				2.2 \pm 0.3			4.3 \pm 0.6
	Average	18.7	273.9							
PV59	2014-Feb-08	-38.6 \pm 0.3	289.5 \pm 0.4				16 \pm 2			17 \pm 3
	2014-Feb-10	-38.3 \pm 0.3	290.6 \pm 0.4			13 \pm 2	18 \pm 3			21 \pm 3
	2014-Mar-12	-42.2 \pm 1.9	292.4 \pm 2.2				7.9 \pm 1.5			
	2014-Oct-31	-37.9 \pm 1.0	286.5 \pm 1.8				4.7 \pm 0.7			3.2 \pm 0.5
	2014-Dec-02	-37.0 \pm 0.9	289.1 \pm 1.0							1.9 \pm 0.3
	2015-Mar-31	-37.0 \pm 1.0	293.6 \pm 0.8			1.1 \pm 0.2	1.5 \pm 0.3			1.7 \pm 0.3
	2015-Apr-02	-38.4 \pm 1.1	290.6 \pm 2.7							2.5 \pm 0.5
	2015-Dec-25	-38.8 \pm 0.5	285.9 \pm 1.6		4.3 \pm 0.6	5.3 \pm 0.8	7.1 \pm 1.1			12 \pm 2

Table A.2 continued on next page

Table A.2 (continued)

Hot Spot	Date	Lat	Lon	K-cont	H ₂ O	PAH	L'	Br α -cont	Br α	Ms
				$\lambda = 2.27 \mu\text{m}$	$3.06 \mu\text{m}$	$3.29 \mu\text{m}$	$3.78 \mu\text{m}$	$3.99 \mu\text{m}$	$4.05 \mu\text{m}$	$4.67 \mu\text{m}$
	[UT]	[°N]	[°W]				[GW/ $\mu\text{m}/\text{sr}$]			
	2016-Dec-23	-39.0 \pm 0.6	288.8 \pm 1.7					4.5 \pm 0.7	3.2 \pm 0.5	7.7 \pm 1.2
	2017-Jan-03	-38.4 \pm 0.7	288.9 \pm 1.4				2.9 \pm 0.4	4.0 \pm 0.6	4.6 \pm 0.7	6.3 \pm 0.9
	2017-Jan-08	-38.4 \pm 1.2	285.1 \pm 1.3				3.0 \pm 0.5	3.1 \pm 0.8	2.2 \pm 0.6	5.6 \pm 0.8
	2017-Jan-24	-39.5 \pm 1.4	287.0 \pm 0.4				2.4 \pm 0.4			4.6 \pm 0.7
	2017-May-07	-35.4 \pm 1.3	291.9 \pm 1.8				3.4 \pm 0.6			
	2017-May-14	-35.8 \pm 1.3	288.3 \pm 2.3				3.9 \pm 0.7			
	2017-May-23	-33.6 \pm 1.3	294.0 \pm 1.5				6.8 \pm 1.2			
	2017-May-25	-37.4 \pm 1.4	293.3 \pm 2.7				13 \pm 2			
	2017-May-28	-37.2 \pm 0.4	293.7 \pm 2.5			13 \pm 4	13 \pm 2	19 \pm 4	15 \pm 2	18 \pm 3
	2017-May-30	-34.7 \pm 1.4	287.2 \pm 1.8				8.3 \pm 1.4			
	2017-Jun-15	-37.6 \pm 1.5	292.6 \pm 1.7				3.3 \pm 0.6			
	2017-Jul-31	-38.5 \pm 0.4	293.1 \pm 0.8					2.0 \pm 0.3	1.9 \pm 0.3	5.9 \pm 0.9
	2018-Jan-12	-38.2 \pm 2.0	288.9 \pm 0.6				2.5 \pm 0.4			4.4 \pm 0.7
	2018-Jun-18	-38.4 \pm 1.4	289.8 \pm 2.1				5.7 \pm 0.9			
	Average	-38.2	289.7							
N Lerna Regio	2013-Nov-18	-56.8 \pm 1.4	279.7 \pm 4.7							2.7 \pm 1.4
	2013-Dec-06	-58.0 \pm 2.0	285.7 \pm 3.1				7.1 \pm 3.6			
	2014-Feb-10	-56.1 \pm 1.0	294.0 \pm 1.5			4.0 \pm 0.6				
	2014-Oct-31	-56.0 \pm 1.4	281.1 \pm 1.9				5.6 \pm 1.4			5.5 \pm 0.8
	2014-Dec-02	-60.0 \pm 1.1	284.1 \pm 1.3				5.4 \pm 1.2			4.3 \pm 0.6
	2015-Mar-31	-57.5 \pm 2.9	295.2 \pm 0.8		5.3 \pm 0.8	3.6 \pm 0.5	3.2 \pm 1.1			3.3 \pm 0.5
	2015-Nov-23	-58.3 \pm 1.7	285.3 \pm 2.5				4.5 \pm 2.3			7.0 \pm 1.1
	2015-Dec-25	-56.6 \pm 1.0	290.6 \pm 2.4				3.1 \pm 1.1			4.3 \pm 0.6
	2016-May-04	-51.9 \pm 1.8	294.7 \pm 2.0				5.3 \pm 1.0			
	2016-May-20	-50.8 \pm 1.9	295.2 \pm 2.7				7.4 \pm 1.5			
	2016-May-25	-54.6 \pm 2.1	291.3 \pm 4.6				7.0 \pm 1.5			
	2016-May-27	-53.1 \pm 2.0	291.6 \pm 2.4				6.7 \pm 1.3			
	2016-Jun-12	-53.9 \pm 2.1	293.2 \pm 3.3				8.0 \pm 1.6			
	2016-Jun-19	-50.5 \pm 2.0	289.9 \pm 2.3				5.8 \pm 1.1			
	2017-Jan-03	-55.1 \pm 1.7	292.9 \pm 1.8				3.3 \pm 0.5			4.5 \pm 0.7
	2017-Jan-08	-54.8 \pm 1.0	283.2 \pm 1.8				4.0 \pm 0.6			
	2017-Jan-24	-59.4 \pm 1.0	288.8 \pm 0.6				3.5 \pm 0.5			3.5 \pm 0.5
	2017-Jul-31	-54.8 \pm 1.0	295.9 \pm 1.5							5.3 \pm 0.8
	2018-Jan-12	-57.7 \pm 0.5	290.0 \pm 2.0				4.1 \pm 0.6			5.8 \pm 0.9
	Average	-56.0	290.6							
Kibero Patera	2016-Jun-24	-14.8 \pm 1.5	296.6 \pm 4.4				15 \pm 4			
	2016-Jun-28	-10.2 \pm 1.4	297.7 \pm 1.7				9.0 \pm 1.5			
	Average	-12.5	297.1							
Amaterasu Patera	2015-Dec-25	39.4 \pm 0.8	304.3 \pm 1.1		16 \pm 2	28 \pm 4	43 \pm 6			110 \pm 20
	2016-Feb-09	42.0 \pm 1.6	299.8 \pm 2.2				6.8 \pm 1.3			
	2016-Feb-16	40.9 \pm 1.5	305.1 \pm 1.6				5.9 \pm 1.1			
	2016-Feb-23	40.8 \pm 1.5	306.8 \pm 1.7				5.9 \pm 1.1			
	2016-Mar-12	38.8 \pm 1.5	301.3 \pm 2.4				3.8 \pm 0.8			
	2016-May-04	40.3 \pm 1.6	308.4 \pm 1.8				3.5 \pm 0.7			
	2016-May-11	38.5 \pm 1.6	305.4 \pm 2.4				3.5 \pm 0.7			
	2016-May-20	39.8 \pm 1.7	305.5 \pm 1.8				2.5 \pm 0.5			
	2016-May-27	38.4 \pm 1.7	303.3 \pm 1.8				3.3 \pm 0.6			
	2016-Jun-05	37.5 \pm 1.7	301.2 \pm 2.5				3.8 \pm 0.7			
	2017-Jan-03	35.0 \pm 1.9	305.2 \pm 0.3				1.7 \pm 0.2			6.9 \pm 1.0
	2017-Jan-08	33.7 \pm 1.8	302.0 \pm 1.2						1.7 \pm 0.3	5.3 \pm 0.8
	2017-Jan-24	31.6 \pm 0.7	301.2 \pm 1.0							3.1 \pm 0.5
	Average	38.8	304.3							
Sengen Patera	2016-Jun-19	-32.4 \pm 1.6	304.9 \pm 1.8				2.9 \pm 0.6			
	2017-Jan-03	-30.0 \pm 1.0	310.9 \pm 0.6					1.7 \pm 0.3	2.0 \pm 0.3	2.4 \pm 0.4
	2017-Mar-04	-29.6 \pm 1.3	303.0 \pm 3.6				9.6 \pm 1.9			
	2017-Mar-06	-26.4 \pm 1.2	305.4 \pm 1.3				6.0 \pm 1.0			
	Average	-29.8	305.1							
Rarog Patera	2013-Aug-15	-40.5 \pm 2.2	305.5 \pm 2.6	500 \pm 80			330 \pm 80			
	2013-Aug-20	-40.1 \pm 1.4	302.1 \pm 1.4	4.0 \pm 1.9			23 \pm 4			
	2013-Aug-22	-39.3 \pm 1.8	305.4 \pm 1.8				21 \pm 3			35 \pm 5
	2013-Sep-07	-41.0 \pm 1.9	304.8 \pm 2.9				7.7 \pm 1.5			
	2013-Nov-29	-42.1 \pm 2.1	304.9 \pm 2.1				4.3 \pm 0.6			

Table A.2 continued on next page

Table A.2 (continued)

Hot Spot	Date	Lat	Lon	K-cont	H ₂ O	PAH	L'	Bra-cont	Bra α	Ms
				$\lambda = 2.27 \mu\text{m}$	$3.06 \mu\text{m}$	$3.29 \mu\text{m}$	$3.78 \mu\text{m}$	$3.99 \mu\text{m}$	$4.05 \mu\text{m}$	$4.67 \mu\text{m}$
	[UT]	[°N]	[°W]	[GW/ $\mu\text{m}/\text{sr}$]						
	2013-Dec-15	-39.7 \pm 1.8	303.0 \pm 2.3				2.9 \pm 1.4			
	2014-Feb-10	-37.8 \pm 0.4	307.9 \pm 1.1			3.5 \pm 0.5	3.3 \pm 0.5			2.6 \pm 0.4
	2014-Mar-10	-41.9 \pm 1.6	300.2 \pm 3.8				5.2 \pm 2.6			
	2014-Mar-12	-39.0 \pm 1.9	309.9 \pm 2.2				2.7 \pm 1.4			
	2014-Mar-28	-37.2 \pm 1.6	306.0 \pm 2.5				4.9 \pm 1.0			
	2015-Jan-12	-33.7 \pm 1.4	304.9 \pm 1.5				1.9 \pm 0.3			2.0 \pm 0.3
	2015-Mar-31	-37.4 \pm 1.1	307.2 \pm 1.0		2.8 \pm 0.4	1.9 \pm 0.3	1.6 \pm 0.4			0.99 \pm 0.35
	2015-Apr-02	-39.0 \pm 2.9	308.3 \pm 1.2				2.2 \pm 0.8			1.3 \pm 0.5
	2015-Apr-09	-39.1 \pm 1.9	309.0 \pm 2.2				5.5 \pm 0.8			
	Average	-39.2	305.4							
Heno Patera	2013-Aug-15	-55.2 \pm 2.1	307.5 \pm 2.1	92 \pm 15			270 \pm 70			
	2013-Aug-20	-53.0 \pm 2.1	304.0 \pm 3.0	4.9 \pm 2.4			40 \pm 6			
	2013-Aug-22	-55.6 \pm 1.7	309.5 \pm 1.7	9.3 \pm 2.6			50 \pm 8			69 \pm 11
	2013-Aug-29	-55.7 \pm 2.5	309.2 \pm 3.0				31 \pm 6			
	2013-Sep-05	-55.0 \pm 2.5	307.1 \pm 4.6				15 \pm 3			
	2013-Sep-07	-56.2 \pm 2.5	307.5 \pm 4.3				17 \pm 4			
	2015-Apr-02	-57.9 \pm 0.8	305.0 \pm 1.9							2.8 \pm 0.4
	Average	-55.6	307.5							
Loki Patera	2013-Aug-15	12.0 \pm 1.4	309.0 \pm 1.4	7.7 \pm 1.4			60 \pm 10			
	2013-Aug-20	11.9 \pm 0.8	308.7 \pm 1.2	13 \pm 3			130 \pm 30			200 \pm 30
	2013-Aug-22	11.7 \pm 1.2	308.4 \pm 1.0	7.5 \pm 1.3			140 \pm 20			210 \pm 30
	2013-Aug-29	11.3 \pm 1.4	307.1 \pm 1.4				130 \pm 20			
	2013-Sep-03	10.9 \pm 1.5	308.4 \pm 4.7				50 \pm 14			
	2013-Sep-05	11.3 \pm 1.4	307.4 \pm 1.6				73 \pm 11			
	2013-Sep-07	12.0 \pm 1.4	307.0 \pm 1.7				84 \pm 13			
	2013-Sep-09	10.2 \pm 1.5	310.3 \pm 5.0				37 \pm 19			
	2013-Sep-10	12.0 \pm 1.4	295.1 \pm 5.3				15 \pm 5			
	2013-Nov-18	14.2 \pm 0.5	309.5 \pm 3.7							28 \pm 10
	2013-Nov-27	11.9 \pm 1.4	307.0 \pm 2.6				12 \pm 2			
	2013-Nov-29	12.4 \pm 1.1	306.5 \pm 1.1				13 \pm 2			
	2013-Dec-06	12.0 \pm 1.1	307.5 \pm 1.5				11 \pm 2			
	2013-Dec-15	12.5 \pm 1.0	307.3 \pm 1.1				11 \pm 2			
	2014-Jan-20	12.2 \pm 0.6	312.6 \pm 2.9							17 \pm 4
	2014-Feb-08	12.6 \pm 0.9	310.7 \pm 0.3				8.5 \pm 1.3			25 \pm 4
	2014-Feb-10	12.6 \pm 0.3	310.0 \pm 0.3			2.1 \pm 0.3	11 \pm 2			32 \pm 5
	2014-Mar-10	12.1 \pm 1.2	314.0 \pm 2.7				6.4 \pm 3.2			
	2014-Mar-12	11.9 \pm 1.2	311.3 \pm 1.2				7.7 \pm 1.1			
	2014-Mar-28	13.1 \pm 1.3	309.5 \pm 1.5				7.6 \pm 1.1			
	2014-Oct-03	12.2 \pm 1.4	306.9 \pm 1.4				130 \pm 20			
	2014-Oct-10	11.6 \pm 1.4	306.6 \pm 1.6				130 \pm 20			
	2014-Oct-24	10.8 \pm 1.4	304.7 \pm 2.3				66 \pm 10			
	2014-Oct-30	11.1 \pm 0.5	309.9 \pm 4.8				40 \pm 28			43 \pm 25
	2014-Oct-31	12.2 \pm 0.5	306.3 \pm 1.7				78 \pm 12			160 \pm 20
	2014-Nov-25	10.6 \pm 1.2	307.0 \pm 1.5				55 \pm 8			
	2014-Nov-27	11.1 \pm 1.2	305.6 \pm 1.5				54 \pm 8			
	2014-Nov-29	9.4 \pm 1.2	298.9 \pm 7.8				59 \pm 31			
	2014-Nov-30	9.8 \pm 1.2	293.1 \pm 3.7				10 \pm 2			
	2014-Dec-02	10.2 \pm 1.1	305.3 \pm 0.6		12 \pm 2		47 \pm 7			120 \pm 20
	2014-Dec-06	11.7 \pm 1.2	306.0 \pm 1.4				29 \pm 4			
	2014-Dec-09	10.7 \pm 1.3	303.3 \pm 2.6				24 \pm 4			
	2014-Dec-16	11.2 \pm 1.2	305.1 \pm 2.7				14 \pm 3			
	2014-Dec-18	12.0 \pm 1.2	306.5 \pm 1.3				24 \pm 4			
2015-Jan-10	12.9 \pm 1.1	307.2 \pm 1.2				12 \pm 2				
2015-Jan-12	11.2 \pm 0.6	306.3 \pm 0.4				23 \pm 3			66 \pm 10	
2015-Jan-14	12.4 \pm 1.1	307.4 \pm 1.2				19 \pm 3				
2015-Jan-26	11.6 \pm 1.1	307.6 \pm 2.7				7.7 \pm 3.9				
2015-Mar-29	12.7 \pm 1.2	311.7 \pm 4.2				11 \pm 5				
2015-Mar-31	12.3 \pm 0.4	312.0 \pm 0.8			2.4 \pm 0.4	9.8 \pm 1.5			30 \pm 4	
2015-Apr-02	12.7 \pm 1.0	311.5 \pm 0.8				9.3 \pm 1.4			28 \pm 4	
2015-Apr-04	12.7 \pm 0.7	318.9 \pm 1.8							15 \pm 2	
2015-Apr-05	12.0 \pm 1.2	307.0 \pm 2.7				6.0 \pm 3.0				
2015-Apr-09	12.4 \pm 1.2	311.7 \pm 1.2				8.7 \pm 1.3				
2015-Nov-23	11.7 \pm 0.6	308.1 \pm 1.1				2.9 \pm 0.4			13 \pm 2	

Table A.2 continued on next page

Table A.2 (continued)

Hot Spot	Date	Lat	Lon	K-cont	H ₂ O	PAH	L'	Bra-cont	Bra α	Ms
				$\lambda = 2.27 \mu\text{m}$	$3.06 \mu\text{m}$	$3.29 \mu\text{m}$	$3.78 \mu\text{m}$	$3.99 \mu\text{m}$	$4.05 \mu\text{m}$	$4.67 \mu\text{m}$
	[UT]	[°N]	[°W]				[GW/ $\mu\text{m}/\text{sr}$]			
	2015-Dec-25	15.5±0.6	306.4±0.9		17±3	28±4	38±6			85±13
	2016-Feb-09	17.5±1.2	303.3±1.3				100±20			
	2016-Feb-16	16.9±1.1	306.7±1.2				75±13			
	2016-Feb-18	14.8±1.0	296.6±7.2				120±110			
	2016-Feb-21	12.6±1.2	304.7±2.0				44±9			
	2016-Feb-23	16.1±1.1	308.1±1.2				67±13			
	2016-Mar-12	12.4±1.1	306.6±1.4				69±13			
	2016-Mar-14	12.4±0.9	305.5±7.1				63±60			
	2016-May-02	13.5±1.3	311.7±3.3				22±5			
	2016-May-04	16.1±1.2	312.2±1.3				26±5			
	2016-May-09	14.9±1.4	310.1±6.5				11±5			
	2016-May-11	13.6±1.3	309.6±1.6				20±4			
	2016-May-13	13.0±1.3	308.4±1.7				21±4			
	2016-May-15	10.4±0.6	314.0±2.5							18±4
	2016-May-18	13.4±1.3	310.1±2.2				17±3			
	2016-May-20	16.2±1.3	307.3±1.3				21±4			
	2016-May-25	11.7±1.3	310.4±2.4				15±3			
	2016-May-27	13.1±1.3	307.2±1.4				20±4			
	2016-Jun-03	18.3±1.4	309.3±1.8				14±3			
	2016-Jun-05	12.5±1.3	305.0±1.6				16±3			
	2016-Jun-10	16.7±1.4	311.0±2.6				10±2			
	2016-Jun-12	13.5±1.4	308.3±1.4				15±3			
	2016-Jun-17	13.3±1.5	306.7±3.4				11±2			
	2016-Jun-19	14.7±1.4	306.2±1.5				13±2			
	2016-Jun-28	15.5±1.5	309.9±1.6				13±2			
	2016-Nov-18	18.2±1.6	305.8±1.8				8.8±1.5			
	2016-Dec-23	12.4±0.5	306.5±1.4					7.2±1.1	5.4±0.8	17±3
	2017-Jan-03	11.9±0.9	308.5±0.7				6.9±1.0	12±2	14±2	28±4
	2017-Jan-08	11.2±0.9	305.2±0.9				4.5±0.7	6.2±0.9	5.2±0.8	18±4
	2017-Jan-12	13.8±1.4	308.1±1.6				4.4±0.8			
	2017-Jan-24	10.6±0.0	306.2±0.7				4.4±0.7			17±3
	2017-Jan-26	15.0±1.3	302.7±1.4				4.6±0.8			
	2017-Mar-04	14.7±1.3	309.0±3.5				22±5			
	2017-Mar-06	17.3±1.2	307.9±1.2				31±5			
	2017-Mar-29	17.8±1.2	305.4±1.2				56±9			
	2017-Apr-02	16.4±0.9	305.6±6.9				38±28			
	2017-Apr-03	16.7±1.4	303.4±5.5				30±10			
	2017-May-05	17.2±1.3	307.6±2.7				52±10			
	2017-May-07	17.0±1.2	311.1±1.8				65±11			
	2017-May-09	16.1±1.2	306.0±1.4				67±11			
	2017-May-11	16.7±1.0	304.3±6.6				81±52			
	2017-May-14	14.3±1.3	308.0±2.4				61±11			
	2017-May-23	16.4±1.2	311.5±1.5				79±13			
	2017-May-25	16.0±1.2	309.6±1.4				82±14			
	2017-May-27	11.9±0.6	314.6±1.8		27±4	45±8	61±9	100±20	140±40	170±30
	2017-May-28	11.6±1.1	304.8±1.7		9.0±2.8	13±7	27±15	57±23	57±45	49±20
	2017-May-30	15.7±1.3	306.3±1.7				89±15			
	2017-Jun-03	12.7±1.0	312.1±6.6				39±26			
	2017-Jun-15	12.2±1.3	311.1±1.5				73±12			
	2017-Jun-22	13.6±1.3	308.8±1.8				72±12			
	2017-Jun-24	14.4±1.3	308.7±1.4				95±16			
	2017-Jun-29	11.7±1.4	306.7±2.4				47±8			
	2017-Jul-01	12.5±1.3	310.5±1.3				67±11			
	2017-Jul-06	14.2±1.5	308.6±4.5				29±7			
	2017-Jul-08	14.7±1.4	308.6±1.6				40±7			
	2017-Jul-31	9.3±1.1	310.4±1.1		4.8±0.7	12±2	27±4	38±6	34±5	120±20
	2017-Dec-12	10.8±0.7	306.1±1.4				8.2±1.2			
	2018-Jan-12	11.0±0.4	307.8±0.9				10±2			40±6
	2018-Mar-02	14.4±1.3	307.0±1.3				5.3±0.9			
	2018-Apr-24	15.1±1.1	303.1±1.3				2.4±0.4			
	2018-May-10	14.5±1.1	305.7±1.2				3.3±0.6			
	2018-May-31	16.8±1.4	308.4±4.7				21±5			
	2018-Jun-02	17.4±1.2	307.5±1.4				26±4			

Table A.2 continued on next page

Table A.2 (continued)

Hot Spot	Date	Lat	Lon	K-cont	H ₂ O	PAH	L'	Br α -cont	Br α	Ms
				$\lambda = 2.27 \mu\text{m}$	$3.06 \mu\text{m}$	$3.29 \mu\text{m}$	$3.78 \mu\text{m}$	$3.99 \mu\text{m}$	$4.05 \mu\text{m}$	$4.67 \mu\text{m}$
	[UT]	[°N]	[°W]				[GW/ $\mu\text{m}/\text{sr}$]			
	2018-Jun-06	14.9 \pm 1.4	309.4 \pm 3.8				24 \pm 7			
	2018-Jun-15	15.7 \pm 1.5	306.2 \pm 4.6				43 \pm 18			
	2018-Jun-18	16.1 \pm 1.3	309.9 \pm 2.1				40 \pm 6			
	2018-Jun-22	15.5 \pm 1.0	303.8 \pm 6.0				37 \pm 19			
	2018-Jun-25	14.2 \pm 1.3	304.3 \pm 2.7				37 \pm 6			
	Average	12.6	307.5							
Shoshu Patera	2017-Jun-15	-17.6 \pm 1.3	322.9 \pm 1.9				2.7 \pm 0.5			
	Average	-17.6	322.9							
Tol-Ava Patera	2013-Sep-05	0.9 \pm 1.8	325.9 \pm 2.3				7.7 \pm 1.2			
	2013-Sep-07	0.5 \pm 1.3	324.1 \pm 1.4				8.4 \pm 1.5			
	2014-Dec-06	1.0 \pm 1.2	327.0 \pm 1.2				0.87 \pm 0.44			
	2015-Jan-14	0.6 \pm 1.1	327.3 \pm 1.1				0.99 \pm 0.49			
	Average	0.7	326.5							
PV170	2014-Dec-02	-50.0 \pm 1.1	324.9 \pm 3.2		19 \pm 3		12 \pm 2			6.8 \pm 1.0
	2014-Dec-06	-47.9 \pm 2.0	327.8 \pm 2.1				7.2 \pm 1.1			
	2015-Dec-25	-46.0 \pm 0.9	329.3 \pm 1.4			2.1 \pm 0.4	2.5 \pm 0.4			4.0 \pm 0.6
	Average	-47.9	327.8							
Fuchi Patera	2014-Feb-10	28.3 \pm 1.1	328.7 \pm 1.1				1.1 \pm 0.4			
	Average	28.3	328.7							
Surt	2014-Feb-10	44.2 \pm 1.7	336.4 \pm 2.4							0.99 \pm 0.5
	2015-Jan-12	44.6 \pm 2.0	331.7 \pm 2.1							1.5 \pm 0.2
	Average	44.4	334.1							
Pfu1063	2014-Oct-30	38.1 \pm 0.9	358.5 \pm 2.4				2.4 \pm 0.7			4.4 \pm 0.7
	2015-Jan-12	41.8 \pm 0.8	352.9 \pm 0.8							3.1 \pm 0.5
	2015-Apr-02	41.7 \pm 1.2	357.7 \pm 1.7							1.2 \pm 0.4
	Average	41.7	357.7							
Paive Patera	2015-Apr-02	-42.1 \pm 1.5	359.6 \pm 1.6							0.99 \pm 0.35
	2017-May-27	-43.7 \pm 0.7	357.0 \pm 1.1					2.1 \pm 0.5		
	Average	-42.9	358.3							
Paive Patera	2015-Apr-02	-42.1 \pm 1.5	359.6 \pm 1.6							0.99 \pm 0.35
	2017-May-27	-43.7 \pm 0.7	357.0 \pm 1.1					2.1 \pm 0.5		
	Average	-42.9	358.3							

^a All flux densities are corrected for geometric foreshortening.